

# Hydrographic Observations At the Woods Hole Oceanographic Institution Hawaii Ocean Time-series Site: 2017 - 2018



## Data Report #14

Fernando Santiago-Mandujano, Fernando Pacheco, Kellen Rosburg, Andrew King, Ksenia Trifonova, Albert Plueddemann, Robert Weller, Roger Lukas, Jeffrey Snyder, and Nan Galbraith

**December 2019**



**Hydrographic Observations at the Woods Hole Oceanographic Institution Hawaii Ocean  
Time-series Site: 2017 – 2018**

by

Fernando Santiago-Mandujano<sup>1</sup>, Fernando Pacheco<sup>1</sup>, Kellen Rosburg<sup>1</sup>, Andrew King<sup>1</sup>, Ksenia Trifonova<sup>1</sup>, Albert Plueddemann<sup>2</sup>, Robert Weller<sup>2</sup>, Roger Lukas<sup>1</sup>, Jeffrey Snyder<sup>1</sup>, and Nan Galbraith<sup>2</sup>

The University of Hawaii at Manoa  
School of Ocean and Earth Science and Technology  
1000 Pope Road  
Honolulu, Hawaii 96822  
U.S.A

December 2019

**Data Report #14**

Reproduction in whole or in part is permitted for any purpose of the United States Government. This data report should be cited as Santiago-Mandujano, F., et al., 2019, Hydrographic observations at the Woods Hole Oceanographic Institution Hawaii Ocean Time-Series Site: 2017-2018, Data Report #14, School of Ocean Science and Technology publication # 10879, University of Hawaii at Manoa, 117 pp.  
([http://www.soest.hawaii.edu/whots/WHOTS-14\\_datareport.pdf](http://www.soest.hawaii.edu/whots/WHOTS-14_datareport.pdf))

It is approved for public release, distribution unlimited.

<sup>1</sup> The University of Hawaii (UH) at Manoa  
<sup>2</sup> Woods Hole Oceanographic Institution (WHOI)

## Acknowledgments

Many people participated in the WHOTS mooring deployment/recovery cruises. They are listed in Table II-1 and Table II-4. We gratefully acknowledge their contributions and support. Thanks are due to all the personnel of the Upper Ocean Processes Group (UOP) at WHOI who prepared the WHOTS buoy's instrumentation and mooring; to Kelsey Maloney, Svetlana Natarov, Noah Howins, and Garret Hebert, for their technical assistance with the moored and shipboard instrumentation; to Kellie Terada for her excellent project support. We gratefully acknowledge the support from the colleagues at Sea-Bird for helping us maintain the quality of the CTD data. We would also like to thank the captains and crew of the Ship *Hi'ialakai* and the University of Hawaii (UH) Marine Center staff for their efforts. The WHOTS mooring work is funded in part by the Ocean Observing and Monitoring Division, Climate Program Office (FundRef number 100007298), National Oceanic and Atmospheric Administration, U.S. Department of Commerce, under grant NA14OAR4320158 to the Woods Hole Oceanographic Institution. This work was also supported by National Science Foundation grant OCE12-60164.



# Table of Contents

<b>I. INTRODUCTION</b> .....	<b>5</b>
<b>II. DESCRIPTION OF THE WHOTS-14 MOORING CRUISES</b> .....	<b>7</b>
A. WHOTS-14 CRUISE: WHOTS-14 MOORING DEPLOYMENT.....	7
B. WHOTS-15 CRUISE: WHOTS-14 MOORING RECOVERY .....	9
<b>III. DESCRIPTION OF WHOTS-14 MOORING</b> .....	<b>11</b>
<b>IV. WHOTS (14-15) CRUISE SHIPBOARD OBSERVATIONS</b> .....	<b>16</b>
A. CONDUCTIVITY, TEMPERATURE, AND DEPTH (CTD) PROFILING.....	16
1. <i>Data acquisition and processing</i> .....	17
2. <i>CTD sensor calibration and corrections</i> .....	17
B. WATER SAMPLING AND ANALYSIS .....	18
<i>Salinity</i> .....	18
C. THERMOSALINOGRAPH DATA ACQUISITION AND PROCESSING.....	19
1. <i>WHOTS-14 Cruise</i> .....	19
2. <i>WHOTS-15 Cruise</i> .....	21
D. SHIPBOARD ADCP.....	23
1. <i>WHOTS-14 Deployment Cruise</i> .....	23
2. <i>WHOTS-15 Deployment Cruise</i> .....	23
<b>V. MOORED INSTRUMENT OBSERVATIONS</b> .....	<b>24</b>
A. MICROCAT/SEACAT DATA PROCESSING PROCEDURES .....	24
1. <i>Internal Clock Check and Missing Samples</i> .....	25
2. <i>Pressure Drift Correction and Pressure Variability</i> .....	25
3. <i>Temperature Sensor Stability</i> .....	27
4. <i>Conductivity Calibration</i> .....	33
B. ACOUSTIC DOPPLER CURRENT PROFILER .....	43
1. <i>Compass Calibrations</i> .....	43
2. <i>ADCP Configurations</i> .....	46
3. <i>ADCP data processing procedures</i> .....	46
C. VECTOR MEASURING CURRENT METER (VMCM) .....	54
D. GLOBAL POSITIONING SYSTEM RECEIVER AND ARGOS POSITIONS .....	59
<b>VI. RESULTS</b> .....	<b>62</b>
A. CTD PROFILING DATA.....	64
B. THERMOSALINOGRAPH DATA.....	77
C. MICROCAT/SEACAT DATA.....	81
D. MOORED ADCP DATA .....	100
E. MOORED AND SHIPBOARD ADCP COMPARISONS.....	103
F. NEXT GENERATION VECTOR MEASURING CURRENT METER DATA (VMCM) .....	110
G. GPS DATA.....	111
H. MOORING MOTION.....	112
<b>VII. REFERENCES</b> .....	<b>114</b>
<b>VIII. APPENDICES</b> .....	<b>116</b>
A. APPENDIX 1: WHOTS-14 300 KHZ - SERIAL 4981.....	116
B. APPENDIX 2: WHOTS-14 600 KHZ ADCP CONFIGURATION (SERIAL 1825).....	117

# List of Figures

FIGURE I-1. WHOTS-14 MOORING DESIGN. ....	6
FIGURE V-1. LINEARLY CORRECTED PRESSURES FROM MICROCATS DURING WHOTS-14 DEPLOYMENT. ....	26
FIGURE V-2. TEMPERATURE DIFFERENCE BETWEEN MICROCAT SN 1841 AT 1.5 M, AND NEAR-SURFACE TEMPERATURE SENSORS. ....	28
FIGURE V-3. TEMPERATURE DIFFERENCE BETWEEN THE 7-M MICROCAT AND THE 10-M VMCM. ....	30
FIGURE V-4. TEMPERATURE DIFFERENCE BETWEEN THE 25-M MICROCAT AND THE 30-M VMCM. ....	31
FIGURE V-5. TEMPERATURE DIFFERENCE BETWEEN THE 45-M MICROCAT AND THE 47.5-M ADCP. ....	32
FIGURE V-6. TEMPERATURE DIFFERENCE BETWEEN THE 120-M MICROCAT AND THE 125-M ADCP. ....	33
FIGURE V-7. TEMPERATURE DIFFERENCES, AND SALINITY DIFFERENCES BETWEEN MICROCATS DURING WHOTS-1. ....	35
FIGURE V-8. CONDUCTIVITY SENSOR CORRECTIONS FOR MICROCATS FROM 2 TO 7 M DURING WHOTS-14. ....	36
FIGURE V-9. CONDUCTIVITY SENSOR CORRECTIONS FOR MICROCATS FROM 15 TO 35 M DURING WHOTS-14. ....	37
FIGURE V-10. CONDUCTIVITY SENSOR CORRECTIONS FOR MICROCATS FROM 40 TO 50 M DURING WHOTS14. ....	38
FIGURE V-11. CONDUCTIVITY SENSOR CORRECTIONS FOR MICROCATS FROM 55 TO 75 M DURING WHOTS14. ....	39
FIGURE V-12. CONDUCTIVITY SENSOR CORRECTIONS FOR MICROCATS FROM 85 TO 105M DURING WHOTS14. ....	40
FIGURE V-13. CONDUCTIVITY SENSOR CORRECTIONS FOR MICROCATS FROM 120 TO 155 M DURING WHOTS-14. ....	41
FIGURE V-14. CONDUCTIVITY SENSOR CORRECTIONS FOR MICROCATS AT 4715 M DURING WHOTS-14. ....	42
FIGURE V-15. RESULTS OF THE POST-CRUISE COMPASS CALIBRATION ON ADCP SN 4891. ....	45
FIGURE V-16. RESULTS OF THE POST-CRUISE COMPASS CALIBRATION ON ADCP SN 1825. ....	45
FIGURE V-17. TEMPERATURE RECORD FROM THE 300 KHz ADCP DURING WHOTS-14 MOORING. ....	48
FIGURE V-18. SAME AS FIGURE V-17, BUT FOR THE 600 KHz ADCP. ....	48
FIGURE V-19. SOUND SPEED PROFILE DURING THE DEPLOYMENT OF THE WHOTS-14. ....	49
FIGURE V-20. EASTWARD VELOCITY COMPONENT FOR THE 300 KHz AND THE 600 KHz ADCPs. ....	50
FIGURE V-21. HISTOGRAM OF THE VERTICAL VELOCITY OF THE 300 KHz ADCP FOR RAW DATA. ....	52
FIGURE V-22. HISTOGRAM OF THE VERTICAL VELOCITY OF THE 600 KHz ADCP FOR RAW DATA. ....	53
FIGURE V-23. A COMPARISON OF 30 M VMCM AND ADCP U VELOCITY FOR WHOTS-14. ....	55
FIGURE V-24. SAME AS IN FIGURE V-23 BUT FOR THE MERIDIONAL (V) VELOCITY COMPONENT. ....	56
FIGURE V-25. SAME AS IN FIGURE V-23 BUT FOR THE 10 M VMCM. ....	57
FIGURE V-26. SAME AS IN FIGURE V-25, BUT FOR THE MERIDIONAL (V) VELOCITY COMPONENT. ....	58
FIGURE V-27. WHOTS-14 BUOY POSITION FROM ARGOS DATA AND GPS DATA. ....	60
FIGURE V-28. WHOTS-12 BUOY ARGOS POSITIONS AND DISTANCE FROM ITS ANCHOR. ....	61
FIGURE VI-1. PROFILES OF CTD AS A FUNCTION OF PRESSURE FOR STATION 20 CAST 1 DURING WHOTS-14 CRUISE. ....	65
FIGURE VI-2. SAME AS IN FIGURE VI-1, BUT FOR STATION 50, CAST 2 AND 50 CAST 3. ....	66
FIGURE VI-3. SAME AS IN FIGURE VI-1, BUT FOR STATION 50, CAST 4 AND 50 CAST 5. ....	67
FIGURE VI-4. SAME AS IN FIGURE VI-1, BUT FOR STATION 50, CAST 6 AND 52 CAST 1. ....	68
FIGURE VI-5. SAME AS IN FIGURE VI-1, BUT FOR STATION 52, CAST 2 AND 52 CAST 3. ....	69
FIGURE VI-6. SAME AS IN FIGURE VI-1, BUT FOR STATION 52, CAST 4 AND 52 CAST 5. ....	70
FIGURE VI-7. PROFILES OF CTD AS A FUNCTION OF PRESSURE FOR STATION 20 CAST 1 DURING WHOTS-15 CRUISE. ....	71
FIGURE VI-8. SAME AS IN FIGURE VI-7, BUT FOR STATION 50, CAST 2 AND 50 CAST 3. ....	72
FIGURE VI-9. SAME AS IN FIGURE VI-7, BUT FOR STATION 50, CAST 4 AND 50 CAST 5. ....	73
FIGURE VI-10. SAME AS IN FIGURE VI-7, BUT FOR STATION 50, CAST 6 AND 52 CAST 1. ....	74
FIGURE VI-11. SAME AS IN FIGURE VI-7, BUT FOR STATION 52, CAST 2 AND 52 CAST 3. ....	75
FIGURE VI-12. SAME AS IN FIGURE VI-7, BUT FOR STATION 52, CAST 4 AND 52 CAST 5. ....	76
FIGURE VI-13. FINAL PROCESSED CTD DATA FROM THE UNDERWAY SYSTEM DURING WHOTS-14 CRUISE. ....	77
FIGURE VI-14. TIMESERIES OF LATITUDE, LONGITUDE, AND SHIP'S SPEED DURING THE WHOTS-14 CRUISE. ....	78
FIGURE VI-15. FINAL PROCESSED CTD DATA FROM THE UNDERWAY SYSTEM DURING THE WHOTS-15 CRUISE. ....	79
FIGURE VI-16. FINAL PROCESSED CTD DATA FROM THE UNDERWAY SYSTEM DURING WHOTS-15 CRUISE. ....	80
FIGURE VI-17. TEMPERATURES FROM MICROCATS DURING WHOTS-14 DEPLOYMENT AT 1.5, 7, 15, AND 25 M. ....	82
FIGURE VI-18. SAME AS IN FIGURE VI-17, BUT AT 35, 40, 45, AND 50 M. ....	83
FIGURE VI-19. SAME AS IN FIGURE VI-17, BUT AT 55, 65, 75, AND 85 M. ....	84
FIGURE VI-20. SAME AS IN FIGURE VI-17, BUT AT 95, 105, 120, AND 135 M. ....	85
FIGURE VI-21. SAME AS IN FIGURE V-17, BUT AT 155 M. ....	86
FIGURE VI-22. SALINITIES FROM MICROCATS DURING WHOTS-14 DEPLOYMENT AT 1.5, 7, 15, AND 25 M. ....	87
FIGURE VI-23. SAME AS IN FIGURE VI-22, BUT AT 35, 40, 45, AND 50 M. ....	88
FIGURE VI-24. SAME AS IN FIGURE VI-22, BUT AT 55, 65, 75, AND 85 M. ....	89
FIGURE VI-25. SAME AS IN FIGURE VI-22, BUT AT 95, 105, 120, AND 135 M. ....	90
FIGURE VI-26. SAME AS IN FIGURE V-22, BUT AT 155 M. ....	91

FIGURE VI-27. POTENTIAL DENSITIES FROM MICROCATs DURING WHOTS-14 AT 1.5, 7, 15, AND 25 M. ....	92
FIGURE VI-28. SAME AS IN FIGURE VI-28, BUT AT 35, 40, 45, AND 50 M. ....	93
FIGURE VI-29. SAME AS IN FIGURE VI-28, BUT AT 55, 65, 75, AND 85 M. ....	94
FIGURE VI-30. SAME AS IN FIGURE VI-28, BUT AT 95, 105, 120, AND 135 M. ....	95
FIGURE VI-31. SAME AS IN FIGURE VI-28, BUT AT 155 M. ....	96
FIGURE VI-32. PLOTS OF T-S VERSUS DEPTH FROM SEACATs/ MICROCATs DURING WHOTS-1 TO WHOTS-14 ....	97
FIGURE VI-33. PLOTS OF POTENTIAL DENSITY, DEPTH, AND OF SALINITY DURING WHOTS-1 TO WHOTS-14 .....	98
FIGURE VI-34. POTENTIAL T-S TIME-SERIES FROM THE ALOHA CABLED OBSERVATORY AND WHOTS-14 MICROCATs.....	99
FIGURE VI-35. PLOT OF EAST COMPONENT VERSUS DEPTH AND TIME FROM WHOTS-1-14 DEPLOYMENTS. ....	100
FIGURE VI-36. PLOT OF NORTH COMPONENT VERSUS DEPTH AND TIME FROM THE WHOTS-1-14 DEPLOYMENTS. ....	101
FIGURE VI-37. PLOT OF VERTICAL COMPONENT VERSUS DEPTH AND TIME FROM THE WHOTS-1-14 DEPLOYMENTS. ....	101
FIGURE VI-38. TIME-SERIES OF EAST COMPONENT OF THE 600 AND 300 KHz MOORED ADCPs DURING WHOTS-14 .....	102
FIGURE VI-39. SAME AS FIGURE VI-39 BUT FOR NORTH VELOCITY COMPONENT.....	102
FIGURE VI-40. SAME AS FIGURE VI-39, BUT FOR VERTICAL VELOCITY COMPONENT. ....	103
FIGURE VI-41. ZONAL CURRENTS FROM 75 KHz SHIPBOARD ADCP AND THE MOORED 300 KHz ADCP FROM THE WHOTS-14 .....	104
FIGURE VI-42. MERIDIONAL CURRENTS FROM 75 KHz SHIPBOARD ADCP AND THE MOORED 300 KHz ADCP FROM THE WHOTS-14 .....	105
FIGURE VI-43. ZONAL CURRENTS FROM 75 KHz SHIPBOARD ADCP AND THE MOORED 300 KHz ADCP FROM THE WHOTS-15 .....	106
FIGURE VI-44. MERIDIONAL CURRENTS FROM 75 KHz SHIPBOARD ADCP AND THE MOORED 300 KHz ADCP FROM THE WHOTS-15 .....	107
FIGURE VI-45. MEAN CURRENT PROFILES DURING SHIPBOARD ADCP VERSUS MOORED 300 KHz ADCP INTERCOMPARISONS FROM HOT-295 THROUGH HOT-305 AND FROM WHOTS-14 AND WHOTS-15 CRUISES. .....	109
FIGURE VI-46. MEAN CURRENT PROFILES DURING SHIPBOARD ADCP VERSUS MOORED 600 KHz ADCP INTERCOMPARISONS FROM HOT-295 THROUGH HOT-305 AND FROM WHOTS-14 AND WHOTS-15 CRUISES. .....	109
FIGURE VI-47. HORIZONTAL VELOCITY DATA DURING WHOTS-14 FROM VMCMs AT 10 M DEPTH AND AT 30 M ...	110
FIGURE VI-48. GPS LATITUDE AND LONGITUDE TIME SERIES FROM THE WHOTS-14 DEPLOYMENT. ....	111
FIGURE VI-49. THE POWER SPECTRUM OF LATITUDE AND LONGITUDE FOR THE WHOTS-14 DEPLOYMENT.....	112
FIGURE VI-50. PLOTS OF ADCP TILT AND DISTANCE OF THE BUOY FOR THE 300 KHz, AND THE 600 KHz ADCP .....	113

## List of Tables

TABLE II-1. SCIENTIFIC PERSONNEL ON SHIP HI'IALAKAI DURING THE WHOTS-14 DEPLOYMENT CRUISE. ....	7
TABLE II-2. CTD STATIONS OCCUPIED DURING THE WHOTS-14 CRUISE.....	8
TABLE II-3. CONFIGURATION OF THE OCEAN SURVEYOR 75kHz ADCP ON BOARD THE SHIP HI'IALAKAI DURING THE WHOTS-14 CRUISE. ....	9
TABLE II-4. SCIENTIFIC PERSONNEL ON SHIP HI'IALAKAI DURING THE WHOTS-15 CRUISE (WHOTS-14 MOORING RECOVERY) .....	9
TABLE II-5. CTD STATIONS OCCUPIED DURING THE WHOTS-15 CRUISE (WHOTS-14 MOORING RECOVERY).....	10
TABLE II-6. CONFIGURATION OF THE OCEAN SURVEYOR 75kHz ADCP ON BOARD THE SHIP HI'IALAKAI DURING THE WHOTS-15 CRUISE. ....	11
TABLE III-1. WHOTS-14 MOORING SUBSURFACE INSTRUMENT DEPLOYMENT INFORMATION. ....	13
TABLE III-2. WHOTS-14 MICROCAT AND SBE-56 TEMPERATURE SENSOR INFORMATION .....	13
TABLE III-3. WHOTS-14 MOORING ADCP DEPLOYMENT AND CONFIGURATION INFORMATION.....	13
TABLE III-4. WHOTS-14 MICROCAT RECOVERY INFORMATION. ALL TIMES STATED ARE IN UTC. ....	14
TABLE III-5. WHOTS-14 MOORING ADCP RECOVERY INFORMATION. ALL TIMES ARE IN UTC.....	15
TABLE IV-1. THE PRECISION OF SALINITY MEASUREMENTS OF SECONDARY LAB STANDARDS. ....	19
TABLE IV-2. ADCP RECORD TIMES FOR THE NARROW BAND 75 kHz ADCP DURING THE WHOTS-14 CRUISE.....	23
TABLE IV-3. ADCP RECORD TIMES (UTC) FOR THE 75 kHz ADCP DURING THE WHOTS-15 CRUISE. ....	24
TABLE V-1. WHOTS-14 MICROCAT TEMPERATURE SENSOR CALIBRATION DATES AND SENSOR DRIFT .....	24
TABLE V-2. PRESSURE BIAS OF MICROCATs WITH PRESSURE SENSORS.....	25
TABLE V-3. SPECIFICATIONS OF THE ADCP'S USED FOR THE WHOTS-14 MOORING. ....	43
TABLE V-4. RESULTS FROM THE WHOTS-14 PRE-DEPLOYMENT 300 kHz ADCP COMPASS FIELD CALIBRATION. ....	44
TABLE V-5. RESULTS FROM THE WHOTS-14 PRE-DEPLOYMENT 600 kHz ADCP COMPASS FIELD CALIBRATION. ....	44
TABLE V-6. RESULTS FROM THE WHOTS-14 POST-DEPLOYMENT 300kHz ADCP COMPASS FIELD CALIBRATION. ....	44
TABLE V-7. RESULTS FROM THE WHOTS-14 POST-DEPLOYMENT 600kHz ADCP COMPASS FIELD CALIBRATION P. ....	44
TABLE V-8. ADCP RECORD TIMES (UTC) DURING WHOTS-14 DEPLOYMENT .....	47
TABLE V-9. RECORD TIMES (UTC) FOR THE VMCMs AT 10 M AND 30 M DURING THE WHOTS-14 DEPLOYMENT ....	54
TABLE V-10. GPS AND ARGOS RECORD TIMES (UTC) DURING WHOTS-14.....	59

# I. Introduction

In 2003, Robert Weller (Woods Hole Oceanographic Institution [WHOI]), Albert Plueddemann (WHOI), and Roger Lukas (University of Hawaii [UH]) proposed to establish a long-term surface mooring at the Hawaii Ocean Time-series (HOT) Station ALOHA (22°45'N, 158°W) to provide sustained, high-quality air-sea fluxes and the associated upper ocean response as a coordinated part of the HOT program, and as an element of the global array of ocean reference stations supported by the National Oceanic and Atmospheric Administration's (NOAA) Office of Climate Observation.

With support from NOAA and the National Science Foundation (NSF), the WHOI HOT Site (WHOTS) surface mooring has been maintained at Station ALOHA since August 2004. The objective of this project is to provide long-term, high-quality air-sea fluxes as a coordinated part of the HOT program and contribute to the goals of observing heat, freshwater, and chemical fluxes at a site representative of the oligotrophic North Pacific Ocean. The approach is to maintain a surface mooring outfitted for meteorological and oceanographic measurements at a site near Station ALOHA by successive mooring turnarounds. These observations are being used to investigate air-sea interaction processes related to climate variability and change.

The original mooring system is described in the mooring deployment/recovery cruise reports (Plueddemann et al., 2006; Whelan et al., 2007). Briefly, a Surlyn foam surface buoy is equipped with meteorological instrumentation including two complete Air-Sea Interaction Meteorological (ASIMET) systems (Hosom et al. (1995), Colbo and Weller (2009)), measuring air and sea surface temperatures, relative humidity, barometric pressure, wind speed and direction, incoming shortwave and longwave radiation, and precipitation. Complete surface meteorological measurements are recorded every minute, as required to compute air-sea fluxes of heat, freshwater, and momentum. Each ASIMET system also transmits hourly averages of the surface meteorological variables via the Argos satellite system and via iridium. The mooring line is instrumented in order to collect time series of upper ocean temperatures, salinities, and velocities with the surface forcing record. This mooring includes conductivity, salinity and temperature recorders, two Vector Measuring Current Meters (VMCMs), and two Acoustic Doppler current profilers (ADCPs). See the WHOTS-14 mooring diagram in 1.

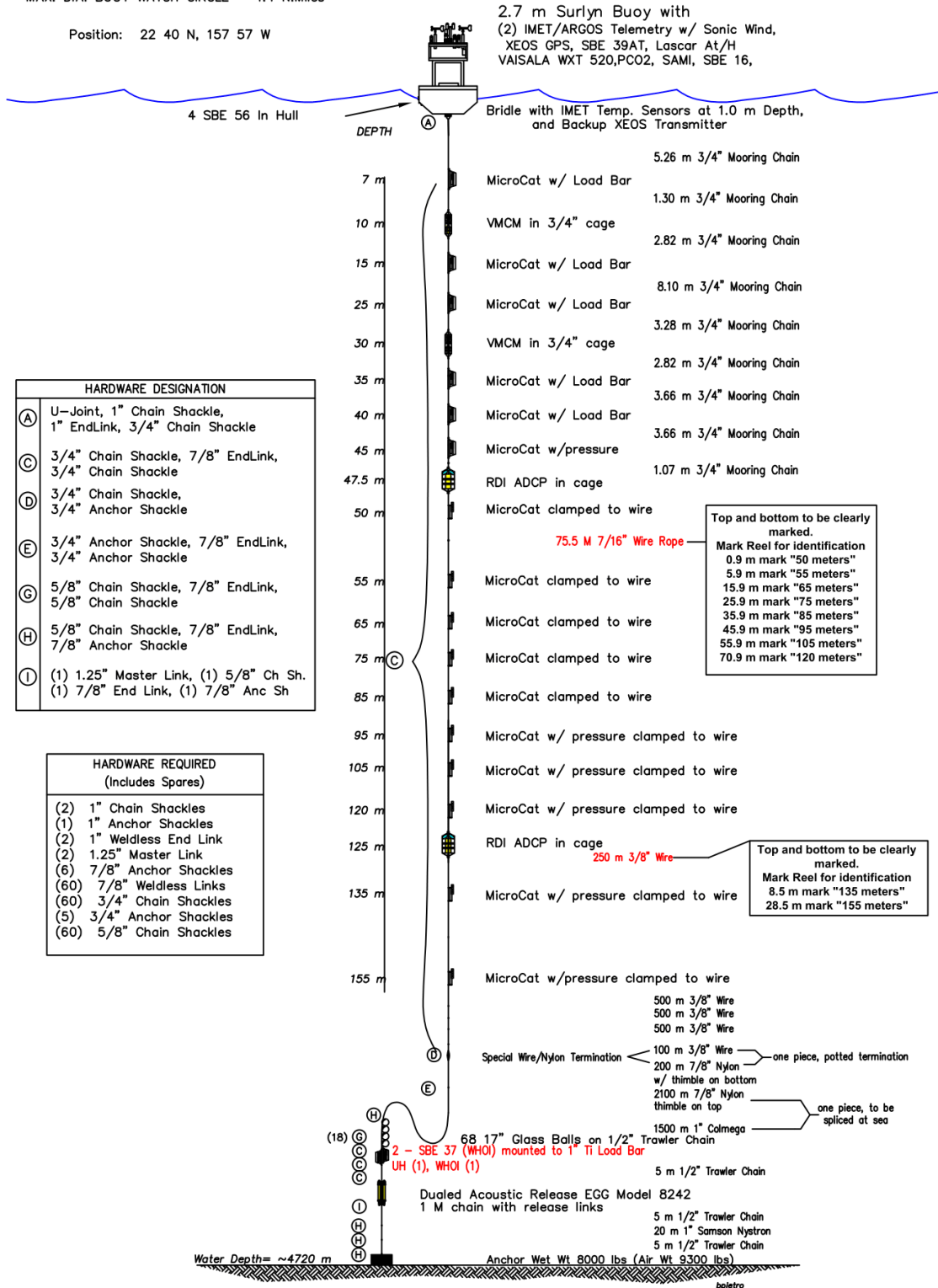
The subsurface instrumentation is located vertically to resolve the temporal variations of shear and stratification in the upper pycnocline to support the study of mixed layer entrainment. Experience with moored profiler measurements near Hawaii suggests that Richardson's number estimates over 10 m scales are adequate. Salinity is crucial to water mass stratification, as salt-stratified barrier layers are observed at HOT and in the region (Kara et al., 2000). Thus Sea-Bird MicroCATs with vertical separation ranging from 5-20 m were used to measure temperature and salinity. A Teledyne RD Instruments (TRDI) ADCP obtains current profiles across the entrainment zone and another in the mixed layer. Both ADCPs are in an upward-looking configuration, one is at 125 m, using 4 m bins, and the other is at 47.5 m using 2 m bins. To provide near-surface velocity (where the ADCP estimates are less reliable), we deploy two VMCMs. The simple mooring design is a balance between resolving extremes versus the typical annual cycling of the mixed layer (see WHOTS Data Report 1-2, Santiago-Mandujano et al., 2007).

# PO # 1278

Feb. 06, 2017

MAX. DIA. BUOY WATCH CIRCLE = 4.4 N.Miles

Position: 22 40 N, 157 57 W



HARDWARE DESIGNATION	
(A)	U-Joint, 1" Chain Shackle, 1" EndLink, 3/4" Chain Shackle
(C)	3/4" Chain Shackle, 7/8" EndLink, 3/4" Chain Shackle
(D)	3/4" Chain Shackle, 3/4" Anchor Shackle
(E)	3/4" Anchor Shackle, 7/8" EndLink, 3/4" Anchor Shackle
(G)	5/8" Chain Shackle, 7/8" EndLink, 5/8" Chain Shackle
(H)	5/8" Chain Shackle, 7/8" EndLink, 7/8" Anchor Shackle
(I)	(1) 1.25" Master Link, (1) 5/8" Ch Sh. (1) 7/8" End Link, (1) 7/8" Anc Sh

HARDWARE REQUIRED (Includes Spares)	
(2)	1" Chain Shackles
(1)	1" Anchor Shackles
(2)	1" Weldless End Link
(2)	1.25" Master Link
(6)	7/8" Anchor Shackles
(60)	7/8" Weldless Links
(60)	3/4" Chain Shackles
(5)	3/4" Anchor Shackles
(60)	5/8" Chain Shackles

## WHOTS MOORING

14 th Deployment - v2

Figure I-1. WHOTS-14 mooring design.

The fourteenth WHOTS mooring (WHOTS-14 mooring) was deployed on June 28<sup>th</sup>, 2017, during a nine-day cruise (WHOTS-14 cruise), and was recovered on September 26<sup>th</sup>, 2018 during a nine-day cruise (WHOTS-15 cruise); both cruises were aboard the NOAA Ship *Hi'ialakai*. A fifteenth mooring (WHOTS-15 mooring) was deployed during the WHOTS-15 cruise; to be recovered in October 2019.

This report documents and describes the oceanographic observations made on the 14<sup>th</sup> WHOTS mooring during nearly one year, and from shipboard measurements during the two cruises when the mooring was deployed and recovered. Sections II and III include a detailed description of the cruises and the mooring, respectively. Sampling and processing procedures of the hydrographic casts, thermosalinograph, and shipboard ADCP data collected during these cruises are described in Section IV. Section V includes the processing procedures for the data collected by the moored instruments: SeaCATs, MicroCATs, VMCMs, and moored ADCPs. Plots of the resulting data and preliminary analysis are presented in Section VI.

## II. Description of the WHOTS-14 Mooring Cruises

### A. WHOTS-14 Cruise: WHOTS-14 Mooring Deployment

The Woods Hole Oceanographic Institution Upper Ocean Processes Group (WHOI/UOP), with the assistance of the UH group, conducted the 14<sup>th</sup> deployment of the WHOTS mooring onboard the NOAA Ship *Hi'ialakai* during the WHOTS-14 cruise between July 26<sup>th</sup> and August 3<sup>rd</sup>, 2017. The WHOTS-14 mooring was deployed at HOT Station 52 on July 28<sup>th</sup>, 2017, and the anchor was dropped at 02:19 UTC at 22° 40.16'N, 157° 56.80'W. Scientific personnel who participated in the cruise are listed in Table II-1.

Table II-1. Scientific personnel on Ship *Hi'ialakai* during the WHOTS-14 deployment cruise.

Cruise	Name	Title or function	Affiliation
WHOTS-14	Weller, Robert	Chief Scientist	WHOI
	Hasbrouck, Emerson	Deck and Instruments	WHOI
	Adams, Samantha	Teacher-at-Sea	WHOI
	Clabaugh, Abby	Undergrad Summer Fellow	WHOI
	Blomquist, Byron	ESRL Meteorologist	NOAA
	Snyder, Jeffrey	Marine Electronics Technician	UH
	Santiago-Mandujano, Fernando	Research Associate	UH
	King, Andrew	Research Associate	UH
	Rosburg, Kellen	Research Associate	UH
	Natarov, Svetlana	Research Associate	UH
	Hebert, Garret	Undergraduate Volunteer	UH
	Howins, Noah	Undergraduate Volunteer	UH
	Maloney, Kelsey	Student Assistant	UH

The UH group conducted the shipboard oceanographic observations during the cruise.

A Sea-Bird CTD (conductivity, temperature, and depth) system was used to measure T, S, and O<sub>2</sub> profiles during CTD casts. The time, location, and maximum CTD pressure for each of the profiles are listed in Table II-2

Thirteen CTD casts were conducted during the WHOTS-14 cruise. CTD profile data were collected at Station 50 (near the WHOTS-13 buoy), and Station 52 (near the WHOTS-14 buoy). A test cast was conducted at Station 20 (21°30.76'N, 158°22.65'W) offshore of Makaha, HI, to a depth of 1500 m in order to test three acoustic releases. Five 200 m yo-yo casts and one cast to 3500 dbar were conducted at both stations; at Station 50 for comparison with subsurface instruments on the WHOTS-13 mooring before recovery, and at Station 52 for comparison with subsurface instruments on the WHOTS-14 mooring just after deployment. Four of the five yo-yo casts consisted of five up-down cycles between 5 and 200 dbar each, and one yo-yo cast consisted of ten cycles between 5 and 200 dbar. Four water samples were taken from each cast for salinity analysis at UH, except for Station 52 cast 2 due to the bottles breaking upon recovery. For Station 52 cast 6, only three out of four depths were sampled because the lanyard of one Niskin bottle was misplaced on the CTD carousel, and no water was collected at that depth.

Table II-2. CTD stations occupied during the WHOTS-14 cruise

Station/cast	Date	Time (GMT)	Location (using NMEA data)	Maximum pressure (dbar)
20 / 1	07/26/17	04:19	21° 30.76' N, 158° 22.65' W	1525
52 / 1	07/28/17	16:08	22° 38.84' N, 157° 59.13' W	216
52 / 2	07/28/17	19:45	22° 39.23' N, 157° 58.85' W	210
52 / 3	07/29/17	00:01	22° 39.20' N, 157° 58.86' W	218
52 / 4	07/29/17	03:48	22° 39.09' N, 157° 59.06' W	494
52 / 5	07/29/17	07:52	22° 39.34' N, 157° 58.95' W	214
50 / 1	07/29/17	16:00	22° 46.00' N, 157° 55.81' W	216
50 / 2	07/29/17	19:48	22° 46.07' N, 157° 55.78' W	216
50 / 3	07/29/17	23:46	22° 46.05' N, 157° 55.76' W	214
50 / 4	07/30/17	03:51	22° 45.76' N, 157° 56.39' W	216
50 / 5	07/30/17	07:49	22° 45.96' N, 157° 56.59' W	212
50 / 6	07/30/17	22:57	22° 45.61' N, 157° 55.93' W	3504
52 / 6	08/01/17	23:26	22° 39.31' N, 158° 03.56' W	3212

Also, continuous ADCP and near-surface thermosalinograph data were obtained while underway.

The NOAA Ship *Hi'ialakai* was equipped with an RD Instruments Ocean Surveyor 75 kHz ADCP, set to function in broadband and narrowband configurations. The configuration information is shown in Table II-3. The ADCP used input from an S.G. Brown gyrometer and a Furuno GP 90 GPS receiver to establish the heading and attitude of the ship, while an Applanix POSMV4 system archived attitude data for use in post-processing.

A complete description of these operations is available in the WHOTS-14 cruise report (Hasbrouck *et al.*, 2019).

Table II-3. Configuration of the Ocean Surveyor 75kHz ADCP on board the Ship *Hi'ialakai* during the WHOTS-14 cruise.

	<b>OS75BB</b>	<b>OS75NB</b>
Sample interval (s)	900	900
Number of bins	80	60
Bin Length (m)	8	16
Pulse Length (m)	8	16
Transducer depth (m)	5	5
Blanking length (m)	16	24

Near-surface temperature and salinity data during the WHOTS-14 cruise were acquired through the use of a thermosalinograph (TSG) system aboard the Ship *Hi'ialakai*. The sensors were sampling water from the continuous seawater system running through the ship. They were comprised of one thermosalinograph model SBE-21 (SN 3155) and a micro-thermosalinograph model SBE-45 (SN 4540403-0150), both with (internal) temperature and conductivity sensors located in the ship's wet lab, about 67 m from the intake; and an SBE-38 (SN 0215) external temperature sensor located at the seawater intake. The SBE-21 recorded data every 5 seconds, and the other two instruments recorded data every second. The *Hi'ialaki* has a water intake depth of 2 m located at the bow of the ship, next to the starboard side bow thruster. The system's pressure gauge indicated between 16 and 17 psi at the sampling spigot when the valve was opened for sampling. Both thermosalinograph systems had a debubbler.

Data from the SBE-45 exhibited conductivity and temperature glitches, indicating a possible problem with the system; SBE-21 data and calculated salinities were of good quality. The records from the external and internal temperature sensors are also of good quality.

## B. WHOTS-15 Cruise: WHOTS-14 Mooring Recovery

The WHOI/UOP Group conducted the mooring turnaround operations during the WHOTS-15 cruise between September 21<sup>st</sup> and 30<sup>th</sup>, 2018. The WHOTS-15 mooring was deployed at Station 50 on September 23<sup>rd</sup>, 2018, 01:17 UTC at 22° 45.94 'N, 157° 53.70 'W, and the WHOTS-14 mooring were recovered on September 27<sup>th</sup>. The scientific personnel that participated during the cruise are listed in Table II-4.

Table II-4. Scientific personnel on Ship *Hi'ialakai* during the WHOTS-15 cruise (WHOTS-14 mooring recovery)

<b>Cruise</b>	<b>Name</b>	<b>Title or function</b>	<b>Affiliation</b>
WHOTS-15	Plueddeman, Albert	Chief Scientist	WHOI
	Pietro, Ben	Senior Engineering Assistant	WHOI
	Hasbrouck, Emerson	Engineering Assistant	WHOI
	Greenwood, Ben	Research Associate	WHOI
	Snyder, Jeffrey	Marine Electronics Technician	UH
	Santiago-Mandujano, Fernando	Research Associate	UH
	Natarov, Svetlana	Research Associate	UH
	Hebert, Garret	Undergraduate Volunteer	UH
	Howins, Noah	Undergraduate Volunteer	UH
	Maloney, Kelsey	Student Assistant	UH
Todd, James	Program Manager	CPO	

The UH group conducted the shipboard oceanographic observations during the cruise. A complete description of these operations is available in the WHOTS-15 cruise report (Santiago-Mandujano *et al.*, 2019).

A Sea-Bird CTD system was used to measure T, S, and O<sub>2</sub> profiles during CTD casts. The time, location, and maximum CTD pressure for each of the profiles are listed in Table II-5

. Twelve CTD casts were conducted during the WHOTS-15 cruise, from September 21<sup>st</sup> through September 30<sup>th</sup>, 2018. CTD profile data were collected on Station 52 (near the WHOTS-14 buoy), and Station 50 (near the WHOTS-15 buoy). A test cast was conducted at Station 20 (21°29.06'N 158°22.04'W) offshore of Makaha, HI, to an approximate depth of 1500 m in order to test three acoustic releases. Six CTD yo-yo casts were conducted to obtain profiles for comparison with subsurface instruments on the WHOTS-15 mooring after deployment, and five yo-yo casts were conducted for comparison with the WHOTS-14 mooring before recovery. These casts were started less than 0.5 nm from the buoys with varying drift during each cast and consisted of 5 up-down cycles between near the surface and 200 m.

Water samples were taken from all casts; 4 samples for each of them. These samples were to be analyzed for salinity at UH and used to calibrate the CTD conductivity sensors.

Table II-5. CTD stations occupied during the WHOTS-15 cruise (WHOTS-14 mooring recovery).

Station/cast	Date	Time (UTC)	Location (using NMEA data)	Maximum pressure (dbar)
20 / 1	09/22/2018	03:19	21° 29.06' N, 158° 22.04' W	1518
52 / 1	09/23/2018	15:52	22° 41.69' N, 157° 56.44' W	202
52 / 2	09/23/2018	19:52	22° 41.62' N, 157° 56.63' W	204
52 / 3	09/23/2018	23:57	22° 41.73' N, 157° 56.91' W	204
52 / 4	09/24/2018	03:53	22° 41.87' N, 157° 56.45' W	204
52 / 5	09/24/2018	07:46	22° 41.65' N, 157° 56.58' W	204
50 / 1	09/25/2018	15:52	22° 47.28' N, 157° 52.64' W	202
50 / 2	09/25/2018	19:54	22° 47.59' N, 157° 52.43' W	204
50 / 3	09/25/2018	23:57	22° 47.28' N, 157° 52.78' W	204
50 / 4	09/26/2018	03:55	22° 47.37' N, 157° 52.25' W	204
50 / 5	09/26/2018	07:50	22° 47.25' N, 157° 52.45' W	204
50 / 6	09/28/2018	15:51	22° 44.21' N, 157° 53.37' W	214

Also, continuous ADCP and near-surface thermosalinograph data were obtained while underway.

The NOAA Ship *Hi'ialakai* was equipped with a TRDI Ocean Surveyor 75 kHz ADCP, set to function in broadband and narrowband configurations. The configuration information is shown in Table II-6. The ADCP used input from an S.G. Brown gyrometer and a Furuno GP 90

GPS receiver to establish the heading and attitude of the ship, while an Applanix POSMV4 system archived attitude data for use in post-processing.

Table II-6. Configuration of the Ocean Surveyor 75kHz ADCP on board the Ship *Hi'ialakai* during the WHOTS-15 cruise.

	<b>OS75BB</b>	<b>OS75NB</b>
Sample interval (s)	900	900
Number of bins	80	60
Bin Length (m)	8	16
Pulse Length (m)	8	16
Transducer depth (m)	5	5
Blanking length (m)	16	24

Near-surface temperature and salinity data during the WHOTS-14 cruise were acquired through the use of a thermosalinograph (TSG) system aboard Ship *Hi'ialakai*. The sensors were sampling water from the continuous seawater system running through the ship and were comprised of one thermosalinograph model SBE-21 (SN 3155) and a micro-thermosalinograph model SBE-45 (SN 4540403-0150), both with (internal) temperature and conductivity sensors located in the ship's wet lab, about 67 m from the intake; and an SBE-38 (SN 0215) external temperature sensor located at the seawater intake. The SBE-21 recorded data every 5 seconds, and the other two instruments recorded data every second. The *Hi'ialaki* has a water intake depth of 2 m located at the bow of the ship, next to the starboard side bow thruster. The system's pressure gauge indicated between 16 and 17 psi at the sampling spigot when the valve was opened for sampling. Both thermosalinograph systems had a debubbler.

Both thermosalinographs exhibited many conductivity and temperature glitches, especially the SBE-21. The temperature differences between the internal SBE-45 and SBE-21 were between 0.4 and 0.8 °C. However, the computed salinity differences between these two instruments were between -0.03 and 0.03 g/kg.

### III. Description of WHOTS-14 Mooring

The WHOTS-14 mooring, deployed on July 28<sup>th</sup>, 2017 from NOAA's Ship *Hi'ialakai*, was outfitted with two complete sets of ASIMET sensors on the buoy and underneath, and subsurface instruments from 7 to 155 m depth and near the bottom. See Hasbrouck *et al.* (2019) for a complete description of the buoy. The WHOTS-14 recovery on September 27<sup>th</sup>, 2018, resulted in about 425 days on station.

The buoy tower also contains a radar reflector, two marine lanterns, and Argos and Iridium satellite transmission systems that provide continuous monitoring of buoy position. A Xeos Melo Global Positioning System (GPS) receiver, an SBE-39 temperature sensor adapted to measure air temperature and a Vaisala WXT-536 multi-variable (temperature, humidity, pressure, wind, and precipitation) were also mounted on the tower. A fourth positioning system (Xeos Sable transmitter) was mounted beneath the hull. Several other instruments were mounted on the buoy. A Battelle pCO<sub>2</sub> system, a pumped SBE-16 CTD, and a SEAFET pH sensor were mounted to the underside of the buoy. A Sea-Bird SBE63 hosted a dissolved oxygen sensor. Three down-looking radiometers were mounted on the buoy. One hyperspectral sensor is mounted facing

upward near the radiometers as a reference for the incoming spectral irradiance. A Wetlabs ECOFLNTUS chlorophyll fluorometer was also mounted on the buoy hull.

Four internally-logging Sea-Bird SBE-56 temperature sensors and two SBE-37 MicroCATs were bolted to the underside of the buoy hull measuring sea surface temperature (SST) and salinity. The SBE-56s measured SST once every 60 sec between 80-90 cm below the surface, and the MicroCATs were at 1.51 m (see Table III-2).

Instrumentation provided by UH for the WHOTS-14 mooring included 16 SBE-37 Microcats, and two TRDI Workhorse ADCPs, transmitting in 300 kHz 600 kHz, respectively. The Microcats all measured temperature and conductivity, with seven of them measuring pressure. All MicroCATs were deployed with antifoulant capsules. In addition to the instrumentation on the buoy, WHOI provided two Vector Measuring Current Meters (VMCMs), two deep Microcats (SBE-37) installed near the bottom of the mooring, and all required subsurface mooring hardware.

Table III-1 provides a listing of the WHOTS-14 subsurface instrumentation at their nominal depths on the mooring, along with serial numbers, sampling rates, and other pertinent information. A cold water spike was induced to the UH MicroCATs before deployment (Table III-1) and after recovery (Table III-4) by placing an ice pack in contact with their temperature sensor to check for any drift in their internal clock. To produce a spike in the ADCP data, each instrument's transducer was rubbed gently by hand for 20 seconds (Tables III-3, III-5).

The RDI 300 kHz Workhorse Sentinel ADCP, SN 4891, with an additional external battery pack, was deployed at 125 m with transducers facing upwards. The instrument was set to ping at 4-second intervals for 160 seconds every 10 minutes. This burst sampling was designed to minimize aliasing by occasional large ocean swell orbital motions. The bin size was set for 4 m. The total number of ensemble records was 62,355. The first ensemble was at 07/24/2017 00:00:00Z, and the last was at 09/30/2018 00:19:59.56Z (see Table III-3 and Table III-5 for more configuration). This instrument also measured temperature.

The RDI 600 kHz Workhorse Sentinel ADCP, SN 1825, with an additional external battery pack, was deployed at 47.5 m with transducers facing upwards. The instrument was set to ping at 2-second intervals for 160 seconds every 10 minutes. This burst sampling was designed to minimize aliasing by occasional large ocean swell orbital motions. The bin size was set for 2 m. The total number of ensemble records was 62,075. The first ensemble was on 07/26/2017 00:00:00Z, and the last was on 09/30/2018 01:39:59.96Z (see Table III-3 and Table III-5 for more configuration). This instrument also measured temperature.

The two VMCMs, SN 42 and 68, were deployed at 10 m and 30 m depth, respectively. The instruments were prepared for deployment by the WHOI/UOP group and set to sample at 1-minute intervals. These instruments also measured temperature.

Table III-1. WHOTS-14 mooring subsurface instrument deployment information. All times are in UTC.

SN:	Instrument	Depth (m)	Pressure SN	Sample Interval (sec)	Start Logging Data		Cold Spike begin		Cold Spike end		Time in Water	
3617	MicroCAT	7	N/A	180	7/24/17	00:00:00	7/25/17	02:36:00	7/25/17	03:00:00	7/27/17	18:29:00
042	VMCM	10	N/A	60	7/27/17	00:00:17	7/27/17	18:25:00*	N/A	N/A	7/27/17	18:26:00
6893	MicroCAT	15	N/A	60	7/24/17	0:00:00	7/25/17	02:36:00	7/25/17	03:00:00	7/27/17	18:19:00
6894	MicroCAT	25	N/A	60	7/24/17	0:00:00	7/25/17	02:36:00	7/25/17	03:00:00	7/27/17	18:15:00
068	VMCM	30	N/A	60	7/26/17	19:54:00	7/27/17	18:10:00*	N/A	N/A	7/27/17	18:10:00
6895	MicroCAT	35	N/A	60	7/24/17	0:00:00	7/25/17	02:36:00	7/25/17	03:00:00	7/27/17	18:07:00
6896	MicroCAT	40	N/A	60	7/24/17	0:00:00	7/25/17	02:36:00	7/25/17	03:00:00	7/27/17	18:04:00
6887	MicroCAT	45	2651319	75	7/24/17	0:00:00	7/25/17	02:36:00	7/25/17	03:00:00	7/27/17	18:02:00
1825	600 kHz ADCP	47.5	N/A	600	7/26/17	00:00:00	N/A	See Table 2	N/A	See Table 2	7/27/17	19:30:00
6897	MicroCAT	50	N/A	60	7/24/17	0:00:00	7/25/17	02:36:00	7/25/17	03:00:00	7/27/17	19:31:00
6898	MicroCAT	55	N/A	60	7/24/17	0:00:00	7/25/17	02:36:00	7/25/17	03:00:00	7/27/17	19:33:00
6899	MicroCAT	65	N/A	60	7/24/17	0:00:00	7/25/17	02:36:00	7/25/17	03:00:00	7/27/17	19:35:00
3618	MicroCAT	75	N/A	180	7/24/17	0:00:00	7/25/17	02:36:00	7/25/17	03:00:00	7/27/17	19:36:00
3634	MicroCAT	85	N/A	180	7/24/17	0:00:00	7/25/17	02:36:00	7/25/17	03:00:00	7/27/17	19:38:00
3670	MicroCAT	95	5701	240	7/24/17	0:00:00	7/25/17	02:36:00	7/25/17	03:00:00	7/27/17	19:40:00
6889	MicroCAT	105	2651321	75	7/24/17	0:00:00	7/25/17	02:36:00	7/25/17	03:00:00	7/27/17	19:42:00
6890	MicroCAT	120	2651322	75	7/24/17	0:00:00	7/25/17	02:36:00	7/25/17	03:00:00	7/27/17	19:54:00
4891	300 kHz ADCP	125	N/A	600	7/24/17	0:00:00	N/A	See Table 2	N/A	See Table 2	7/27/17	19:55:00
6888	MicroCAT	135	3418742	75	7/24/17	0:00:00	7/25/17	02:36:00	7/25/17	03:00:00	7/27/17	19:57:00
6891	MicroCAT	155	2651323	75	7/24/17	0:00:00	7/25/17	02:36:00	7/25/17	03:00:00	7/27/17	19:59:00
9988	MicroCAT	39 m off bottom	N/A	60	7/24/17	0:00:00	7/25/17	02:36:00	7/25/17	03:00:00	7/28/17	02:02:00
10602	MicroCAT	39 m off bottom	10602	60	7/20/17	1:00:00	7/25/17	02:36:00	7/25/17	03:00:00	7/28/17	02:02:00

Table III-2. WHOTS-14 MicroCAT and SBE-56 Temperature Sensor Information. All times stated are in UTC.

Instrument	SN	Depth (m)	Sample Interval (sec)
SBE-56	7215	0.8	60
SBE-56	7214	0.9	60
SBE-56	7213	0.8	60
SBE-56	7212	0.8	60
MicroCAT	1834	1.5	60
MicroCAT	1841	1.5	60

Table III-3. WHOTS-14 mooring ADCP deployment and configuration information. All times are in UTC.

	ADCP S/N 4891	ADCP S/N 1825
<b>Frequency (kHz)</b>	300	600
<b>Number of Depth Cells</b>	30	25
<b>Depth Cell Size (m)</b>	4 m	2 m
<b>Pings per Ensemble</b>	40	80
<b>Time between Ensembles</b>	10 min	10 min
<b>Ping interval</b>	4 sec	2 sec
<b>Time of First Ping</b>	07/24/17, 00:00:00	07/26/17, 00:00:00
<b>Transducer 1 Spike Time</b>	07/26/17, 00:30:00	07/26/17, 00:30:00

<b>Transducer 2 Spike Time</b>	07/26/17, 00:30:15	07/26/17, 00:30:15
<b>Transducer 3 Spike Time</b>	07/26/17, 00:30:30	07/26/17, 00:30:30
<b>Transducer 4 Spike Time</b>	07/26/17, 00:30:45	07/26/17, 00:30:45
<b>Time in Water</b>	07/27/17, 19:55:00	07/27/17, 19:30:00
<b>Depth (m)</b>	125 m	47.5 m

All WHOTS-14 instruments were successfully recovered; recovery information for the C-T instruments is shown in Table III-4. Most of the instruments had some degree of biofouling, with the most substantial fouling near the surface. The fouling extended down to the ADCP at 125 m, although it was minor at that level.

All MicroCATs were in good condition after recovery. MicroCAT 6896 (40 m) had a barnacle attached at the top end of its conductivity cell, partially blocking the flow, and MicroCAT 6894 (25 m) had its anti-fouling plug slightly displaced. The data from all instruments were downloaded onboard the ship, and all instruments returned full data records. A post-cruise evaluation showed no missing samples in all the MicroCATs and both ADCPs. Table III-4 has an initial evaluation of the data quality; more details are in Section

Table III-4. WHOTS-14 MicroCAT recovery Information. All times stated are in UTC.

<b>Depth (m)</b>	<b>Sea-Bird Serial #</b>	<b>Time out of water</b>	<b>Time of Spike</b>	<b>Time Logging Stopped</b>	<b>Samples Logged</b>	<b>Data Quality</b>
7	SBE 37-3617	9/27/18 01:45:00	9/27/18 05:21:00	9/27/18 06:55:00	206538	Good
15	SBE 37-6893	9/27/18 01:49:00	9/27/18 05:21:00	9/28/18 04:34:00	620915	Good
25	SBE 37-6894	9/27/18 01:54:00	9/27/18 05:21:00	9/28/18 04:29:30	620910	Good
35	SBE 37-6895	9/27/18 01:58:00	9/27/18 05:21:00	9/29/18 01:11:30	622153	Good
40	SBE 37-6896	9/27/18 01:59:00	9/27/18 05:21:00	9/28/18 01:05:00	620706	Good
45	SBE 37-6887	9/27/18 02:03:00	9/27/18 05:21:00	9/28/18 04:32:00	496730	Good
47.5	ADCP-1825	9/27/18 00:34:00	N/A	9/30/18 01:42:00	62074	Good
50	SBE 37-6897	9/27/18 00:34:00	9/27/18 05:21:00	9/27/18 06:32:00	619593	Good
55	SBE 37-6898	9/27/18 00:33:00	9/27/18 05:21:00	9/27/18 06:27:30	619589	Good
65	SBE 37-6899	9/27/18 00:32:00	9/27/18 05:21:00	9/27/18 06:39:00	619600	Good
75	SBE 37-3618	9/27/18 00:25:00	9/27/18 05:21:00	9/27/18 06:58:00	206538	Good
85	SBE 37-3634	9/27/18 00:24:00	9/27/18 05:21:00	9/27/18 06:52:30	206537	Good
95	SBE 37-3670	9/27/18 00:23:00	9/27/18 05:21:00	9/27/18 06:49:00	154902	Good
105	SBE 37-6889	9/27/18 00:23:00	9/27/18 05:21:00	9/27/18 06:15:00	495660	Good
120	SBE 37-6890	9/27/18 00:21:00	9/27/18 05:21:00	9/27/18 06:18:00	495663	Good
125	ADCP-4891	9/27/18 00:19:00	N/A	9/30/18 00:15:00	62354	Good
135	SBE 37-6888	9/27/18 00:15:00	9/27/18 05:21:00	9/27/18 06:06:30	495654	Good
155	SBE 37-6891	9/27/18 00:14:00	9/27/18 05:21:00	9/27/18 06:12:30	495658	Good
39 mab	SBE 37-9988	9/26/18 20:18:00	9/27/18 05:21:00	9/27/18 06:36:00	619597	Good
39 mab	SBE 37-10602	9/26/18 20:18:00	9/27/18 05:21:00	9/27/18 04:27:30	125322	Good

The data from the upward-looking 300 and 600 kHz ADCP at 125 and 47,5m, respectively, were considered as good; the instruments were pinging upon recovery. There appeared to be no questionable data from both ADCP at this time, apart from near-surface artifacts.

*Table III-5. WHOTS-14 mooring ADCP recovery information. All times are in UTC.*

	<b>ADCP S/N 4891</b>	<b>ADCP S/N 1825</b>
<b>Time of First Ping</b>	07/24/17, 00:00:00	07/26/17, 00:00:00
<b>Transducer 1 Spike Time</b>	09/28/18, 02:31:10	09/28/18, 02:36:50
<b>Transducer 2 Spike Time</b>	09/28/18, 02:31:20	09/28/18, 02:37:00
<b>Transducer 3 Spike Time</b>	09/28/18, 02:31:30	09/28/18, 02:37:10
<b>Transducer 4 Spike Time</b>	09/28/18, 02:31:40	09/28/18, 02:37:20
<b>Time in Water</b>	07/27/17, 19:55:00	07/27/17, 19:30:00
<b>Time out of Water</b>	09/27/18, 00:19:00	09/27/18, 00:34:00

## **IV. WHOTS (14-15) cruise shipboard observations**

The hydrographic profile observations made during the WHOTS cruises were obtained with a Sea-Bird CTD package with dual temperature, salinity, and oxygen sensors. This CTD was installed on a rosette-sampler with 5 L Niskin bottles for calibration water samples. Furthermore, the *Hi'ialakai* came equipped with a thermosalinograph system which provided a continuous depiction of temperature and salinity of the near-surface layer. Horizontal currents over the depth range of 30-1000 m were measured from the shipboard 75 kHz Ocean Surveyor (OS75) ADCP (narrowband) with a vertical resolution of 16m for the WHOTS-14 and WHOTS-15 cruises. Broadband mode for the OS75 provided additional current data over the range of 20-650 m with a vertical resolution of 8m.

Data gaps occurred when the system was shut down temporarily during communications with the acoustic releases used for the moorings during both cruises. Periods of missing data between 300 and 450 m in the broadband ADCP were apparent due to the lack of scattering material in the water.

### **A. Conductivity, Temperature, and Depth (CTD) profiling**

Continuous measurements of temperature, conductivity, dissolved oxygen, and pressure were made with the UH Sea-Bird SBE-9/11Plus CTD underwater unit #09P43777-0850 (referred to as #850) during the WHOTS-14 and WHOTS-15 cruises. The CTD was equipped with an internal Digiquartz pressure sensor and pairs of external temperature, conductivity, and oxygen sensors.

Each of the temperature-conductivity sensor pairs used a Sea-Bird TC duct, which circulated seawater through independent pump and plumbing installations. The CTD configuration also included two oxygen sensors, installed in the plumbing for each sensor set. In both cruises, the CTD was mounted in a vertical position in the lower part of a rosette sampler, with the sensors' water intakes located at the bottom of the rosette.

The package was deployed on a conducting cable, which allowed for real-time data acquisition and display. The deployment procedure consisted of lowering the package to approximately 10 dbar and waiting until the CTD pumps started operating. The CTD was then raised until the sensors were close to the surface to begin the CTD cast. The time and position of each cast were obtained via a GPS connection to the CTD deck box. Six Niskin bottles were used on the rosette. Four salinity samples were taken on each cast for calibration of the conductivity sensors.

## 1. Data acquisition and processing

CTD data were acquired at the instrument's highest sampling rate of 24 samples per second. Digital data were stored on a laptop computer, and, for redundancy, the analog signal was recorded on VHS videotapes. Backups of CTD data were made onto USB storage cards.

The raw CTD data were quality controlled and screened for spikes as described in the WHOTS Data Report 1 (Santiago-Mandujano et al., 2007). Data alignment, averaging, correction, and reporting were done as described in Tupas *et al.* (1993). Spikes in the data occur when the CTD samples the disturbed water of its wake. Therefore, samples from the downcast were rejected when the CTD was moving upward or when its acceleration exceeded  $0.5 \text{ m s}^{-2}$  in magnitude. The data were subsequently averaged into 2-dbar pressure bins after calibrating the CTD conductivity with the bottle salinities.

The data were additionally screened by comparing the T-C sensor pairs. These differences permitted the identification of problems with the sensors. The data from only one T-C pair, whichever was deemed most reliable, is reported here. Only data from the downcast are reported, as upcast data are commonly contaminated by wake effects from the rosette.

Temperature is reported on the ITS-90 scale. Salinity and all derived units were calculated using the UNESCO (1981) routines; salinity is reported in the practical salinity scale (PSS-78). Oxygen is reported in  $\mu\text{mol kg}^{-1}$ .

## 2. CTD sensor calibration and corrections

### *Pressure*

The pressure calibration strategy for CTD pressure transducers SN 75434 used during WHOTS-14 and SN 101430 used during WHOTS-15 cruises employed a high-quality quartz pressure transducer as a transfer standard. Periodic recalibrations of this lab standard were performed with a primary pressure standard. The only corrections applied to the CTD pressures were a constant offset determined at the time that the CTD first enters the water on each cast. Also, a span correction determined from bench tests on the sensor against the transfer standard was applied. These procedures and corrections are thoroughly documented in the HOT-2017 data report (Fujieki et al. 2019).

### *Temperature/Conductivity*

Sea-Bird SBE-3-Plus temperature and SBE 4C conductivity transducers were used during WHOTS-14 and -15 cruises. The history and performance of these sensors have been monitored during HOT cruises, and calibrations and drift corrections applied during WHOTS cruises are thoroughly documented in the HOT-2017 data report (Fujieki et al. 2019).

## *Dissolved Oxygen*

Sea-Bird SBE-43 oxygen sensors were used during the WHOTS-14 and -15 cruises. Oxygen data from the WHOTS-14 cruise were calibrated using empirical calibration coefficients obtained during the HOT-294 cruise conducted on 19-23 June 2017, before the WHOTS-14 cruise, which used the same oxygen sensors. Fujieki, et al. (2019) have details on these calibrations. Similarly, the WHOTS-15 oxygen data were calibrated using calibration coefficients obtained during the HOT-305 cruise conducted on 9-13 September 2018, before the WHOTS-15 cruise, which used the same oxygen sensors. The CTD empirical calibration was conducted using oxygen water samples and the procedure from Owens and Millard (1985). See Tupas et al. (1997) for details on these calibrations procedures.

## **B. Water sampling and analysis**

### **Salinity**

Salinity samples were collected by a rosette sampler during CTD casts at selected depths during WHOTS-14 and -15, and sub-sampled in 250 ml glass bottles. The top of each bottle and thimble were thoroughly dried before being tightly capped to prevent water from being trapped between the cap or thimble and the bottle's mouth. It has been observed that residual water trapped in this way increases its salinity due to evaporation, and it can leak into the sample when the bottle is opened for measuring. Samples from each cruise were measured after the cruise in the laboratory at the UH using a Guildline Autosol 8400B (SN 70168). IAPSO<sup>1</sup> standard seawater samples were measured to standardize the Autosol, and samples from a large batch of "secondary standard" (substandard) seawater were measured after every 24-48 samples to detect drift in the Autosol. Standard deviations of the secondary standard measurements were less than  $\pm 0.001$  for WHOTS-14 and -15 cruises (Table IV-1).

The substandard water was collected by a rosette sampler from 1020 m at station ALOHA during HOT cruises and drained into a 50-liter Nalgene plastic carboy. In the laboratory, the water was then thoroughly mixed in a glass carboy for 20 minutes by manually shaking, rolling and tilting the carboy vigorously, after which a 2-inch protective layer of white oil was added on top to deter evaporation. The substandard water was allowed to stand for approximately three days before it was used, and was stored in the same temperature-controlled room as the Autosol, protecting it from the light with black plastic bags to inhibit biological growth. Substandard seawater batches #61 and #65 were prepared on June 9<sup>th</sup>, 2016, and October 23<sup>rd</sup>, 2018, and used for WHOTS-14 and -15 samples, respectively.

Samples from the WHOTS-14 and WHOTS-15 cruises were measured during the same session as the HOT-295 and HOT-306 samples, respectively. The substandard statistics in Table IV-1 include the combined substandard samples measured for the WHOTS-14 and HOT-295 samples and the WHOTS-15 and HOT-306 samples, respectively.

---

<sup>1</sup> International Association for Physical Sciences of the Ocean

Table IV-1. The precision of salinity measurements of secondary lab standards.

Cruise	Mean Salinity +/- SD	# Samples	Substandard Batch #	IAPSO Batch #
WHOTS-14 / HOT-295	34.4681 ± 0.0009	4	61	P158
WHOTS-15 / HOT-306	34.8661 ± 0.0016	4	65	P160

## C. Thermosalinograph data acquisition and processing

### 1. WHOTS-14 Cruise

Near-surface temperature and salinity data during the WHOTS-14 cruise were acquired from the thermosalinograph (TSG) system installed on the NOAA Ship *Hi'ialakai*. The *Hi'ialakai* has a water intake depth of 2 m located at the bow of the ship, next to the starboard side bow thruster. The sensors located in the ship's wet lab about 67 m from the intake, were sampling water from the continuous seawater system running through the ship, and were comprised of one thermosalinograph model SBE-21 (SN 3155) and a micro-thermosalinograph model SBE-45 (SN 4540403-0150), both with (internal) temperature and conductivity sensors; and an SBE-38 (SN 215) external temperature sensor located at the water intake. The SBE-21 recorded data every 5 seconds, and the other two instruments recorded data every second. The system had a pressure gauge showing a flow pressure between 16 and 17 psi. Both thermosalinograph systems had a de-bubbler.

#### *Temperature Calibration*

External temperature data from the SBE-38 sensor (last calibrated at Sea-Bird on January 20<sup>th</sup> 2017) were used as a measure of the seawater temperature. These data were compared to the data collected during CTD casts.

#### *Nominal Conductivity Calibration*

Data from the SBE-21 conductivity and temperature sensors were used to calculate the intake seawater salinity. These sensors were last calibrated at Sea-Bird on January 18<sup>th</sup> 2017. All conductivity data from the thermosalinograph were nominally calibrated with coefficients from this calibration. However, all the final salinity data reported here were calibrated against bottle data, as explained below.

## ***Data Processing***

Daily files containing navigation data recorded every second were concatenated with the thermosalinograph data. The thermosalinograph data were then screened for gross errors, with upper and lower bounds of 18 °C and 35 °C for temperature and 3 and 6 Siemens m<sup>-1</sup> for conductivity. There were no points outside the valid temperature range and no points outside the valid conductivity range.

A 5-point running median filter was used to detect one- or two-point temperature and conductivity glitches in the thermosalinograph data. Glitches in temperature and conductivity detected by the 5-point median filter were immediately replaced by the median. Threshold values of 0.3 °C for temperature and 0.1 Siemens m<sup>-1</sup> for conductivity were used for the median filter. After running the filter, there were no temperature or conductivity points replaced by the median. A 3-point triangular running mean filter was used to smooth the temperature and conductivity data after passing the glitch detection.

The thermosalinograph aboard the Ship Hi'ialakai was set to record data every five seconds. However, occasionally, due to an error in the acquisition software rounding routine, a record is written at a longer interval. Only two-timing errors occurred during this cruise; both were greater than 20 seconds. The most substantial gap lasted 473 seconds.

Data were visually scanned to flag spikes likely caused by contamination due to the introduction of bubbles to the flow-through system during transits or rough conditions. Of a total of 754,531 data points, 6,773 conductivity data points (0.9%) were flagged as bad.

### ***Bottle salinity and CTD Salinity Comparisons***

The thermosalinograph salinity was calibrated by comparing it to bottle salinity samples drawn from a water intake next to the thermosalinograph every 8 hours throughout the cruise. Of the 24 bottles sampled, six were considered outliers and discarded from the analysis. Samples were analyzed as described in Section IV.B. The comparison was made in conductivity in order to eliminate the effects of temperature. The conductivity of each bottle sample was computed using the salinity of the bottle, thermosalinograph temperature, and a pressure of 3.44 dbar, which includes the pressure of the flow through system's pump.

Salinity samples were drawn from the flow through system, located less than 0.5 m from the SBE-21. Consequently, there should be virtually no delay between when the water passes through the thermosalinograph and it being sampled. A 90-second average centered on the sample draw time was chosen for processing purposes.

The CTD salinity data at 2 dbar from the 13 casts conducted during the cruise were used for comparisons with the thermosalinograph conductivity. Using the thermosalinograph temperature data and a pressure of 3.44 dbar, the CTD conductivity was calculated for the 13 casts conducted while the thermosalinograph was running. Six CTD casts were excluded from processing as outliers.

A cubic spline was fit to the time series of the differences between the bottle and TSG conductivity, and a correction was obtained for the TSG conductivities. Salinity was calculated

using these corrected conductivities, the thermosalinograph temperatures, and 3.44 dbar pressure. After correction, the mean difference between the bottle and thermosalinograph salinities was 0.000000 psu with a standard deviation of 0.00099 psu. The mean CTD - thermosalinograph difference was -0.002269 psu with a standard deviation of 0.00098 psu.

### ***CTD Temperature Comparisons***

There were 13 CTD casts conducted during WHOTS -14, one of which was a test cast offshore Honolulu (Station 20) and six casts each at Station 52 (WHOTS-14) and Station 50 (WHOTS-13), respectively. The 4 dbar downcast CTD temperature data from those casts were used to compare with the thermosalinograph data at the time of the casts. This comparison gives an estimate of the quality of the thermosalinograph measurements. Of the 13 casts, four were identified as temperature outliers after comparing it against the thermosalinograph data and removed from the analysis. The mean difference between the internal sensor and the CTD was -0.25903 °C, with a standard deviation of  $\pm 0.07119$  °C.

## **2. WHOTS-15 Cruise**

Near-surface temperature and salinity data during the WHOTS-15 cruise were acquired from the thermosalinograph (TSG) system installed on the NOAA Ship *Hi'ialakai*. The *Hi'ialakai* has a water intake depth of 2 m located at the bow of the ship, next to the starboard side bow thruster. The sensors located in the ship's wet lab about 67 m from the intake, were sampling water from the continuous seawater system running through the ship, and were comprised of one thermosalinograph model SBE-21 (SN 3155) and a micro-thermosalinograph model SBE-45 (SN 0150), both with (internal) temperature and conductivity sensors; and an SBE-38 (SN 0215) external temperature sensor located at the water intake. The SBE-21 recorded data every 5 seconds, and the other two instruments recorded data every second. The system had a pressure gauge showing a flow pressure between 10 to 15 psi when the water intake was open. Both thermosalinograph systems had a de-bubbler.

### ***Temperature Calibration***

External temperature data from the SBE-38 sensor (last calibrated at Sea-Bird on January 16<sup>th</sup>, 2018) were used as a measure of the seawater temperature. These data were compared to the data collected during CTD casts.

### ***Nominal Conductivity Calibration***

Data from the SBE-21 conductivity and temperature sensors were used to calculate the intake seawater salinity. These sensors were last calibrated at Sea-Bird on November 8<sup>th</sup>, 2017. All conductivity data from the thermosalinograph were nominally calibrated with coefficients from this calibration. However, all the final salinity data reported here were calibrated against bottle data, as explained below.

## ***Data Processing***

Daily files containing navigation data recorded every second were concatenated with the thermosalinograph data. The thermosalinograph data were then screened for gross errors, with upper and lower bounds of 18 °C and 35 °C for temperature and 3 and 6 Siemens m<sup>-1</sup> for conductivity. There were no points outside the valid temperature range and no points outside the valid conductivity range.

A 5-point running median filter was used to detect one- or two-point temperature and conductivity glitches in the thermosalinograph data. Glitches in temperature and conductivity detected by the 5-point median filter were immediately replaced by the median. Threshold values of 0.3 °C for temperature and 0.1 Siemens m<sup>-1</sup> for conductivity were used for the median filter. After running the filter, there were no temperature or conductivity points replaced by the median. A 3-point triangular running mean filter was used to smooth the temperature and conductivity data after passing the glitch detection.

The thermosalinograph aboard the Ship Hi'ialakai was set to record data every five seconds. However, occasionally, due to an error in the acquisition software rounding routine, a record is written at a longer interval. There were no timing errors during WHOTS-15.

Data were visually scanned to flag spikes likely caused by contamination due to the introduction of bubbles to the flow-through system during transits or rough conditions. Of a total of 799,508 data points, 22,555 conductivity data points (2.8%) were flagged as bad.

### ***Bottle salinity and CTD Salinity Comparisons***

The thermosalinograph salinity was calibrated by comparing it to bottle salinity samples drawn from a water intake next to the thermosalinograph every 8 hours throughout the cruise. Of the 22 thermosalinograph bottles sampled, bottle17 was identified as a conductivity outlier and discarded from the analysis. Samples were analyzed as described in Section IV.B. The comparison was made in conductivity in order to eliminate the effects of temperature. The conductivity of each bottle sample was computed using the salinity of the bottle, thermosalinograph temperature, and a pressure of 3.44 dbar, which includes the pressure of the flow through system's pump.

Salinity samples were drawn from the flow through system, located less than 0.5 m from the SBE-21. Consequently, there should be virtually no delay between when the water passes through the thermosalinograph and it being sampled. A 90-second average centered on the sample draw time was chosen for processing purposes.

In order to make the comparison in conductivity units, the CTD conductivity was calculated using the 4 dbar downcast CTD salinity, the internal thermosalinograph temperature, and a pump pressure of 3.44 dbar. There were 12 CTD casts conducted during WHOTS-15, while the thermosalinograph was running. Casts 1 and 4 were removed from the analysis as temperature outliers and cast 1, 9, and 10 as conductivity outliers.

A cubic spline was fit to the time series of the differences between the bottle and TSG conductivity, and a correction was obtained for the TSG conductivities. Salinity was calculated

using these corrected conductivities, the thermosalinograph temperatures, and 3.44 dbar pressure. After correction, the mean difference between the bottle and thermosalinograph salinities was 0.000005 psu with a standard deviation of 0.003339 psu. The mean CTD - thermosalinograph difference was -0.001385 psu with a standard deviation of 0.001677 psu.

### ***CTD Temperature Comparisons***

There were 12 CTD casts conducted during WHOTS-15, one of which was a test cast offshore Honolulu (Station 20) and five at Station 52 (WHOTS-14) and six at Station 50 (WHOTS-15), respectively. The 4 dbar downcast CTD temperature data from those casts were used to compare with the thermosalinograph data at the time of the casts. This comparison gives an estimate of the quality of the thermosalinograph measurements. Of the 12 casts, two were identified as temperature outliers after comparing it against the thermosalinograph data and removed from the analysis. The mean difference between the CTD and the internal temperature sensor was -0.00992 °C, with a standard deviation of  $\pm 0.04096$  °C.

## **D. Shipboard ADCP**

### **1. WHOTS-14 Deployment Cruise**

Currents were measured for the duration of the cruise over the depth range of 30-1000 m with a 75 kHz RDI Ocean Surveyor (OS75) ADCP working in narrowband mode with a vertical resolution of 16 m, and in broadband mode with a vertical resolution of 8 m. The system yielded useful data (see cruise report). The times of the datasets from the OS75 are shown in Table IV-2.

*Table IV-2. ADCP record times (UTC) for the Narrow Band 75 kHz ADCP during the WHOTS-14 cruise*

<b>WHOTS-14</b>	<b>OS75nb</b>	<b>OS75bb</b>
File beginning time	25-Jul-2017 22:01:17	25-Jul-2017 22:01:17
File ending time	03-Aug-2017 18:03:04	03-Aug-2017 17:58:03

### **2. WHOTS-15 Deployment Cruise**

Currents were measured for the duration of the cruise over the depth range of 30-1000 m with a 75 kHz RDI Ocean Surveyor (OS75) ADCP working in narrowband mode with a vertical resolution of 16 m, and in broadband mode with a vertical resolution of 8 m. The system yielded useful data (see cruise report). The times of the datasets from the OS75 are shown in Table IV-3.

Table IV-3. ADCP record times (UTC) for the 75 kHz ADCP during the WHOTS-15 cruise.

<b>WHOTS-15</b>	<b>OS75nb</b>	<b>OS75bb</b>
File beginning time	21-Sept-2018 19:00:19	21-Sept-2018 19:55:20
File ending time	03-Oct-2018 01:55:22	03-Oct-2018 01:50:21

## V. Moored Instrument Observations

### A. MicroCAT/SeaCAT data processing procedures

Each moored MicroCAT and SeaCAT temperature, conductivity, and pressure (when installed) was calibrated at Sea-Bird before their deployment and after their recovery on the dates shown in Table V-1. The internally-recorded data from each instrument were downloaded onboard the ship after the mooring recovery, and the nominally-calibrated data were plotted for a visual assessment of the data quality. The data processing included checking the internal clock data against external event times, and pressure sensor drifts correction, temperature sensor stability, and conductivity calibration against CTD data from casts conducted near the mooring during HOT and WHOTS cruises. The detailed processing procedures are described in this section.

Table V-1. WHOTS-14 MicroCAT temperature sensor calibration dates and sensor drift during deployments.

<b>Nominal deployment depth (m)</b>	<b>Sea-Bird Serial number</b>	<b>Pre-deployment calibration</b>	<b>Post-recovery calibration</b>	<b>Temperature sensors annual drift during WHOTS-14 (mili°C)</b>
7	SBE 37-3617	4-Aug-2016	21-Nov-2018	-0.60
15	SBE 37-6893	6-Aug-2016	27-Nov-2018	0.20
25	SBE 37-6894	5-Aug-2016	28-Nov-2018	-0.61
35	SBE 37-6895	5-Aug-2016	21-Nov-2018	-0.94
40	SBE 37-6896	5-Aug-2016	27-Nov-2018	-0.31
45	SBE 37-6887	4-Aug-2016	8-Dec-2018	-1.17
50	SBE 37-6897	10-Aug-2016	28-Nov-2018	-0.80
55	SBE 37-6898	5-Aug-2016	28-Nov-2018	-0.97
65	SBE 37-6899	5-Aug-2016	27-Nov-2018	-0.19
75	SBE 37-3618	4-Aug-2016	4-Dec-2018	-0.09
85	SBE 37-3634	4-Aug-2016	21-Nov-2018	-0.86
95	SBE 37-3670	4-Aug-2016	28-Nov-2018	-0.89
105	SBE 37-6889	6-Aug-2016	28-Nov-2018	-0.37
120	SBE 37-6890	6-Aug-2016	28-Nov-2018	-0.59
135	SBE 37-6888	6-Aug-2016	12-Dec-2018	0.00
155	SBE 37-6891	10-Aug-2016	12-Dec-2018	-0.56
4715	SBE 37-9988	5-Aug-2016	21-Nov-2018	-0.66
4715	SBE 37-10602	18-Nov-2016	21-Dec-2018	-0.03

## 1. Internal Clock Check and Missing Samples

Before the WHOTS-14 mooring deployment and after its recovery (before the data logging was stopped), the MicroCATs temperature sensors were placed in contact with an ice pack to create a spike in the data, to check for any problems with their internal clocks, and for possible missing samples (Table III-4). The cold spike was detected by a sudden decrease in temperature. For all the instruments, the clock time of this event matched the time of the spike (within the sampling interval of each instrument) correctly. No missing samples were detected for any of the instruments.

## 2. Pressure Drift Correction and Pressure Variability

Some of the MicroCATs used in the moorings were outfitted with pressure sensors (Table III-1). Biases were detected in the pressure sensors by comparing the on-deck pressure readings (which should be zero for standard atmospheric pressure at sea level of 1029 mbar) before deployment and after recovery. Table V-2 shows the magnitude of the bias for each of the sensors before and after deployment. To correct this offset, a linear fit between the initial and final on-deck pressure offset as a function of time was obtained and subtracted from each sensor. Figure V-1 shows the linearly corrected pressures measured by the MicroCATs located above 200 m during the WHOTS-14 deployment. For all these sensors, the mean difference from the nominal instrument pressure (based on the deployed depth) was less than 1 dbar. The standard deviation of the pressure for the duration of the record was also less than 1 dbar for all sensors, with the deeper sensors showing a slightly larger standard deviation. The range of variability for all sensors was about  $\pm 3$  dbar.

The causes of pressure variability can be several, including density variations in the water column above the instrument; horizontal dynamic pressure (not only due to the currents but also due to the motion of the mooring); mooring position (see WHOTS Data Report 1, Santiago-Mandujano et al., 2007).

Table V-2. Pressure bias of MicroCATs with pressure sensors.

Deployment	Depth (m)	Sea-Bird Serial #	Bias before deployment (dbar)	Bias after recovery (dbar)
WHOTS-14	45	SBE 37-6887	0.025	-0.20
WHOTS-14	95	SBE 37-3670	0.03	-0.40
WHOTS-14	105	SBE 37-6889	0.17	0.06
WHOTS-14	120	SBE 37-6890	0.09	-0.06
WHOTS-14	135	SBE 37-6888	0.02	-0.10
WHOTS-14	155	SBE 37-6891	0.04	-0.09
WHOTS-14	4715	SBE 37-10602	-0.25	-0.15

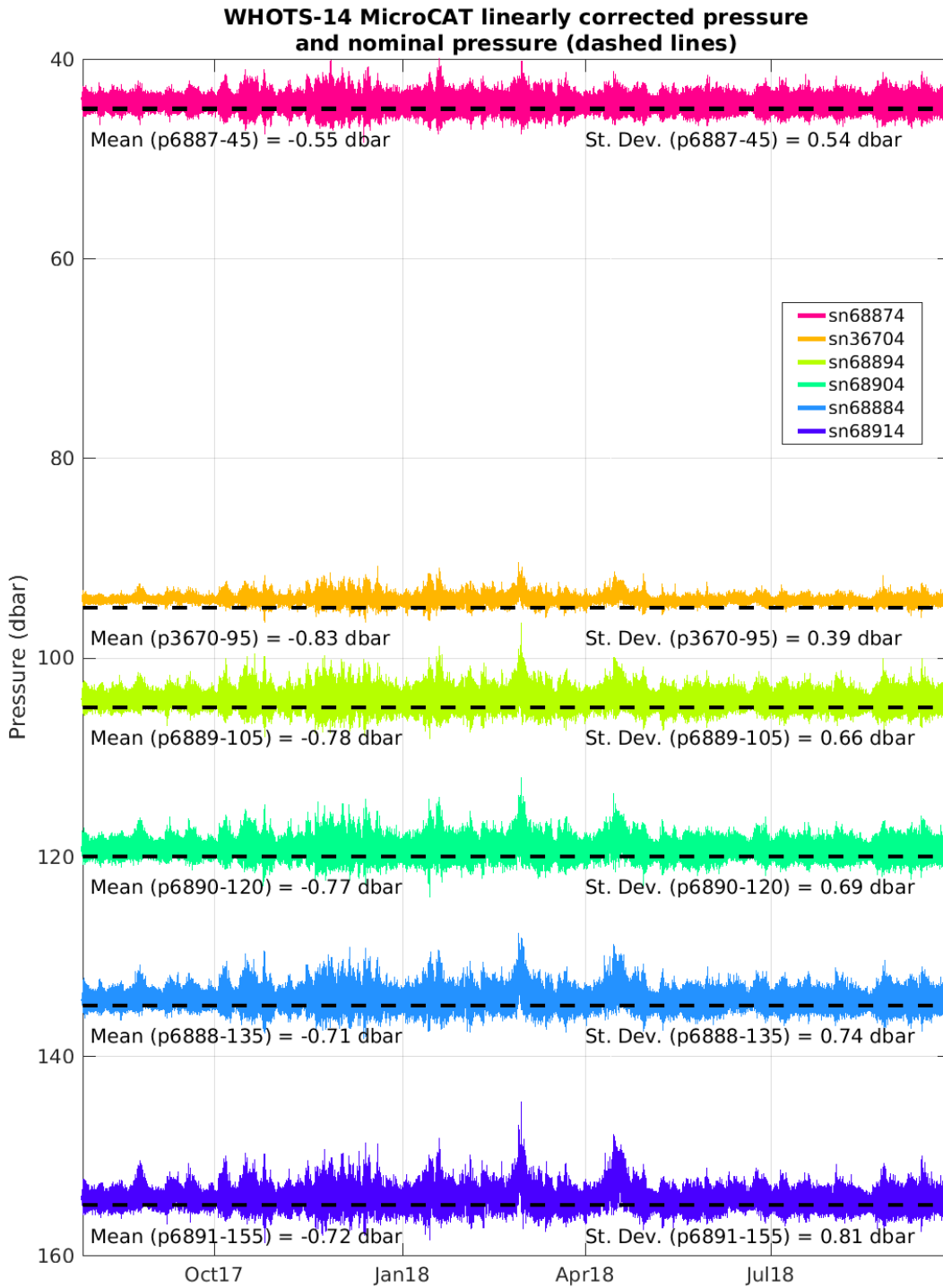


Figure V-1. Linearly corrected pressures from MicroCATs between 45 and 155 m during WHOTS-14 deployment. The horizontal dashed line is the sensor's nominal pressure, based on deployed depth.

### 3. Temperature Sensor Stability

The MicroCAT temperature sensors were calibrated at Sea-Bird before and after each deployment, and their annual drift evaluations based on these calibrations are shown in Table V-1. These values turned out to be insignificant (not higher than 1.2 milli °C) for all sensors. Comparisons between the MicroCAT and CTD data from casts conducted near the mooring during HOT cruises confirmed that the temperature drift of the rest of the moored instruments was insignificant. The two MicroCATs (SN 9988 and SN 10602) deployed near the bottom were drift corrected. Figure V-7 (upper panel) shows the temperature differences between both instruments before and after the correction. After the correction, the temperature differences were in the -1.0 to 2.0 m°C range.

Temperature comparisons between one of the WHOTS-14 near-surface MicroCAT (SN 1841) and the four SBE-56 surface temperature sensors in the buoy hull (Table III-2) are shown in Figure V-2. All of the SBE-56 instruments returned full records, and none of them show any obvious bias when compared to the Microcat measurements.

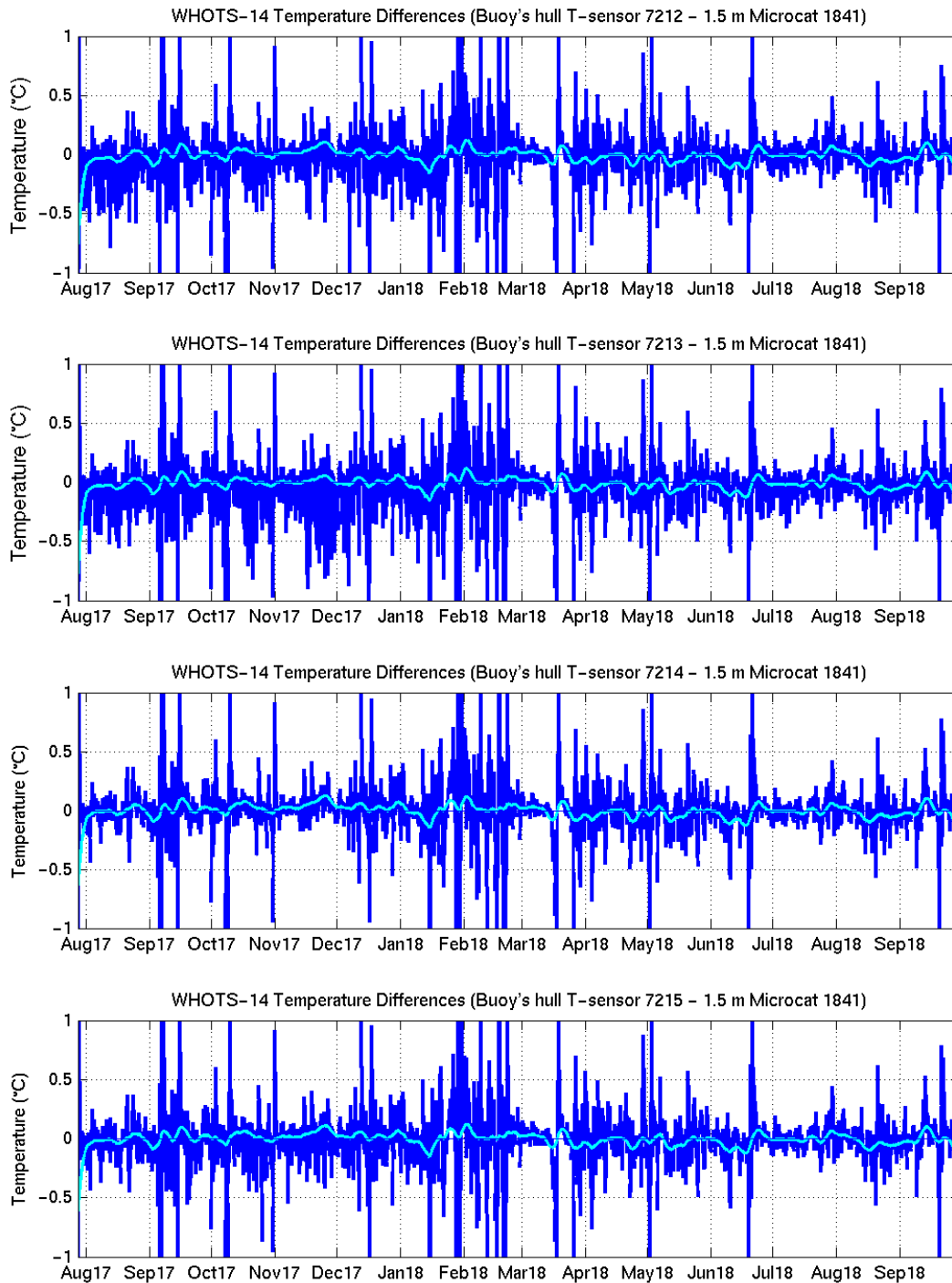


Figure V-2. The temperature difference between MicroCAT SN 1841 at 1.5 m, and near-surface temperature sensors SN 7212 (top panel), 7213 (second panel), 7214 (third panel), and 7215 (bottom panel), during the WHOTS-14 deployment. The light blue line is a 24-hour running of the differences.

In addition to the Sea-Bird temperature sensors, there were additional temperature sensors in the VMCMs (at 10 and 30 m), and in the ADCPs (at 47.5 m and 125 m). In order to evaluate the quality of the temperatures from these sensors, comparisons with the temperatures from adjacent MicroCATs were conducted.

### *Comparisons with VMCM and ADCP temperature sensors*

The upper panel of Figure V-3 shows the difference between the 10-m VMCM and the 7-m MicroCAT temperatures during WHOTS-14, after adding a 0.0263 °C offset correction to the VMCM. The offset was the mean difference between the uncorrected VMCM and the 7-m MicroCAT data. Also shown for comparison in the middle panel of the figure are the differences between MicroCAT temperatures at 15 m. The lower panel shows the temperature fluctuations in the differences between the 7 and 15-m MicroCATs, which seem to be around zero.

Temperature differences between the 30-m VMCM and the temperatures from adjacent MicroCATs at 25 and 35-m during WHOTS-14 are shown in Figure V-4, after adding a 0.0294°C offset correction to the VMCM. The offset was the mean difference between the uncorrected VMCM and the 23-m MicroCAT data. For comparison, the differences between the MicroCATs temperatures are also shown in the lower panel.

Temperature differences between the 47.5-m ADCP and the temperatures from adjacent MicroCATs at 45 and 50-m during WHOTS-14 are shown in Figure V-5. For comparison, the differences between the MicroCATs temperatures are also shown in the lower panel. These plots indicate that there was no offset in the 47.5-m ADCP for the adjacent MicroCATs (top and middle plots).

Temperature differences between the 125-m ADCP and the temperatures from adjacent MicroCATs at 120 and 135-m during WHOTS-14 are shown in Figure V-6. For comparison, the differences between the MicroCATs temperatures are also shown in the lower panel. It is difficult to assess the quality of the ADCP temperature from these comparisons, as these sensors were located at the top of the thermocline, where we expect to find substantial temperature differences between adjacent sensors. However, an indication of the quality of the ADCP temperatures is given in the upper panel plot, which shows temperatures fluctuating closely around zero.

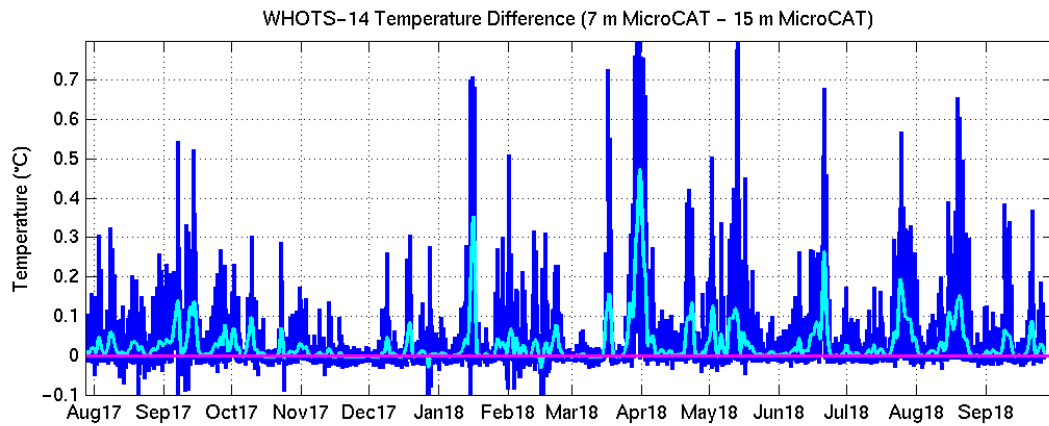
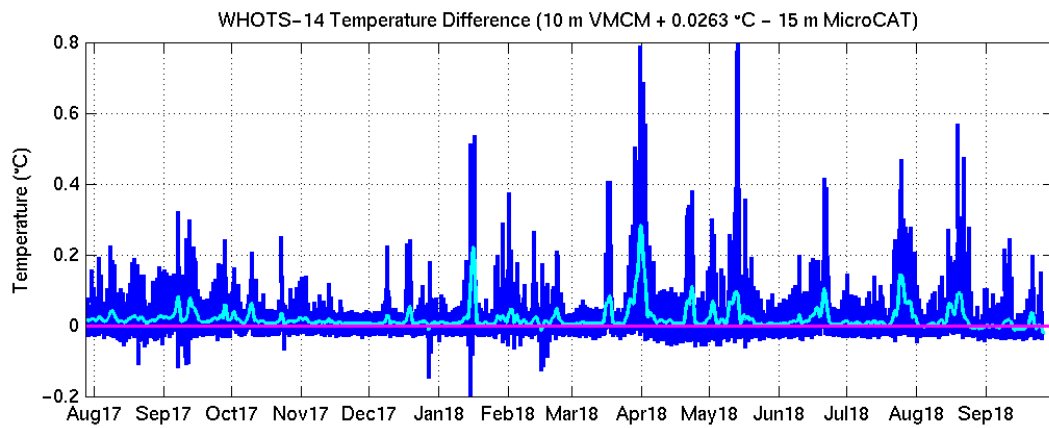
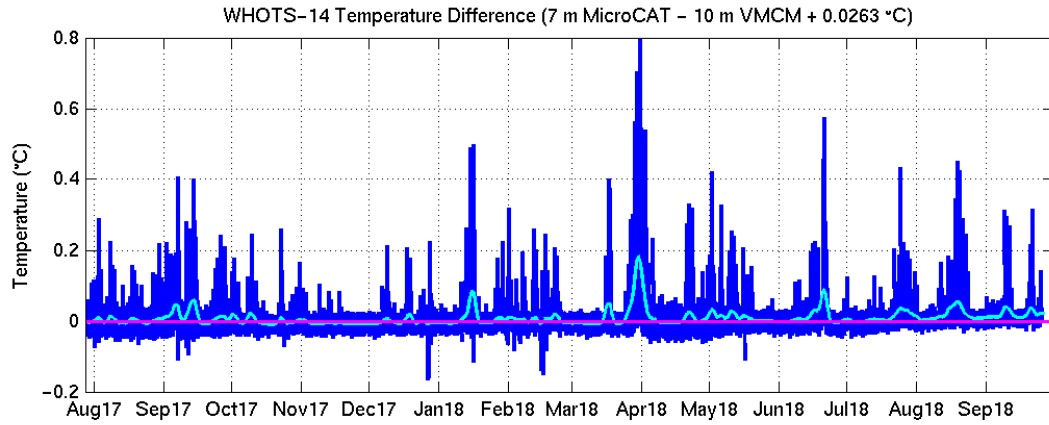


Figure V-3. The temperature difference between the 7-m MicroCAT and the 10-m VMCM (upper pane)l; between the 15-m MicroCAT and the 10-m VMCM (middle panel); and between the 7-m and the 15-m MicroCATs (lower panel ) during the WHOTS-14 deployment. The light blue line is a 24-hour running mean of the differences.

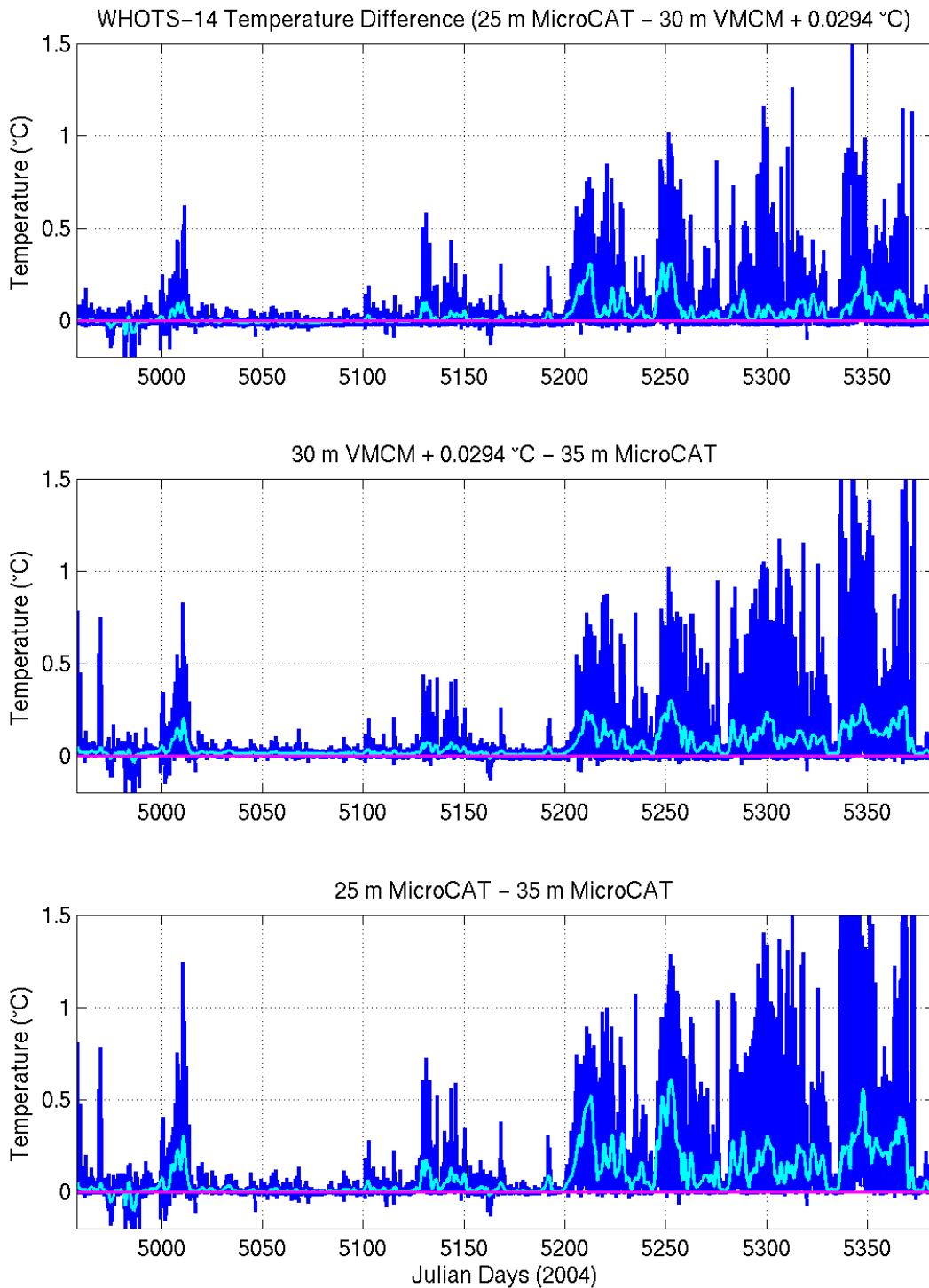


Figure V-4. The temperature difference between the 25-m MicroCAT and the 30-m VMCM (upper panel); between the 35-m MicroCAT and the 30-m VMCM (middle panel); and between the 25-m and the 35-m MicroCATs (lower panel) during the WHOTS-14 deployment. The light blue line is a 24-hour running mean of the differences.

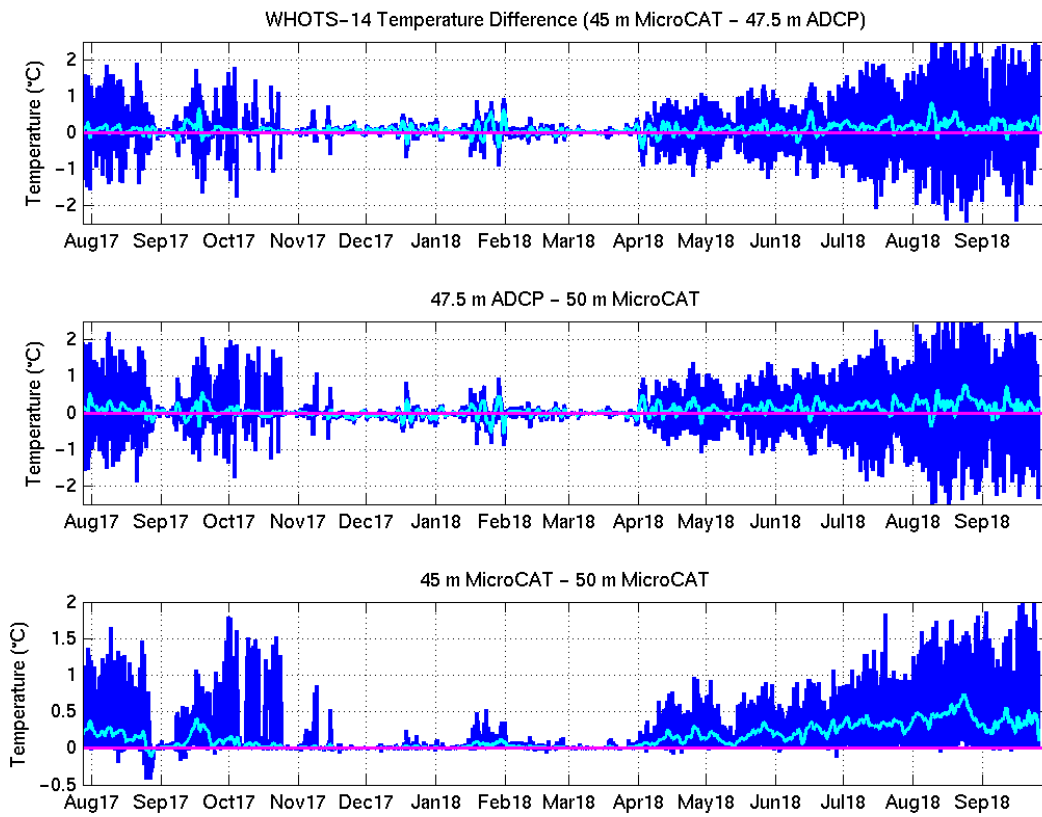


Figure V-5. The temperature difference between the 45-m MicroCAT and the 47.5-m ADCP (upper panel); between the 50-m MicroCAT and the 47.5-m ADCP (middle panel); and between the 45-m and the 50-m MicroCATs (lower panel) during the WHOTS-14 deployment. The light blue line is a 24-hour running mean of the differences.

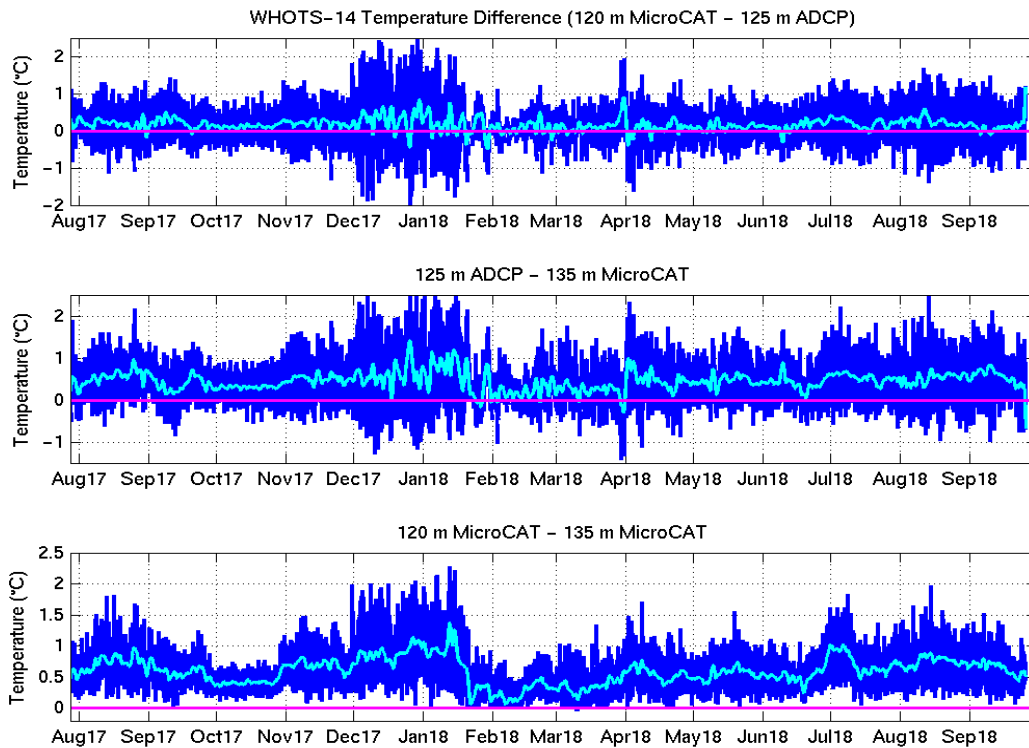


Figure V-6. The temperature difference between the 120-m MicroCAT and the 125-m ADCP (upper panel); between the 135-m MicroCAT and the 125-m ADCP (middle panel); and between the 120-m and the 135-m MicroCATs (lower panel) during the WHOTS-14 deployment. The light blue line is a 24-hour running mean of the differences.

#### 4. Conductivity Calibration

The results of the Sea-Bird post-recovery conductivity calibrations indicated that some of the MicroCAT conductivity sensors experienced relatively large offsets from their pre-deployment calibration. These were qualitatively confirmed by comparing the mooring data against CTD data from casts conducted between 200 m and 5 km from the mooring during HOT cruises. The causes of the conductivity offsets are not clear, and there may have been multiple causes (see Freitag et al., (1999) for a similar experience with conductivity cells during COARE). For some instruments, the offset was negative, caused perhaps by biofouling of the conductivity cell while for others the offset was positive, caused possibly by scouring of the inside of the conductivity cell (possibly by the continuous up and down motion of the instrument in an abundant field of diatoms). A visual inspection of the instruments after recovery did not show any apparent signs of biofouling, and there were no cell scourings reported in the post-recovery inspections at Sea-Bird.

Corrections of the MicroCATs conductivity data were conducted by comparing them against CTD data from profiles and yo-yo casts conducted near the mooring during HOT cruises and during deployment/recovery cruises. Casts conducted between 200 and 1000 m from the mooring were given extra weight in the correction, as compared to those conducted between 1 and 5 km away. Casts more than 5 km away from the mooring were not used. Given that the CTD casts are conducted at least 200 m from the mooring, the alignment between CTD and MicroCAT data was done in density rather than in-depth. For cases in which the alignment in

density was not possible due to large conductivity offsets (causing unrealistic mooring density values), alignment in temperature space was done. A cubic least-squares fit (LSF) to the CTD-MicroCAT/SeaCAT differences against time was applied as a first approximation, and the corresponding correction was applied.

Some of the sensors had large offsets and noticeable variability that could not be explained by a cubic LSF (see below). For these sensors, a stepwise correction was applied to match the data to the available CTD cast data and then to use the differences between consecutive sensors to determine when the sensor started to drift. For instance, during periods of weak stratification, the conductivity difference between neighboring sensors A, B, and C could reach near-zero values, in particular for instruments near the surface, which are the ones most prone to suffer conductivity offsets. A sudden conductivity offset observed during this period between sensors A and B, but not between sensors A and C could indicate the beginning of an offset for sensor B.

Given that the most in-depth instruments on the mooring are less likely to be affected by biofouling and consequent sudden conductivity drift, the deep instruments served as an excellent reference to find any possible malfunction in the shallower ones. Therefore the most profound instruments' conductivity was corrected first, and the correction was continued sequentially upwards toward the shallower ones.

As a quality control to the conductivity corrections, the buoyancy frequency between neighboring instruments was calculated using finite differences. Over- or under-corrected conductivities yielded instabilities in the water column (negative buoyancy frequency) that were easy to detect and were not real when lasting for several days. Based on this, the conductivity correction of the corresponding sensors was revised.

Corrections of the in-depth MicroCATs conductivity data were conducted following similar procedures as for the shallow instruments by comparing them against CTD data from near-bottom profiles conducted during HOT cruises (Figure V-7, bottom panel). After correction, the salinity differences between both instruments were in the  $\pm 0.002$  g/kg range.

Another characteristic of the offsets in the conductivity sensors is that their development is not always linear in time, and their behavior can be highly variable (see WHOTS Data Report 1, Santiago-Mandujano et al., 2007).

The corrections applied to each of the conductivity sensors during WHOTS-14 can be seen from Figure V-8 to Figure V-14. Most of the instruments had a drift of less than 0.015 Siemens/m for the duration of the deployment, which was corrected with a linear or cubic least-squares fit. Most of the instruments deployed above 85 m showed a negative drift starting a few months before the end of the deployment, apparently due to the expiration of the anti-foulant.

# WHOTS-14 Deep MicroCATs

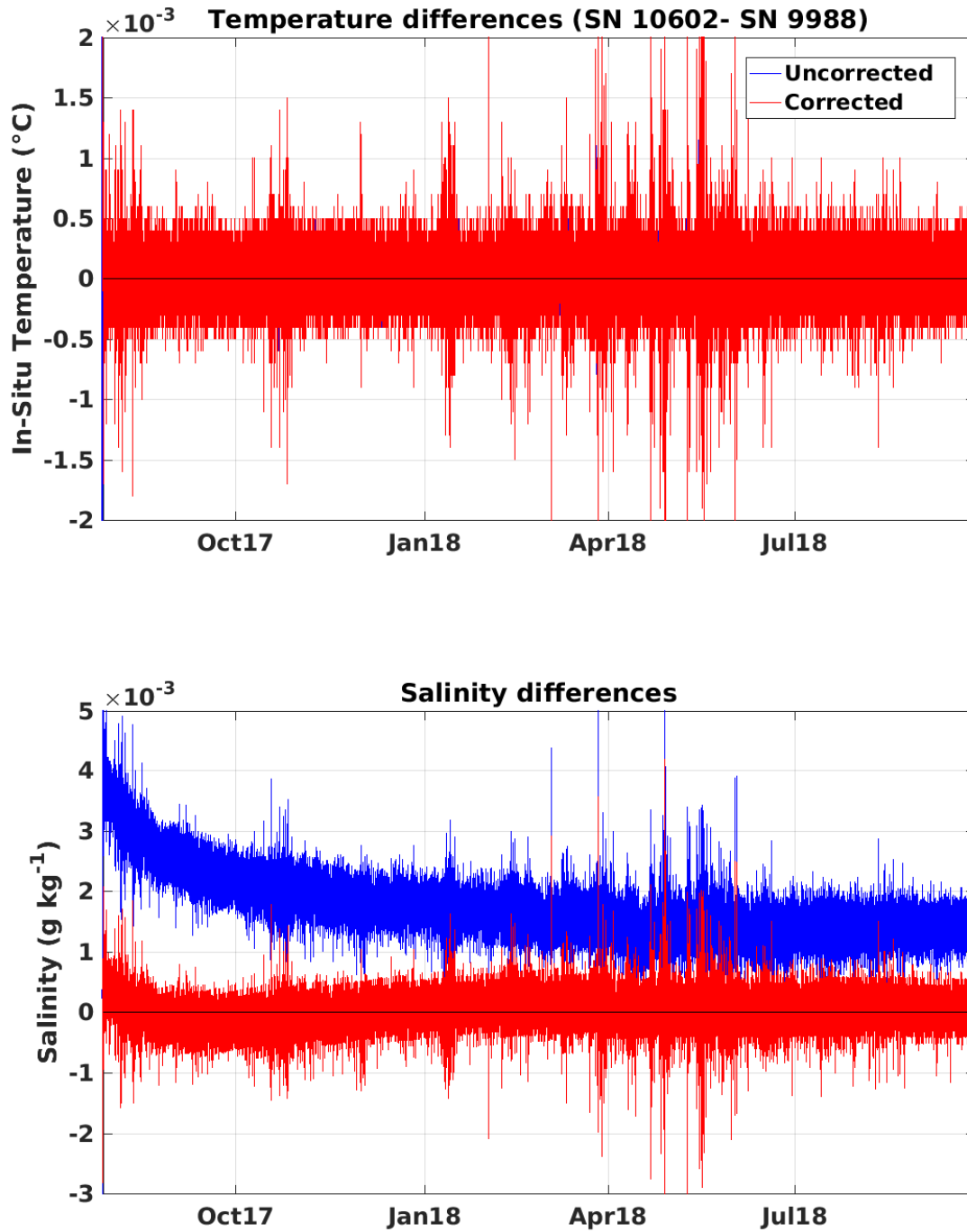


Figure V-7. Temperature differences (top panel), and salinity differences (bottom panel) between MicroCATs #10602 and #9988 during WHOTS-14. The blue (red) lines are the differences before (after) correcting the data following procedures indicated in the text.

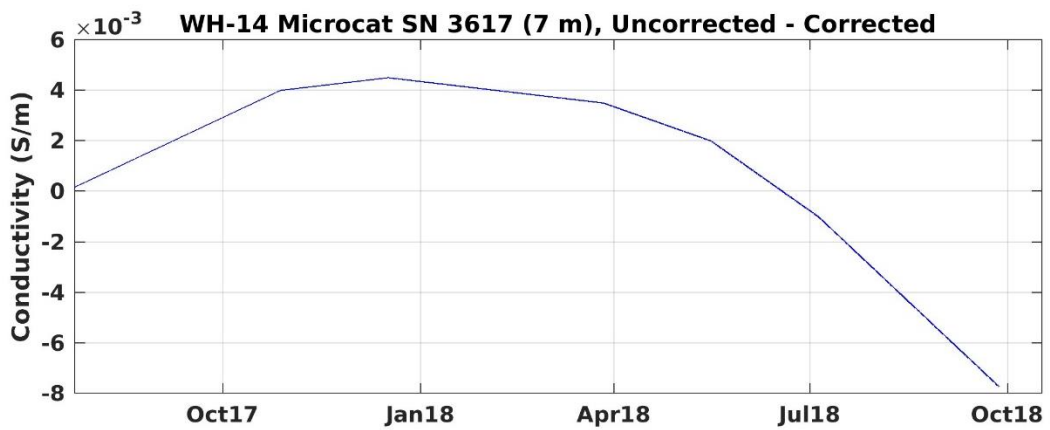
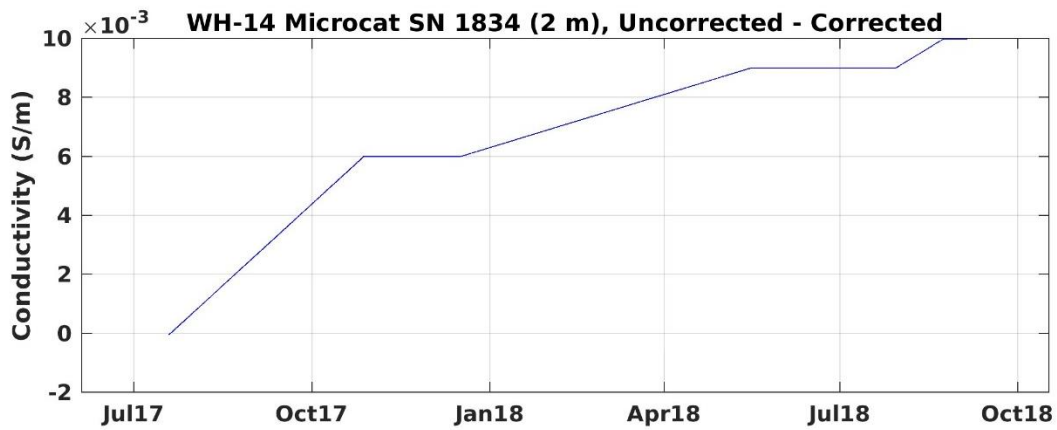
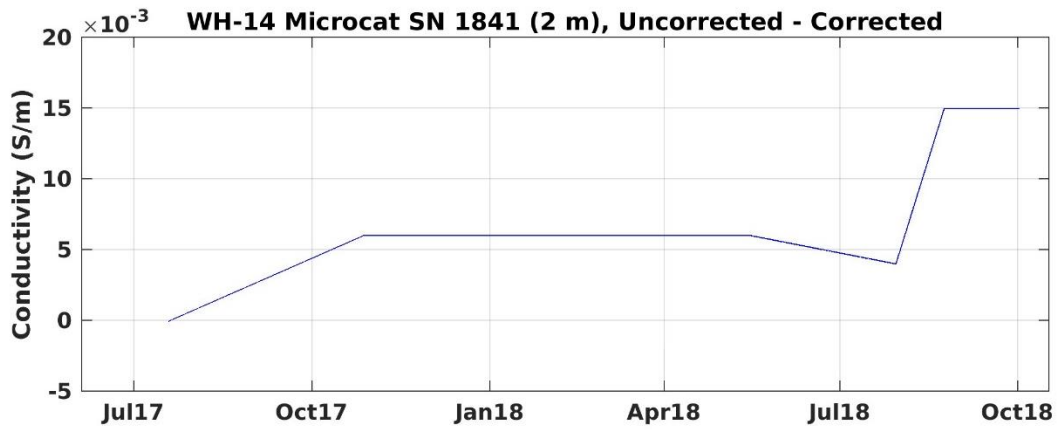


Figure V-8. Conductivity sensor corrections for MicroCATs from 2 to 7 meters during WHOTS-14.

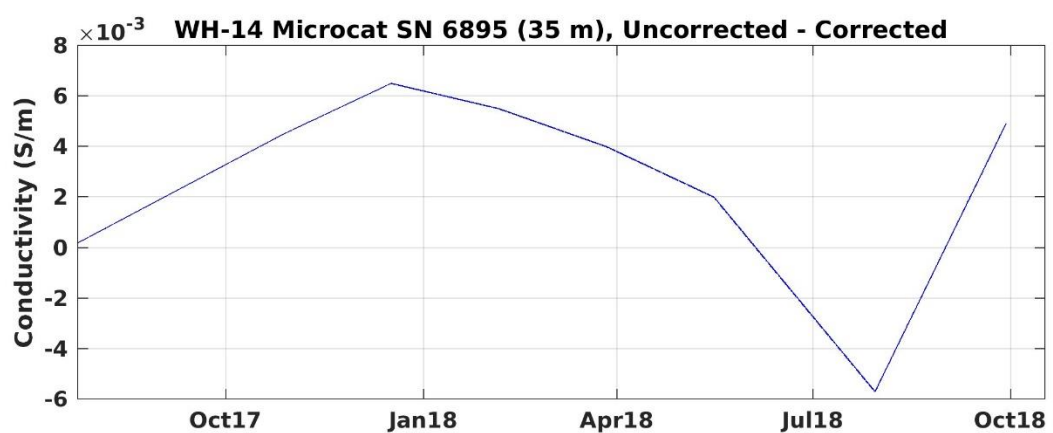
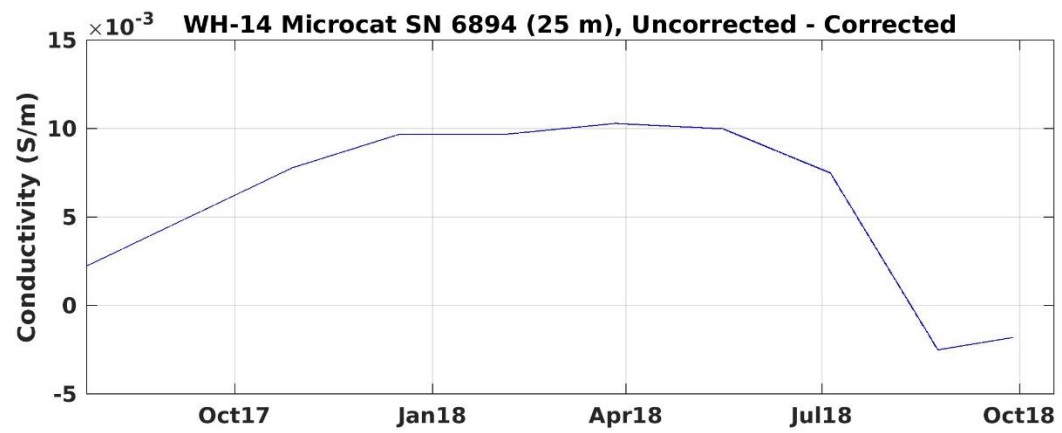
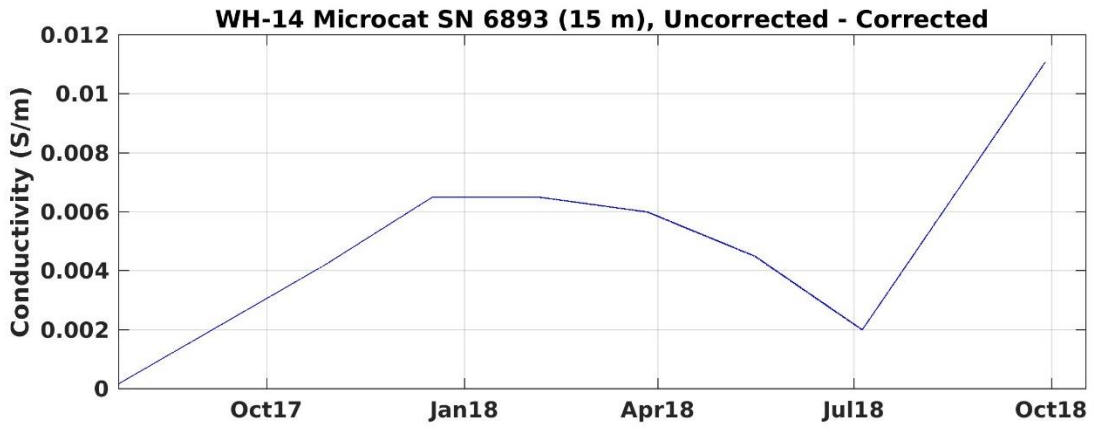


Figure V-9. Conductivity sensor corrections for MicroCATs from 15 to 35 meters during WHOTS-14.

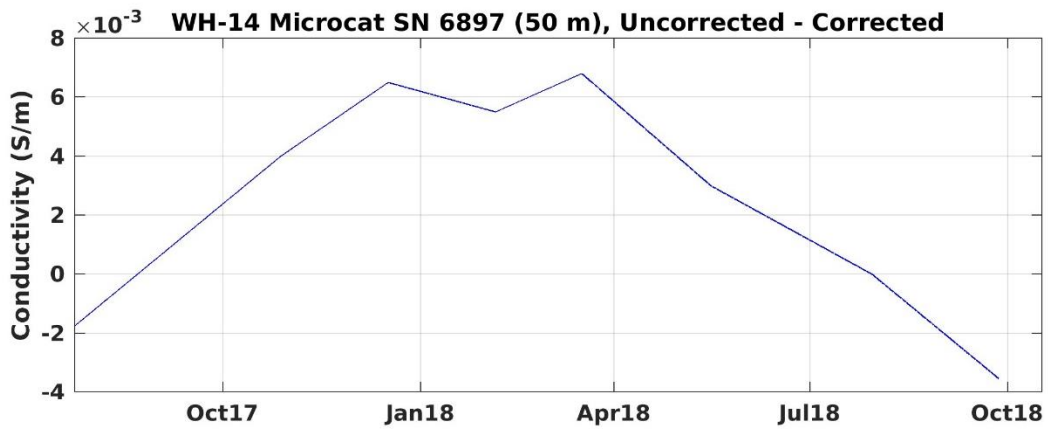
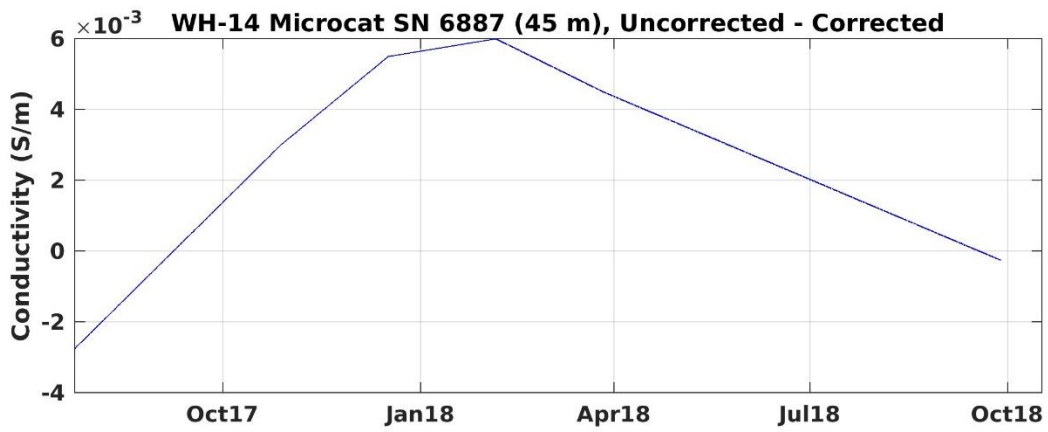
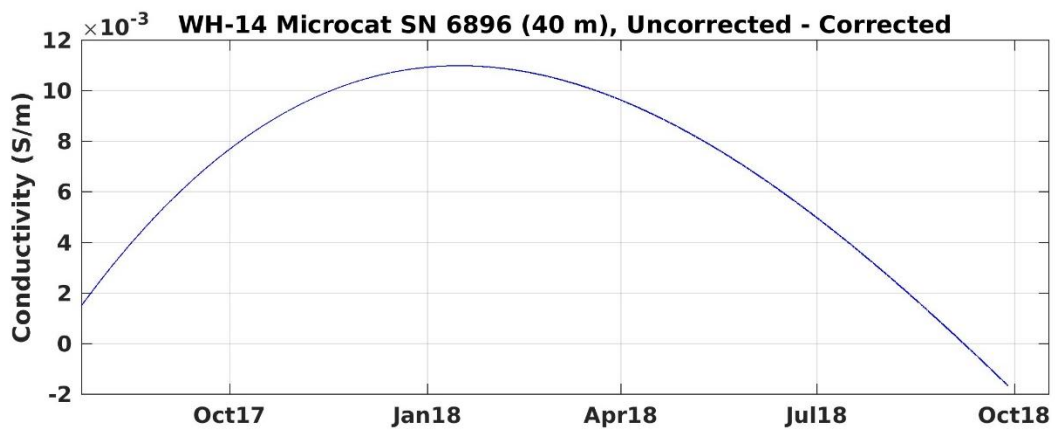


Figure V-10. Conductivity sensor corrections for MicroCATs from 40 to 50 meters during WHOTS-14

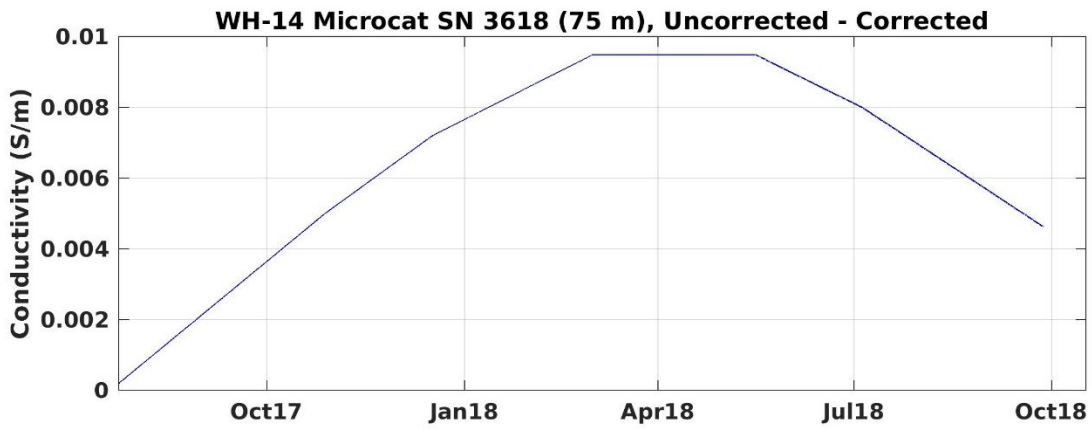
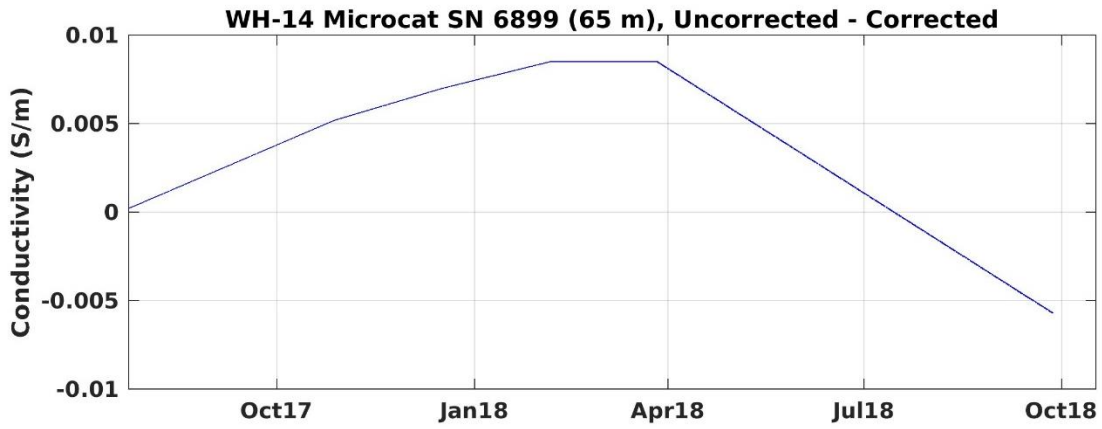
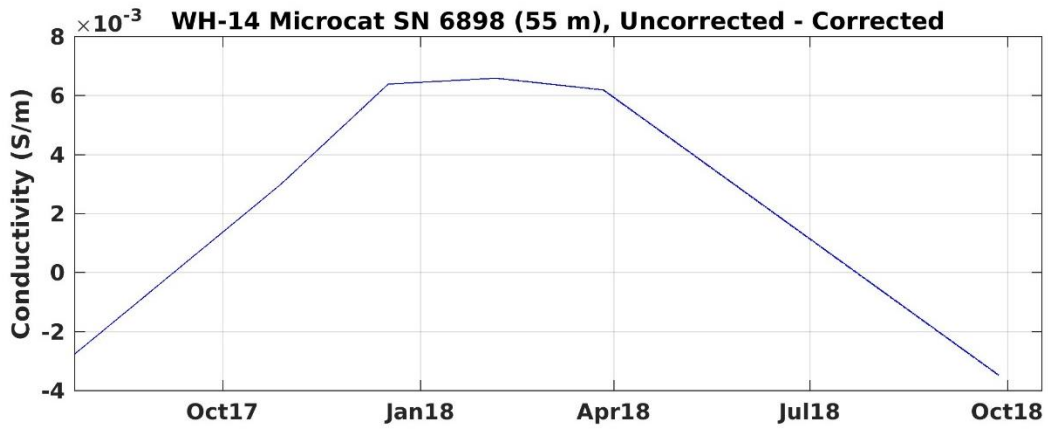


Figure V-11. Conductivity sensor corrections for MicroCATs from 55 to 75 meters during WHOTS-14

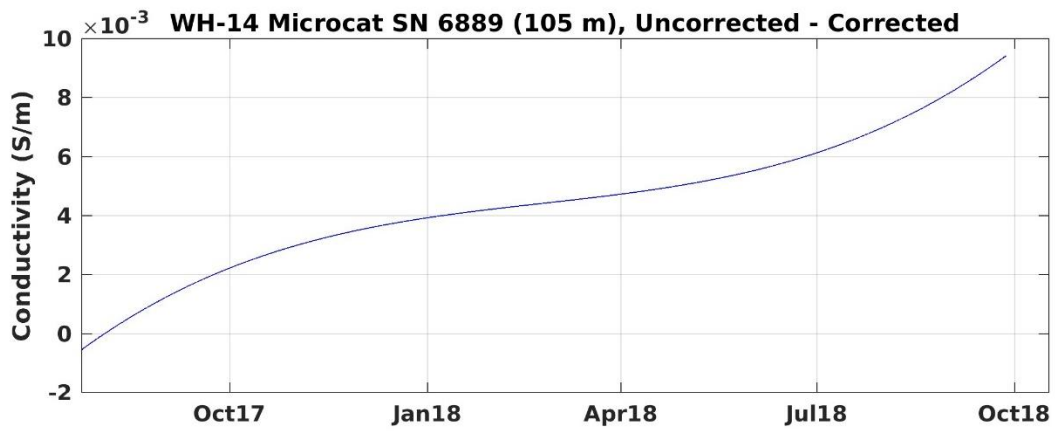
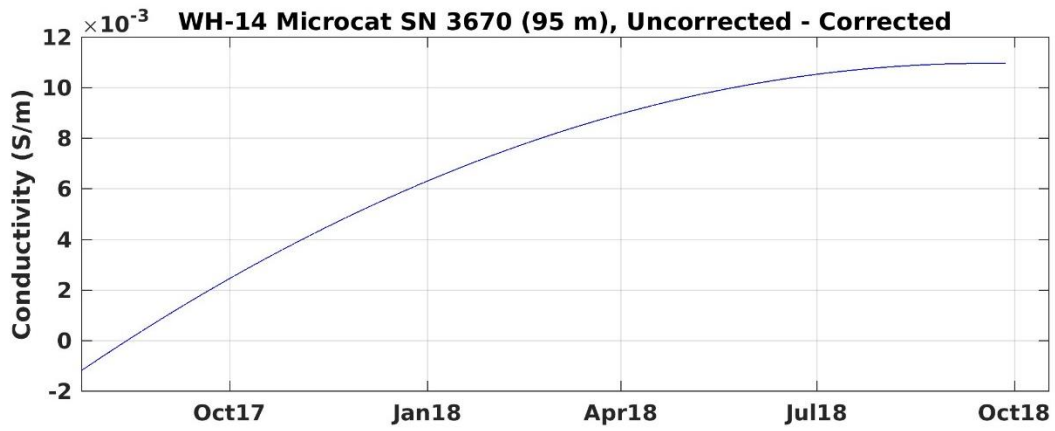
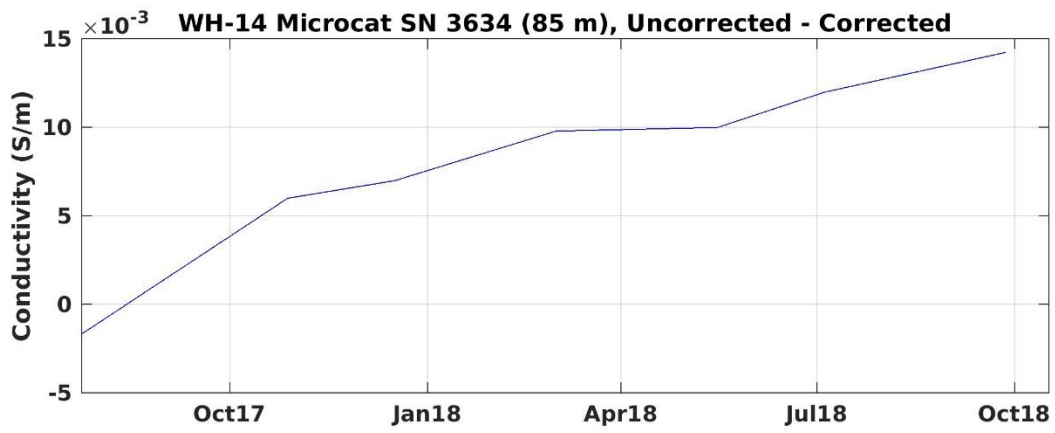


Figure V-12. Conductivity sensor corrections for MicroCATs from 85 to 105 meters during WHOTS-14

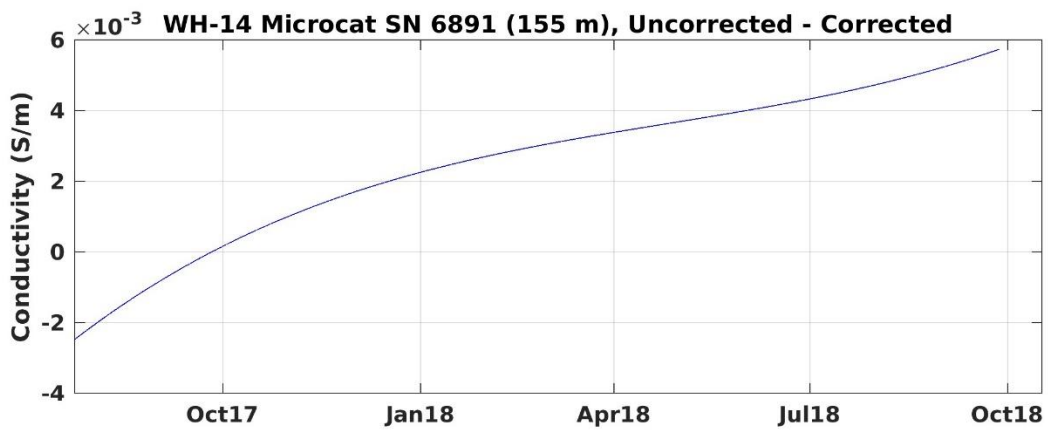
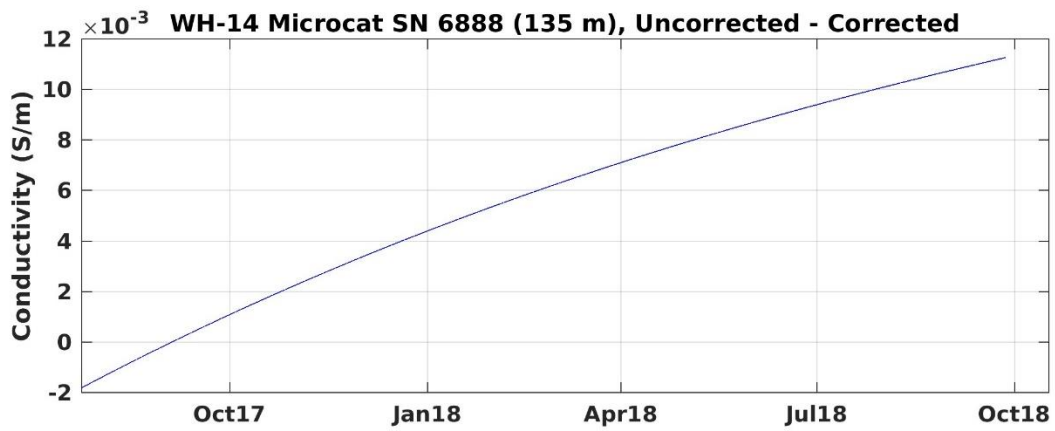
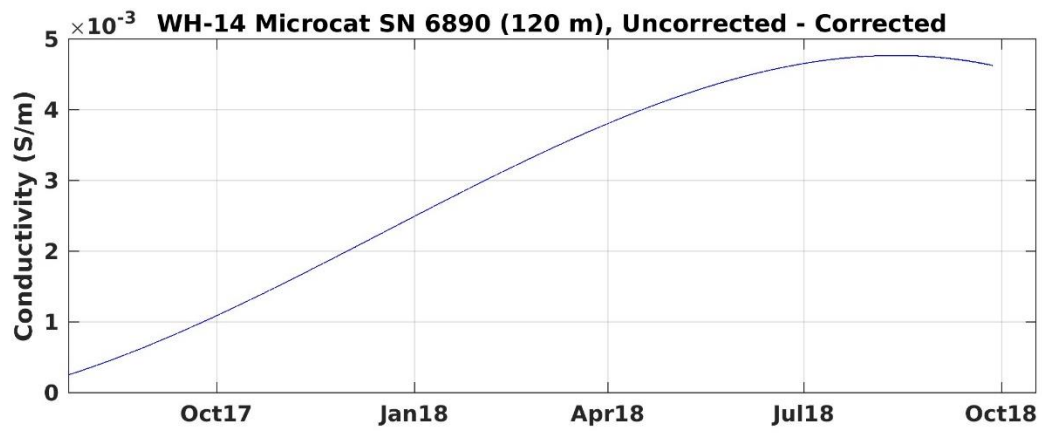


Figure V-13. Conductivity sensor corrections for MicroCATs from 120 to 155 meters during WHOTS-14

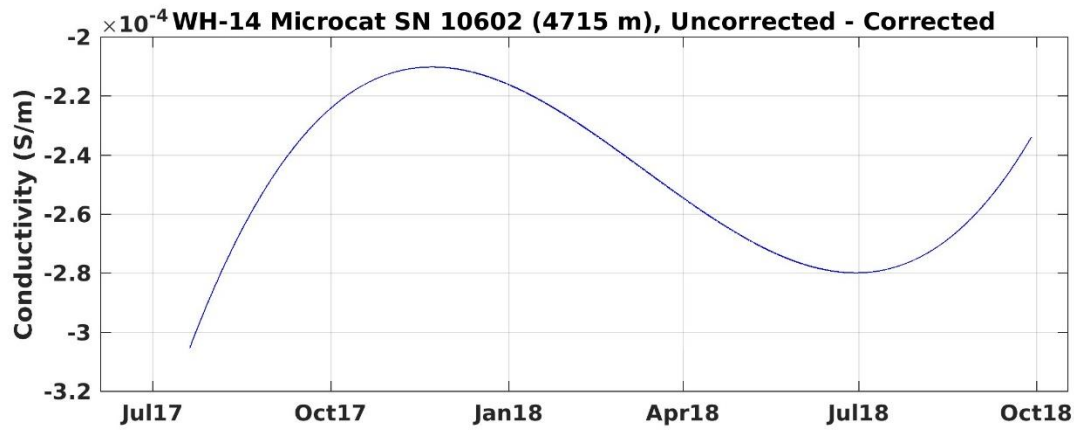
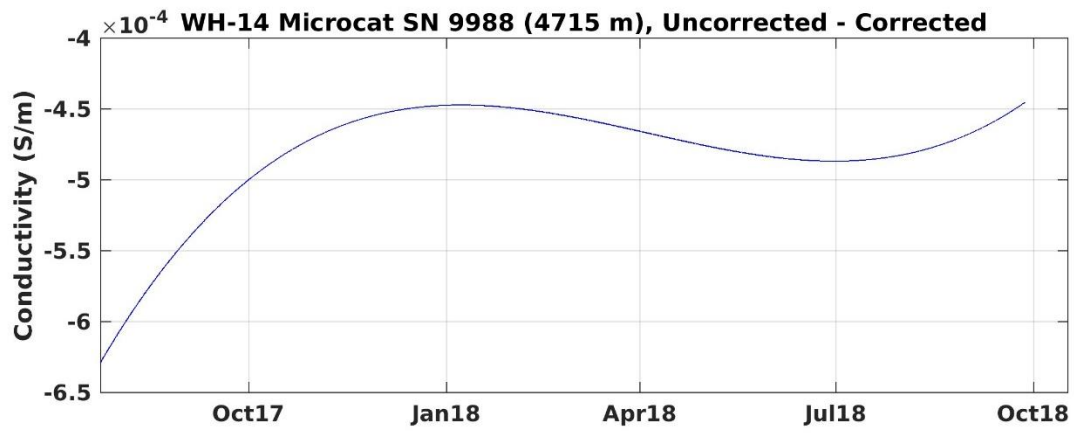


Figure V-14. Conductivity sensor corrections for MicroCATs at 4715 meters during WHOTS-14

## B. Acoustic Doppler Current Profiler

Two TRDI broadband Workhorse Sentinel ADCP's were deployed on the WHOTS-14 mooring. A 600 kHz ADCP was deployed at 47.5 m depth in the upward-looking configuration, and a 300 kHz ADCP was deployed at 125 m, also in the upward-looking configuration. The instruments were installed in aluminum frames along with an external battery module to provide sufficient power for the intended period of deployment. The four ADCP beams were angled at 20° from the vertical line of the instrument. The 300 kHz ADCP was set to profile across 30 range cells of 4 m with the first bin centered at 6.2m from the transducer. The 600 kHz ADCP was set to profile across 25 range cells of 4 m with the first bin centered at 3.11m from the transducer. The specifications of the instrument are shown in Table V-3.

Table V-3. Specifications of the ADCP's used for the WHOTS-14 mooring.

Instrument	Description
ADCP	<i>TRDI Workhorse Sentinel, 300KHz</i> Model: WHS300-I-UG86; Serial Number: 4981 <i>TRDI Workhorse Sentinel, 600KHz</i> Model: WHS600-I; Serial Number: 1825
Battery module	<i>300 kHz</i> Model: WH-EXT-BATTERY; Serial Number: 3169 <i>600 kHz</i> Model: WH-EXT-BCL; Serial Number: 182

### 1. Compass Calibrations

#### Pre-Deployment

Before the WHOTS-14 deployment, field calibration of the internal ADCP compass was performed at the soccer field of the University of Hawai'i at Manoa on June 28<sup>th</sup>, 2017, for both the 300 kHz and the 600 kHz instruments. Each instrument was mounted in the deployment cage along with the external battery module and was located away from potential sources of magnetic field disturbances. The ADCP was mounted to a turntable, which was aligned with the magnetic north using a surveyor's compass. Using the built-in RDI calibration procedure, the instrument was tilted in one direction between 10 and 20 degrees and then rotated through 360 degrees at less than 5 ° per second. The ADCP was then tilted in a different direction, and a second rotation made. Based on the results from the first two rotations, calibration parameters are temporarily loaded, and the instrument, tilted in a third direction is rotated once more to check the calibration. Results from each pre-deployment field calibration are shown in Table V-4 and Table III-5 (Figure V-15 and Figure V-16).

Table V-4. Results from the WHOTS-14 pre-deployment 300 kHz ADCP compass field calibration procedure.

300 kHz (SN 4981)	Single Cycle Error (°)	Double Cycle Error (°)	Largest Double + Single Cycle Error (°)	RMS of 3 <sup>rd</sup> Order and Higher + Random Error (°)	Overall Error (°)	Pitch Mean and Standard Deviation (°)	Roll Mean and Standard Deviation (°)
Before Calibration	2.73	0.24	2.98	0.25	2.73	1.61±1.08	0.26±0.78
After Calibration	0.85	0.61	1.47	0.35	1.26	-17.12 ± 1.05	0.06 ± 1.29

Table V-5. Results from the WHOTS-14 pre-deployment 600 kHz ADCP compass field calibration procedure.

600 kHz (SN 1825)	Single Cycle Error (°)	Double Cycle Error (°)	Largest Double + Single Cycle Error (°)	RMS of 3 <sup>rd</sup> Order and Higher + Random Error (°)	Overall Error (°)	Pitch Mean and Standard Deviation (°)	Roll Mean and Standard Deviation (°)
Before Calibration	2.50	0.57	3.07	0.32	2.61	0.46 ± 0.83	10.73 ± 0.54
After Calibration	2.08	0.44	2.52	0.23	2.15	4.12 ± 0.44	0.08 ± 0.56

## Post-Deployment

After the WHOTS-14 mooring was recovered, the performance of the ADCP compass was tested at the soccer field of the University of Hawai'i at Manoa on November 27<sup>th</sup>, 2018, with an identical compass calibration procedure as during the pre-deployment calibration. Results from the WHOTS-14 post-deployment ADCP compass field calibration procedure are listed in Table V-6 and Table V-7. (Figure V-15 and Figure V-16).

Table V-6. Results from the WHOTS-14 post-deployment 300kHz ADCP compass field calibration procedure.

300 kHz (SN 4981)	Single Cycle Error (°)	Double Cycle Error (°)	Largest Double + Single Cycle Error (°)	RMS of 3 <sup>rd</sup> Order and Higher + Random Error (°)	Overall Error (°)	Pitch Mean and Standard Deviation (°)	Roll Mean and Standard Deviation (°)
After Calibration	1.20	0.20	1.40	0.14	1.22	1.64 ± 0.43	0.1 ± 0.42

Table V-7. Results from the WHOTS-14 post-deployment 600kHz ADCP compass field calibration procedure.

600 kHz (SN 1825)	Single Cycle Error (°)	Double Cycle Error (°)	Largest Double + Single Cycle Error (°)	RMS of 3 <sup>rd</sup> Order and Higher + Random Error (°)	Overall Error (°)	Pitch Mean and Standard Deviation (°)	Roll Mean and Standard Deviation (°)
After Calibration	2.96	0.40	3.36	0.12	3.06	-2.22 ± 0.74	0.51 ± 0.53

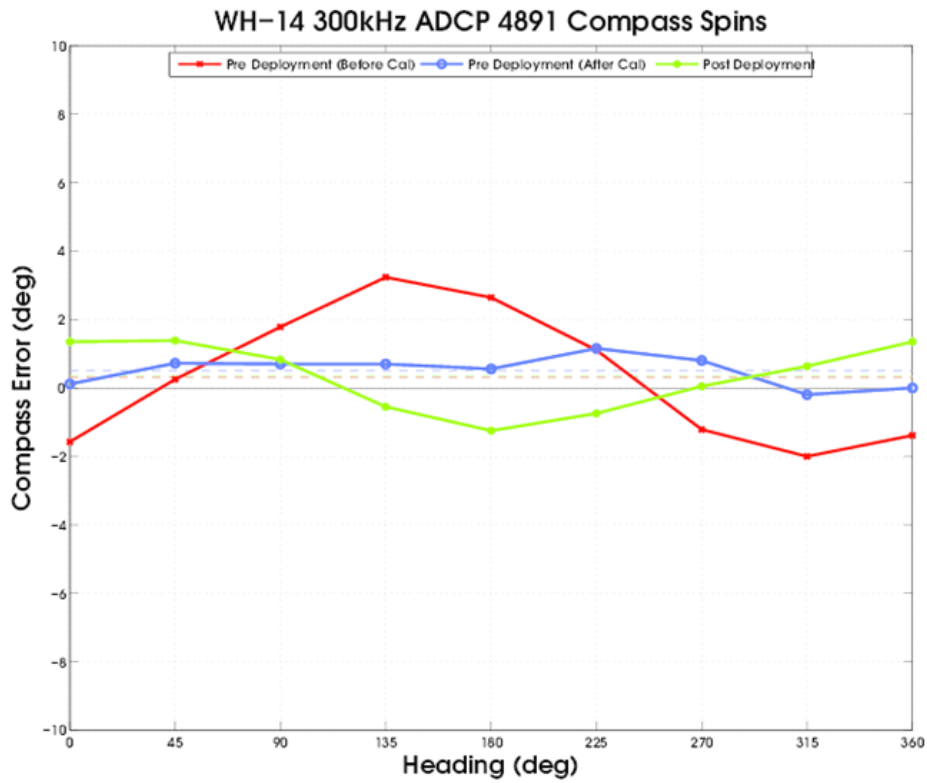


Figure V-15. Results of the post-cruise compass calibration, conducted November 27th, 2018, on ADCP SN 4891 at the University of Hawai'i at Manoa.

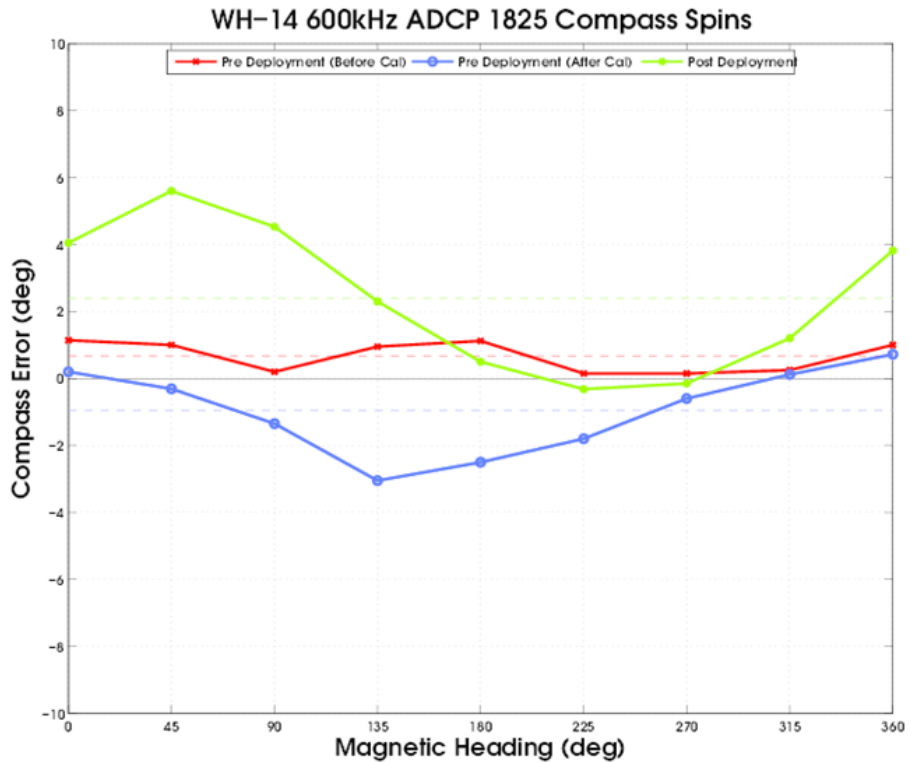


Figure V-16. Results of the post-cruise compass calibration, conducted November 27th, 2018, on ADCP SN 1825 at the University of Hawai'i at Manoa.

## **2. ADCP Configurations**

Individual configurations for the two ADCP's on the WHOTS-14 mooring are detailed in Section VIII.A and VIII.B. The salient differences for each of the ADCP's are summarized below.

### **300 kHz (125m)**

The ADCP, set to a beam frequency of 300 kHz, was configured in a burst sampling mode consisting of 40 pings per ensemble to resolve low-frequency wave orbital motions. The interval between each ping was 4 seconds, so the ensemble length was 160 seconds. The interval between ensembles was 10 minutes. Data were recorded in earth coordinates, with a heading bias of 9.61° E due to magnetic declination. False targets, usually fish, were screened by setting the threshold maximum to 70 counts. Velocity data were rejected if the difference in echo intensity among the four beams exceeded this threshold.

### **600 kHz (47.5m)**

The ADCP, set to a beam frequency of 600 kHz, was configured in a burst sampling mode consisting of 80 pings per ensemble. The interval between each ping was 2 seconds, so the ensemble length was also 160 seconds. The interval between ensembles was 10 minutes. Data were recorded in earth coordinates with a heading bias of 9.61° E. The threshold maximum was also set to 70 counts. Velocity data were rejected if the difference in echo intensity among the four beams exceeded this threshold.

## **3. ADCP data processing procedures**

Binary files output from the ADCP were read and converted to MATLAB™ binary files using scripts developed by Eric Firing's ADCP lab (<http://current.soest.hawaii.edu>). The beginning of the raw data files was truncated to a time after the mooring anchor was released to allow time for the anchor to reach the seabed and for the mooring motions that follow the impact of the anchor on the seafloor to dissipate. The pitch, roll, and ADCP temperature were examined to pick reasonable times that ensured good data quality but without unnecessarily discarding too much data (Figure V-15 and Figure V-16). Truncation at the end of the data files was chosen to be the ensemble before the time that the acoustic release signal was sent to avoid contamination due to the ascent of the instrument. The times of the first ensemble from the raw data, deployment, and recovery time, along with the times of the truncated records of both deployments, are shown in Table V-8.

Table V-8. ADCP record times (UTC) during WHOTS-14 deployment

Activities		300 kHz	600 kHz
Raw file	Beginning	7/24/2017 00:00	7/26/17 00:00
	End	9/30/2018 00:20	9/30/18 01:40
Deployment and Recovery	In water	6/27/2017 19:55	6/27/17 19:30
	Anchor over	7/28/2017 02:19	7/28/17 02:19
	Release fired	9/26/2018 16:57	9/26/18 16:57
	on deck	9/27/2018 00:19	9/27/18 00:34
Processed	Beginning	7/24/2017 00:00	7/26/17 00:00
	End	9/30/2018 00:09	9/30/18 01:29

### ADCP Clock Drift

Upon recovery, a spike was produced in the ADCP data by gently rubbing each instrument's transducer by hand for 20 seconds (see Sect. III, Table III-5) to compare the ADCP clocks with the ship's time server. It was found that for 300 kHz (SN 4891) ADCP, the clock on the instrument was fast by less than 9 minutes. The clock on the 600 kHz (SN 1825) was fast by less than 3 minutes. Past deployments of the ADCP's suggest a 9-minute difference is not unusual. Since the drift represents just one ensemble out of a total of over 58,000, no corrections were made. However, this drift may be significant if the data are used for time-dependent analysis, such as tidal or spectrum analysis. A drift correction needs to be applied in those cases.

### Heading Bias

As mentioned in the ADCP configuration section, the data were recorded in the earth coordinates. A heading bias, the angle between magnetic north and true north, can be included in the setup to obtain output data in true-earth coordinates. Magnetic variation was obtained from the National Geophysical Data Center 'Geomag' calculator. (<https://www.ngdc.noaa.gov/geomag/calculators/magcalc.shtml#declination>). For a yearlong deployment, a constant value is acceptable because the change in declination is small, approximately  $-0.02^{\circ} \text{ year}^{-1}$  at the WHOTS location. A heading bias of  $9.61^{\circ}$  was entered in the setup of the WHOTS-14 ADCP's.

### Speed of sound

Due to the constant of proportionality between the Doppler shift and water speed, the speed of sound needs only be measured at the transducer head (Firing, 1991). The sound speed used by the ADCP is calculated using a constant value of salinity (35) and the temperature recorded by the transducer temperature sensor of the ADCP. Using CTD profiles close to the mooring during HOT cruises, HOT-295 to HOT-305, and from the WHOTS deployment/recovery cruises, the mean salinity at 125 dbar was 35.13 while the mean salinity at 47.5 dbar was 34.98. The mean ADCP temperature at 125 dbar was  $21.93^{\circ}\text{C}$  and  $25.59^{\circ}\text{C}$  at 47.5 dbar (Figure V-17 through Figure V-19 ). The maximum associated mean sound speed variability at 47.5 and 125 dbar is

less than  $10 \text{ m s}^{-1}$ , and  $3 \text{ m s}^{-1}$ , respectively, which represents a change of less than 0.7% and 0.2% respectively, so no correction was made.

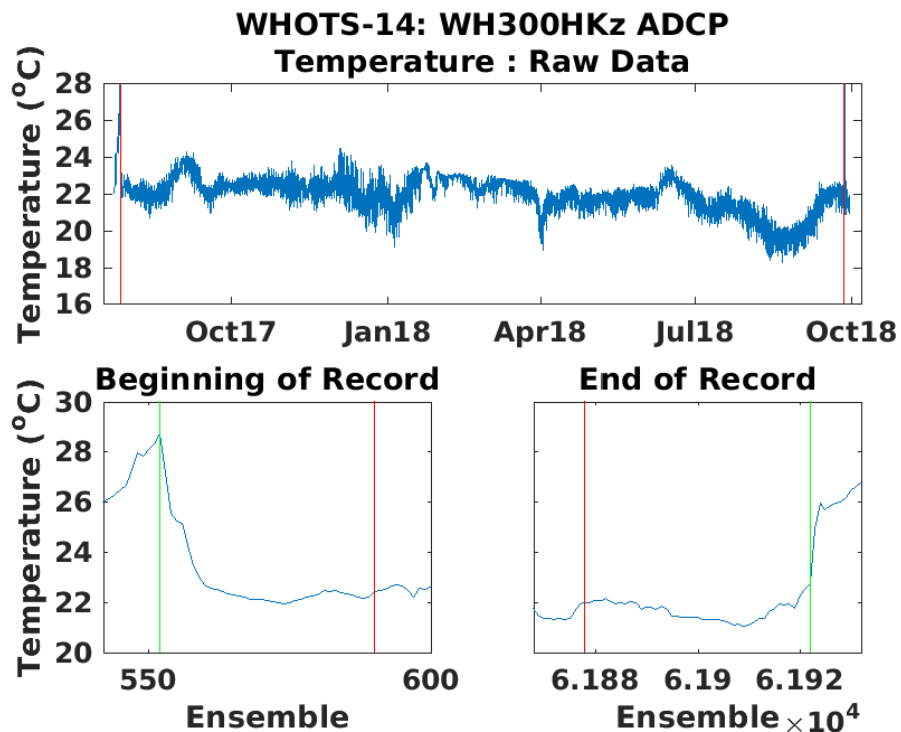


Figure V-17. Temperature record from the 300 kHz ADCP during WHOTS-14 mooring (top panel). The bottom panel shows the beginning and end of the record with the green vertical line representing the in-water time during deployment and out-of-water time for recovery. The red line represents the anchor release and acoustic release trigger for deployment and recovery, respectively.

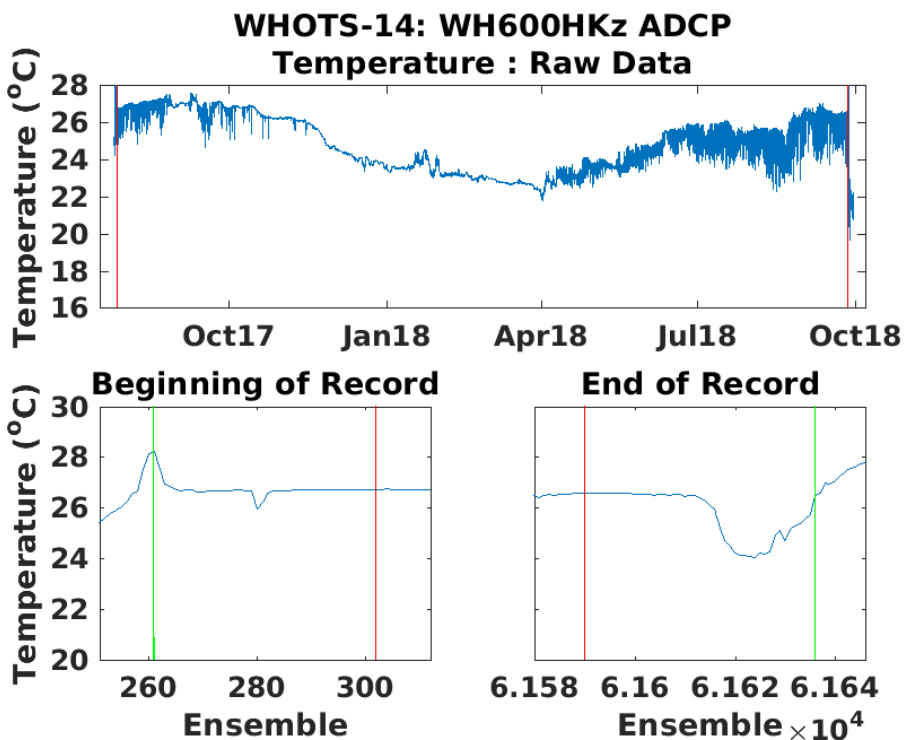


Figure V-18. Same as Figure V-17, but for the 600 kHz ADCP.

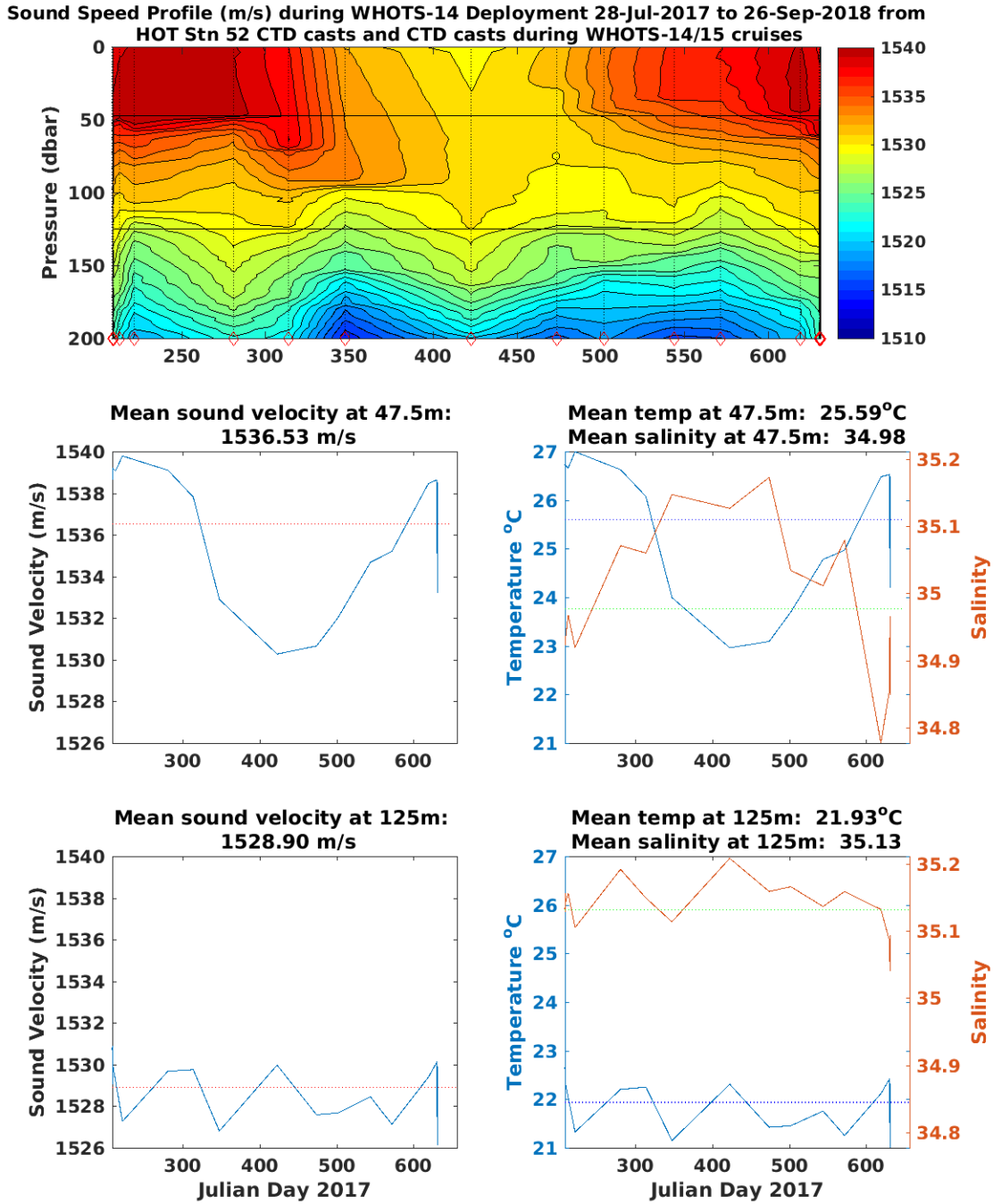


Figure V-19. Sound speed profile (top panel) during the deployment of the WHOTS-14 mooring from 2 dbar CTD data taken during regular HOT cruises and CTD profiles taken during the WHOTS-14 and -15 deployment cruises (individual casts marked with a red diamond). The bottom left panels to show the sound velocity at a depth of the ADCP's (47.5 m and 125 m), with the mean sound velocity indicated with a red line. The lower right panels show the temperature and salinity at each ADCP depth for the time series with the mean temperatures indicated with blue lines and mean salinity indicated with green lines.

## Quality Control

Quality control of the ADCP data involved the thorough examination of the velocity, instrument orientation, and diagnostic fields to develop the basis of the QC flagging procedures. Details of the methods used can be found in the WHOTS Data Report 1 (Santiago-Mandujano et al., 2007). The following QC procedures were applied to the WHOTS-14 deployment of ADCP data.

- 1) The first bin (closest to the transducer) is sometimes corrupted due to what is known as ringing. A period of time is needed for the sound energy produced during a transmit pulse at the transducer to dissipate before the ADCP can adequately receive the returned echoes. This “blanking interval” is used to prevent useless data from being recorded. If it is too short, signal returns can be contaminated from the lingering noise from the transducer. The blanking interval is expressed as a distance. The default value of 1.76 m was used for the 300 kHz ADCP, whereas an interval of 0.88 m was used for the 600 kHz ADCP. As a result, bin one was flagged and replaced with Not a Number (NaN) in the quality-controlled dataset (Figure V-20)

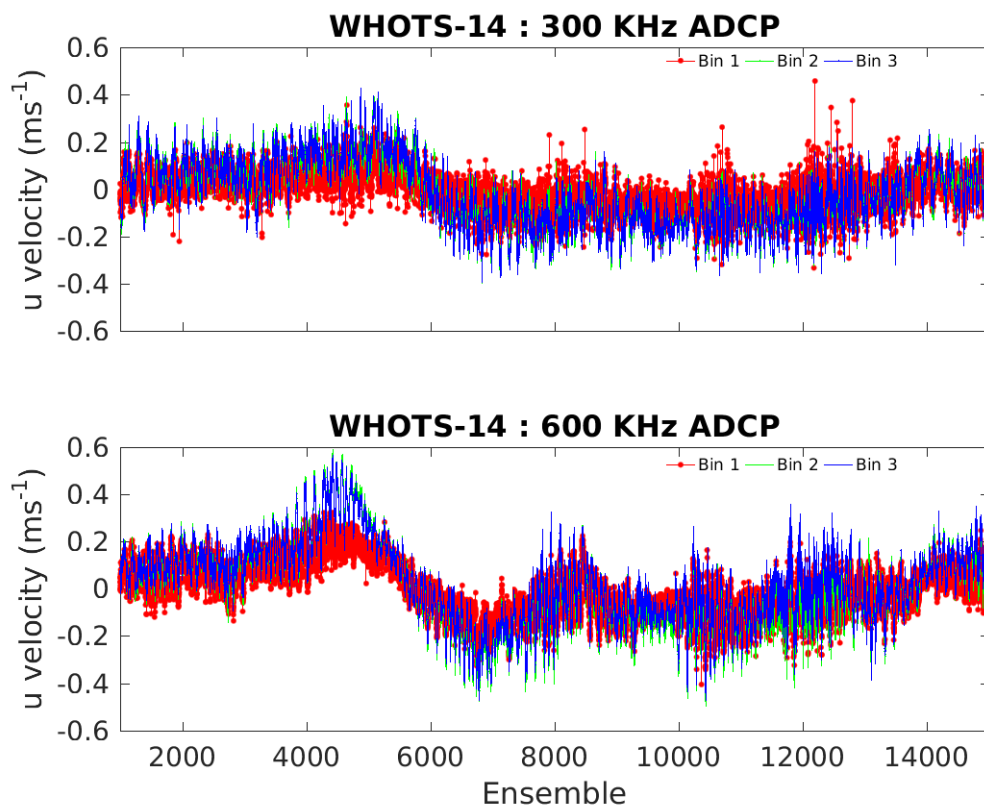


Figure V-20. Eastward velocity component for the 300 kHz (top panel) and the 600 kHz (bottom panel) ADCPs are showing the incoherence between depth bins 1 (red), 2 (green), and 3 (blue).

- 2) For an upward-looking ADCP with a beam angle of  $20^\circ$  within range of the sea surface, the upper 6% of the depth range is contaminated with sidelobe interference (Teledyne RD Instruments, 2011). This contamination is a result of the much stronger signal reflection from the sea surface than from scatters, overwhelming the sidelobe suppression of the transducer. Data quality is quantified using echo intensity, a measure of the strength of the backscattered echo for each depth cell. With distance from the transducer sensor, echo intensity is expected to decrease. Sharp increases in echo intensity indicate contamination from surface reflection. In practice, the majority of the data within the upper four bins (~14% of the vertical range) were flagged. These top four bins range from about 15 m up to the sea surface.
- 3) The Janus configuration of four beams (along with instrument orientation) is used to resolve currents into their component earth-referenced velocities, providing a second estimate of the vertical velocity. The scaled difference between these estimates is defined as the error velocity, and it is useful for assessing data quality. Error velocities with an absolute magnitude more significant than  $0.15 \text{ m s}^{-1}$  (value comparable to the standard deviation of observed horizontal velocities) were flagged and removed.
- 4) An indication of data quality for each ensemble is given by the “percent good” data indicator, which accompanies each beam for each bin. The use of the percent good indicator is determined by the coordinate transformation mode used during the data collection. For profiles transformed into earth coordinates, the percent good field shows the percentage of pings that could be used to create the earth coordinate velocities. The percent good fields show the percentage of data that was made using 4 and 3 beam solutions in each depth cell within an ensemble, and the percentage that was rejected as a result of failing one of the criteria set during the instrument setup (see Appendix 1: WHOTS-14 300 kHz ). Data were flagged when data in each depth cell within an ensemble made from 3 or 4 beam solutions was 20% or less.
- 5) Data were rejected using correlation magnitude, which is the pulse-to-pulse correlation (in ping returns) for each depth cell. Correlation magnitude represents a measure of how the shape of the received signal corresponds to the outgoing signal for each ping. For a given bin, if at least three of the beams exhibited a correlation magnitude more significant than 64 counts, then the profile can be transformed into earth coordinates. Low correlation magnitudes may be indicative of sudden changes in particle density, or sudden changes in ADCP tilt. More research is needed at this time into relationships between ADCP tilt and correlation magnitude. If any beam had a correlation magnitude of 20 counts or less, that data point was flagged.
- 6) Histograms of raw vertical velocity data and partially cleaned data from the ADCP [see Figure V-21 and Figure V-22] and the WHOTS Data Report 1 (Santiago-Mandujano et al., 2007)] showed vertical velocities larger than expected, some exceeding  $1 \text{ m s}^{-1}$ . Recall that the instruments’ burst sampling (4-second intervals for the 300 kHz and 2-second intervals for the 600 kHz, for 160 seconds every 10 minutes) was designed to minimize aliasing by occasional large ocean swell orbital motions (Section III), and therefore are not the source of these tremendous speeds in the data. These significant vertical speeds are possibly fish swimming in the beams based on the histograms of the partially cleaned data; depth cells with an absolute value of vertical velocity greater than  $0.3 \text{ m s}^{-1}$  were flagged.

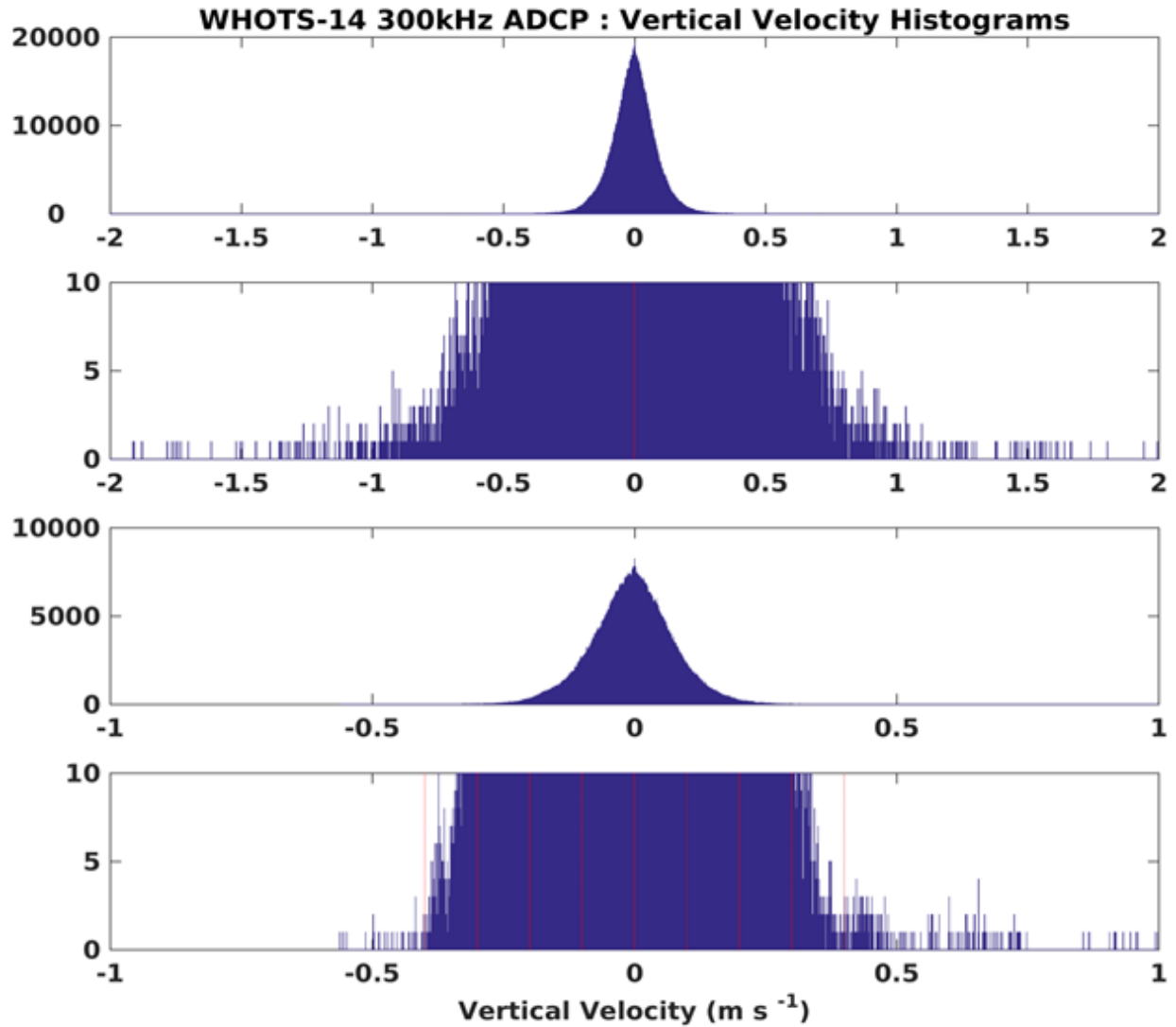


Figure V-21. Histogram of the vertical velocity of the 300 kHz ADCP for raw data (top panel) and enlarged for clarity (upper middle panel), and partial quality controlled data (lower middle panel) and enlarged for clarity (bottom).

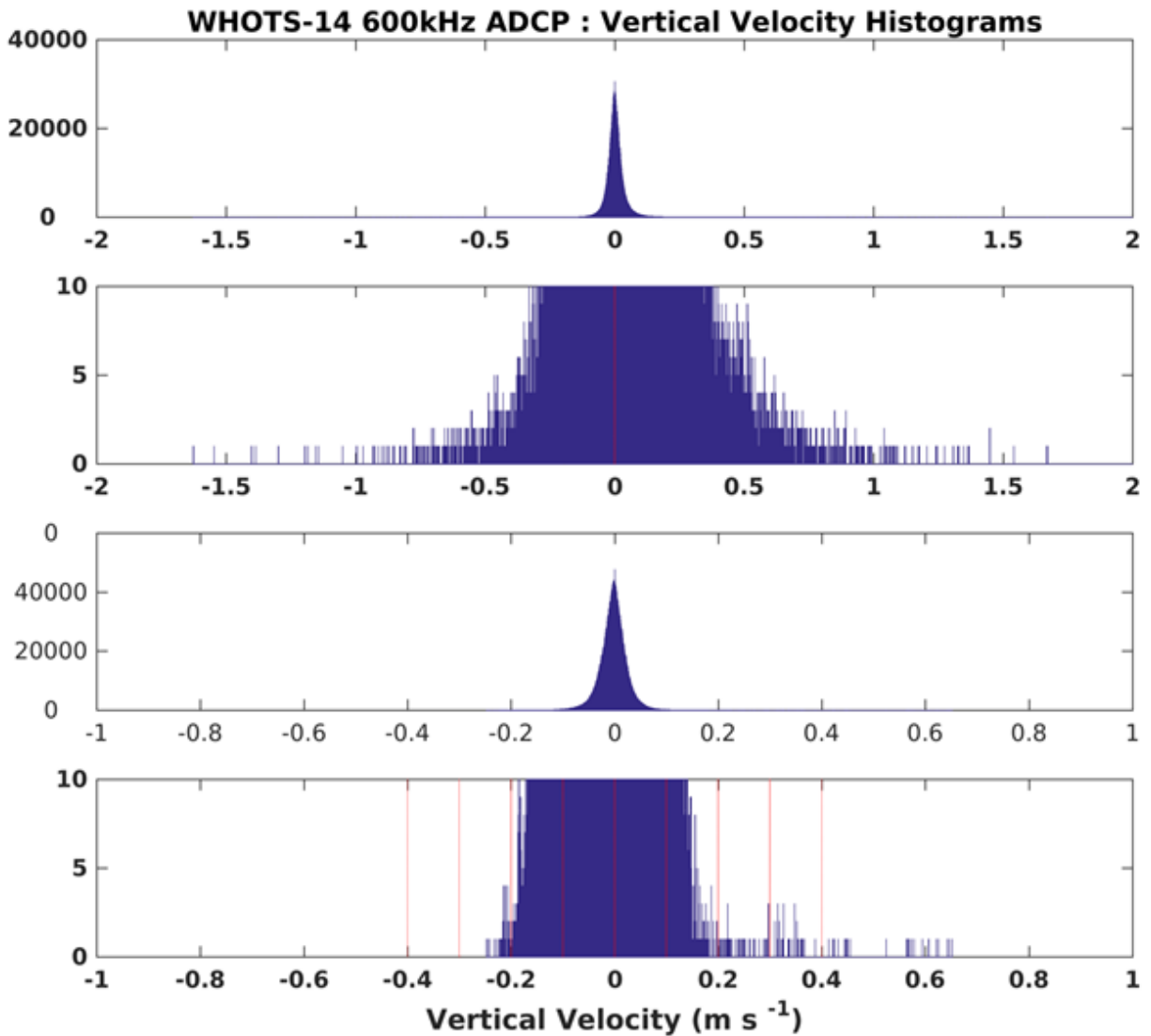


Figure V-22. Histogram of the vertical velocity of the 600 kHz ADCP for raw data (top panel) and enlarged for clarity (upper middle panel), and partial quality controlled data (lower central panel) and expanded for clarity (bottom).

- 7) A quality control routine known as ‘edgers’ identifies outliers in surface bins using a five-point median differencing method. The median velocity from surface bins was calculated for each ensemble, and then a five-point running median of the surface bin median was calculated. This last median was then compared to individual velocity observations in the surface bins, and those differing by greater than 0.48 m/s were flagged.
- 8) A 5-pole low pass Butterworth filter with a cutoff frequency of 1/4 cycles/hour was used upon the length of the time-series to isolate low-frequency flow for each bin independently. The low-frequency flow is then subtracted, giving a time series of high-frequency velocity component fluctuations for each bin. Data points were considered outliers when their values exceeded four standard deviations from the mean (for each bin) and were removed.

- 9) A median residual filter used a 7-point (70 minutes) median differencing method to define velocity fluctuations. A 7-point running median is calculated for each bin independently, and the result is subtracted out, giving time series of variations relative to the running median. Outliers higher than four standard deviations from the mean of the 7 points are flagged and removed for each bin.
  
- 10) Meticulous verification of all the quality control routines was performed through visual inspections of the quality-controlled velocity data. Two methods were utilized; time-series of u and v components for multiple bins were evaluated as well as individual vertical profiles. The time-series methodology involved inspecting u and v components separately, five bins at a time, over 600 ensembles (100 hours). Any instance showing one bin behaving erratically from the other four bins was investigated further. If it seemed that there could be no reasonable rationale for the erratic points from the identified bin, the points were flagged. The intent of the inspection of vertical profiles of u and v components was to find entire profiles that were not aligned with neighboring profiles. Thirty u and v profiles were stacked at a time and were visually inspected for any anomalous data.

### C. Vector Measuring Current Meter (VMCM)

Vector measuring current meters (VMCM) were deployed on the WHOTS-14 mooring at depths of 10 m and 30 m, serial numbers SN 42 and 68 respectively. VMCM data were processed by the WHOI/UOP group, and the record times are shown in Table V-9. Record times (UTC) for the VMCMs at 10 m and 30 m during the WHOTS-14 deployment Table V-9

*Table V-9. Record times (UTC) for the VMCMs at 10 m and 30 m during the WHOTS-14 deployment*

	<b>WHOTS-14</b>	
	<b>VMCM042</b>	<b>VMM068</b>
Deployment and recovery times	27-Jul-2017 18:25 27-Sept-2018 01:47	27-Jul-2017 18:10 27-Sept-2018 01:54

Daily (24 hours) moving averages of quality controlled 600 kHz ADCP data are compared to VMCM data interpolated to the ADCP ensemble times in the top panels of Figure V-23 through Figure V-26, and the difference is shown in the middle panels. The absolute value of the mean difference plus or minus one standard deviation is shown at the top of the middle panel. Velocities are not compared if greater than 80% of the ADCP data within a 24-hour average was flagged. The absolute value of mean differences for all deployments and both velocity components varied between 3 and 4 cm/s, with standard deviations between 2.2 and 3.5 cm/s. The VMCM data does not appear to degrade over time for any deployment. Propeller fouling would dampen measured VMCM velocity magnitudes, but a decrease in VMCM velocity magnitude compared to ADCP velocity magnitude with time is not observed.

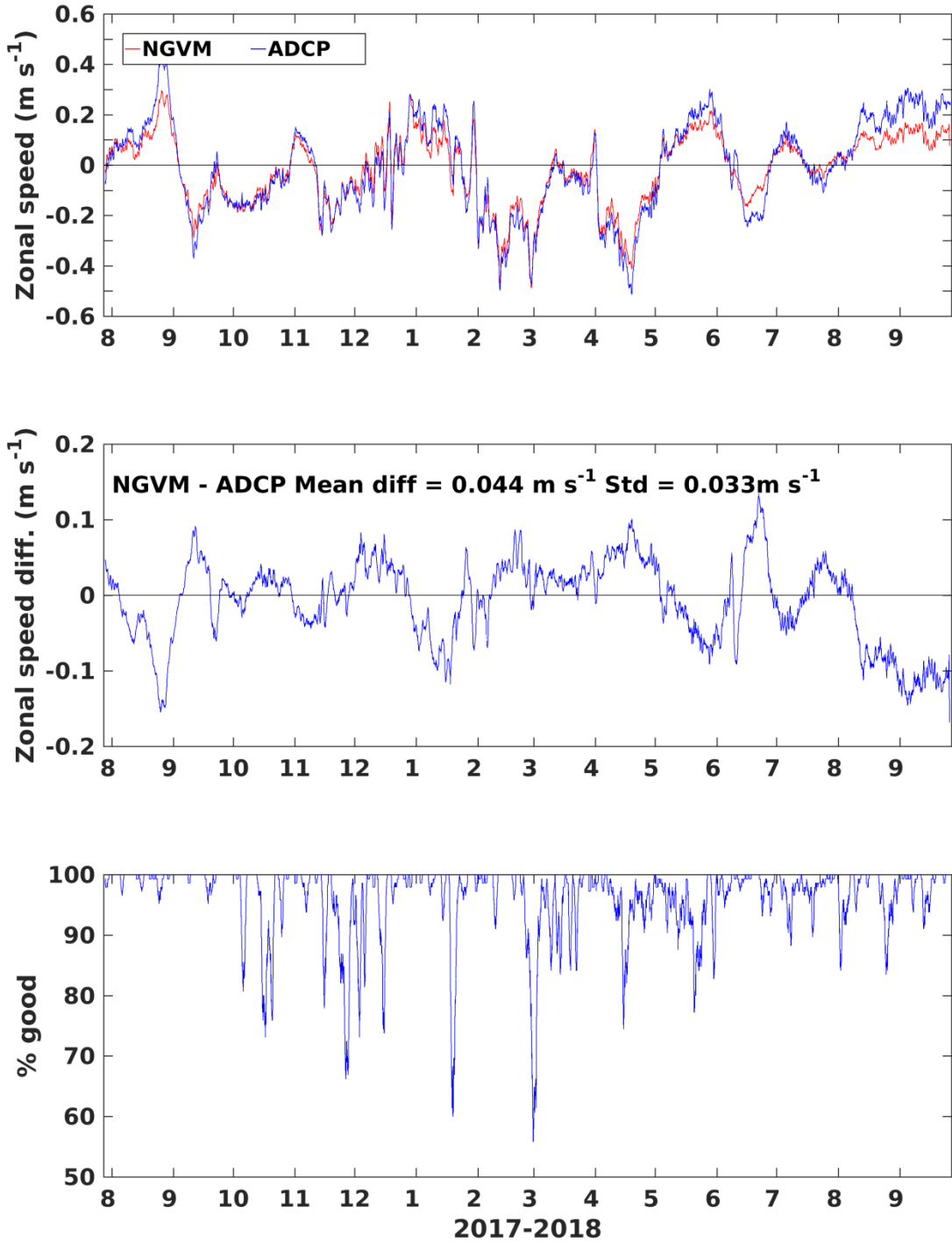


Figure V-23. A comparison of 30 m VMCM and ADCP U velocity for WHOTS-14. The top panel shows 24-hour moving averages of VMCM zonal (U) velocity at 30 m depth (red) and ADCP U velocity from the nearest depth bin to 30 m (30.22 m). The middle panel shows the U velocity difference, and the bottom panel shows the percentage of ADCP data within the moving average not flagged by quality control methods.

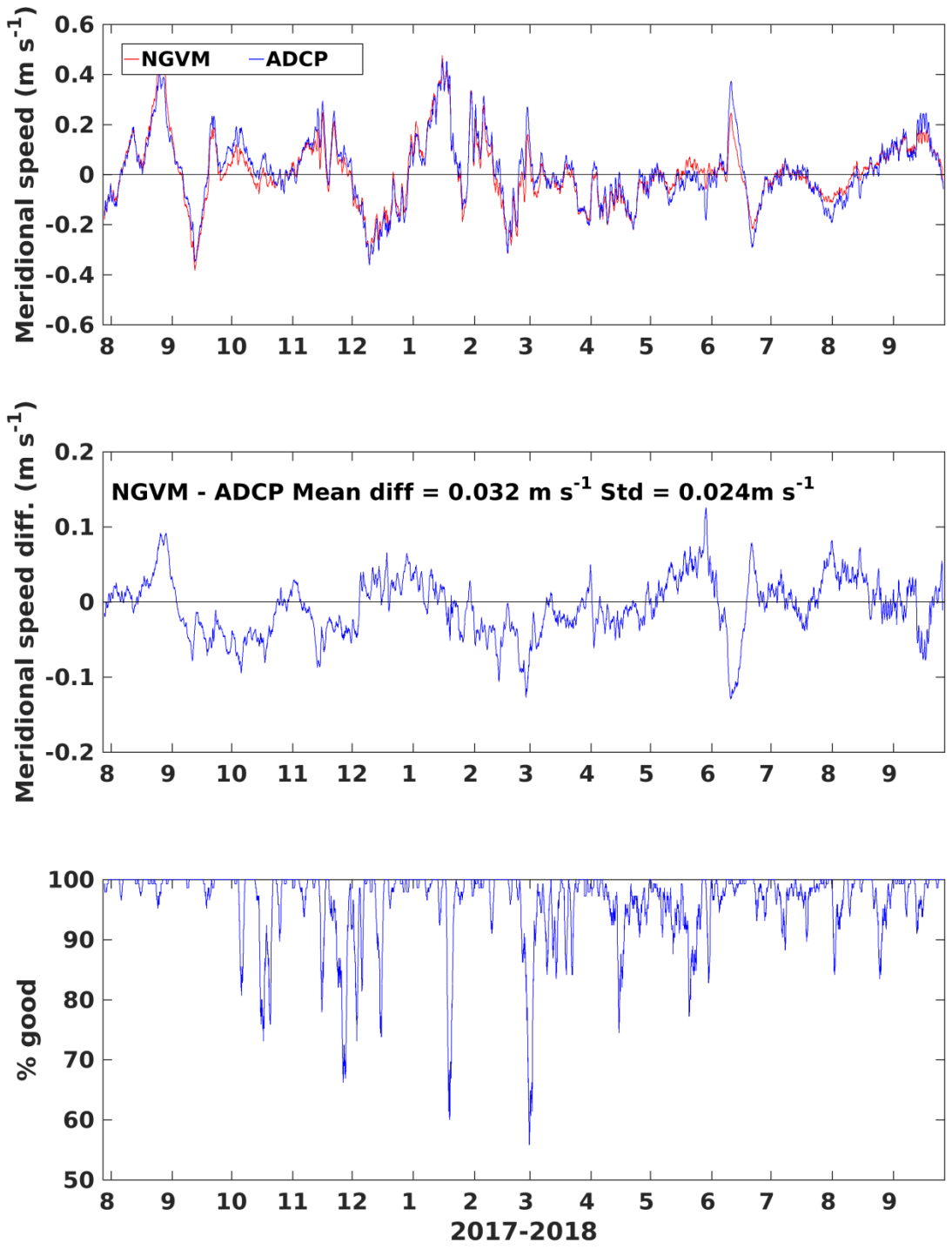


Figure V-24. Same as in Figure V-23 but for the meridional (V) velocity component.

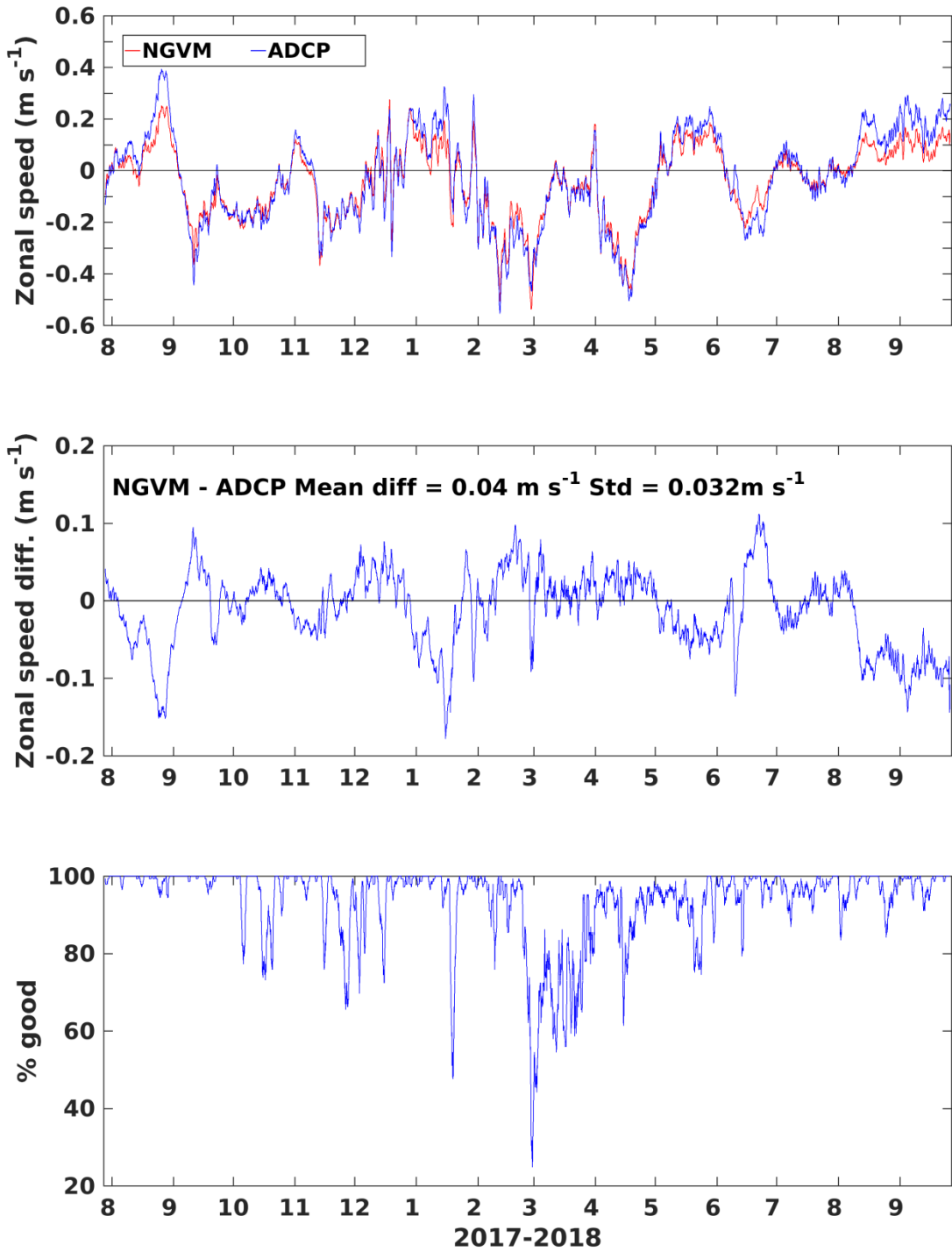


Figure V-25. Same as in Figure V-23 but for the 10 m VMCM.

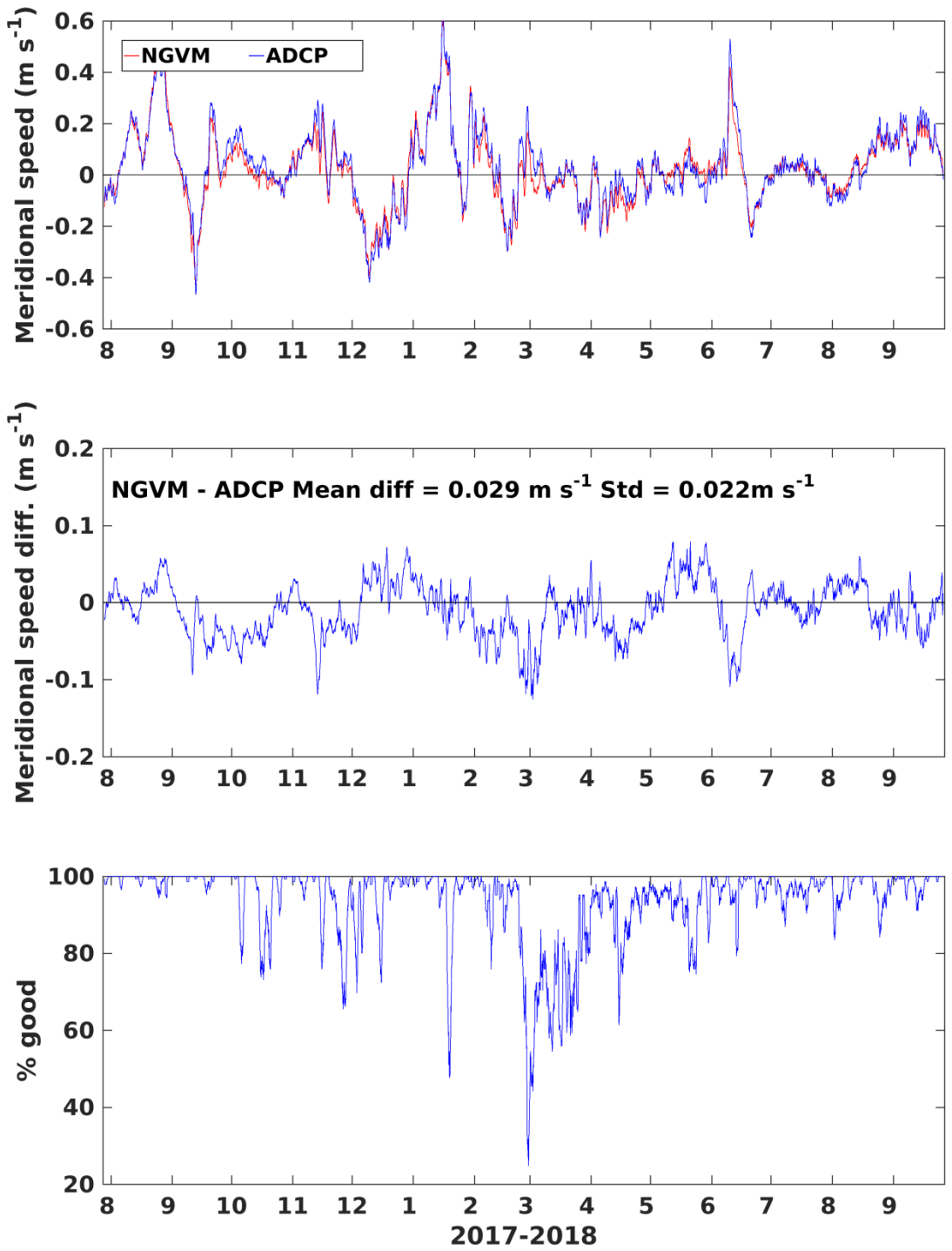


Figure V-26. Same as in Figure V-25, but for the meridional (V) velocity component.

## D. Global Positioning System Receiver and ARGOS Positions

Xeos Global Positioning System receiver (GPS) and ARGOS beacon were attached to the tower top of the buoy during the WHOTS-14 deployment (see Section III). Data returns from the receivers were high (Table V-10), but the GPS failed from November 17<sup>th</sup>, 2017 to April 4<sup>th</sup>, 2018 (Figure V-27). The reason for the failure of the GPS receiver is unknown.

Table V-10. GPS and ARGOS record times (UTC) during WHOTS-14

<b>WHOTS-14</b>	<b>Xeos GPS</b>	<b>ARGOS</b>
Raw file beginning	28-Jul-2017 02:49	28-Jul-2017 03:09
and end times	25-Sept-2018 23:33	27-Sept-2018 08:59

ARGOS positions were available during the WHOTS-14 deployment, and they provided additional information on the buoy's motion. ARGOS data were recorded at 1-minute intervals, although after removing invalid data, the median time interval was 16 minutes. Samples that were taken before mooring deployment were eliminated. Data outside the 2.5 nautical miles buoy watch circle radius were eliminated. The velocity magnitude was calculated, and positions that resulted in speeds higher than  $1 \text{ m s}^{-1}$  were removed. Data were interpolated onto a regular time grid to compute spectra.

For comparison, Figure V-27 shows the ARGOS buoy's positions together with the GPS positions during the WHOTS-14 deployment. The standard deviation of the difference between these two records is about 1 km.

The ARGOS positions of the WHOTS-14 buoy for the duration of the deployment are in Figure V-28. The color-coded positions are shown according to their data quality. Its distance from the satellite track determines the data quality. Data of better quality have a higher flag number three is for a distance less than 150 m, two is for a distance between 150 and 350 m, and one is for a distance between 350 and 1000 m. For the duration of the deployment, the buoy had a mean position of about 1.6 km from the anchor, with a standard deviation of about 500 m.

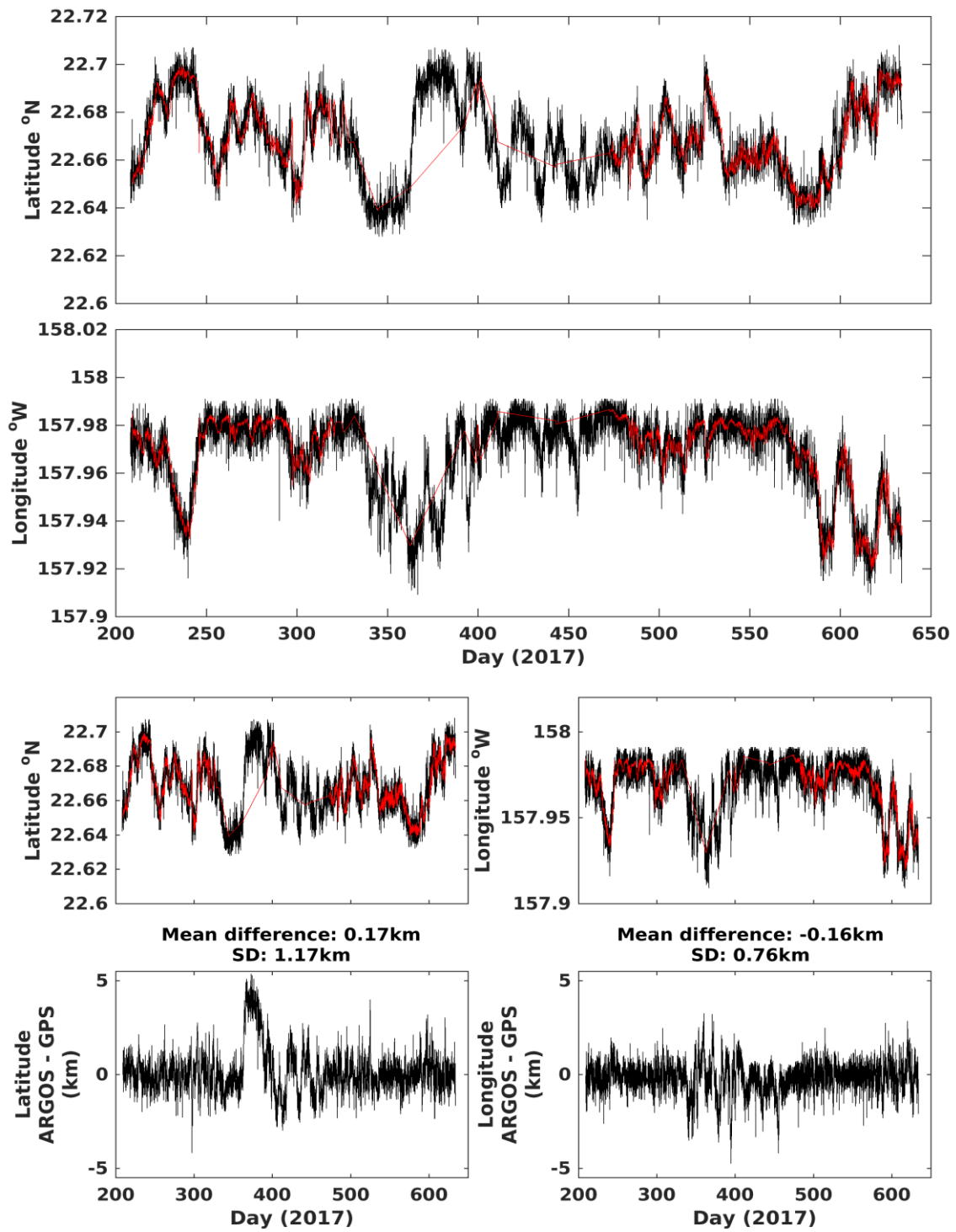


Figure V-27. WHOTS-14 buoy position from ARGOS data (black line), and GPS data (red line). The top and two middle panels show the latitude and longitude of the buoy. The bottom panel shows the difference between the GPS positions and the ARGOS positions interpolated to the GPS times.

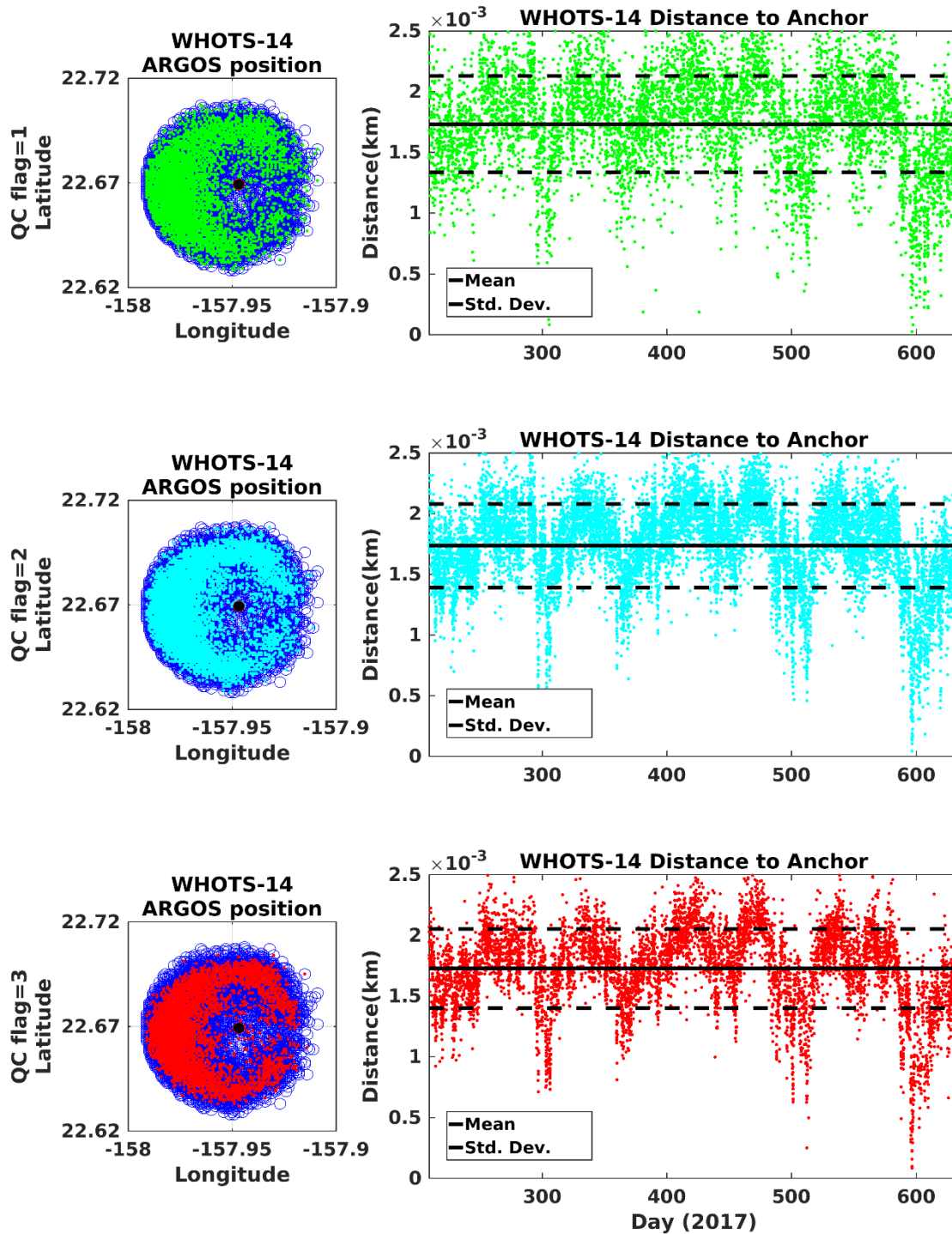


Figure V-28. WHOTS-12 buoy ARGOS positions (circles, left panels), and distance from its anchor (dots, right panels). The data are colored according to their quality control flag, 1: green, 2: light blue, 3: red. The black circle in the center of the left side panels is the location of the mooring's anchor. The black line in the right panel plots is the mean distance between the buoy and its anchor, and the dashed line is the mean plus one standard deviation.

## VI. Results

During the WHOTS-14 cruise (WHOTS-14 mooring deployment), Station ALOHA was under the influence of the eastern North Pacific high-pressure system, and the associated east-northeasterly trade winds. Moisture associated with former Tropical Cyclone Fernanda, which passed north of the islands during the days before the cruise was moving westward away from the state with a drier air-mass gradually filling in from the east at the beginning of the cruise. By July 27<sup>th</sup>, 2017, moisture associated with the remnants of former Tropical Cyclone Greg, passing 400 miles SE of Hilo started to bring increased humidity.

CTD casts conducted near the mooring site (Station 52) after the deployment (Figure VI-4 through Figure V-6, displayed a subsurface salinity maximum at 140 dbar, and a mixed layer nearly 60 m deep. Near-surface currents during the cruise were nearly 1 kt SSWward during transit to Station ALOHA, turning SWward and Wward upon arrival to Station ALOHA, and remained so for approximately four days, at which point currents swung counter-clockwise to the SE and dropped to an average of  $\sim 0.4 \text{ m s}^{-1}$ . There was a nearly stationary cyclonic eddy NW of ALOHA, suggesting a possible increasing geostrophic flow towards the SW.

During the WHOTS-15 cruise (WHOTS-14 mooring recovery), a low-pressure system north-northwest of Kauai was drawing up tropical moisture from the south, producing light south to southeasterly winds at Station ALOHA creating hot and humid weather conditions. A hurricane that developed SW of the Big Island was forecast to pass over French Frigate Shoals, where NOAA scientists were conducting observations. Consequently, science operations were stopped on September 28<sup>th</sup>, 2018, at 18:40, and the ship was re-routed to evacuate the observers and their equipment.

CTD casts conducted near the mooring site (Station 52) before the recovery (Figure VI-10 through Figure VI-12, displayed a subsurface salinity maximum at 130 dbar, and a mixed layer nearly 60 m deep. Near-surface currents during the cruise were nearly 1 kt NWward during transit to Station ALOHA, turning Nward and Eward upon arrival to Station ALOHA, and remained so for approximately five days. There was a nearly stationary cyclonic eddy east of ALOHA, suggesting a possible increasing geostrophic flow towards the E, NE.

The temperature MicroCAT records during the WHOTS-14 deployment (Figure V-17 through Figure VI-21 show noticeable seasonal variability in the upper 100 m, and a sudden increase during January 2017, apparent above 65 m; and a decrease between June and September 2018 evident in the instruments below 55 m. The salinity records (Figure VI-22 through Figure VI-26 do not show an apparent seasonal cycle, but instances of salinity decrease were recorded during September 2017 and June 2018, and to a minor extent in September 2018 by the instruments located above 135 m.

Figure VI-32 and Figure VI-33 show contours of the WHOTS-14 MicroCAT data in context with data from the previous 13 deployments. The seasonal cycle is evident in the temperature record, with record temperatures (higher than 26 °C) in the summer of 2004, and again in the summer of 2014, 2015 and 2017. Salinities in the subsurface salinity maximum were relatively low during the first 6 years of the record, only to increase drastically after 2008 through 2015,

with some episodes of lower salinity in mid-2011 and early 2012. The salinity maximum extended to near the surface in some instances in early 2010, 2011, late 2012-early 2013 and during February-March 2013. Salinities in the salinity minimum decreased after 2015, showing record low salinities above 100 m in 2016, 2017 and 2018. The low salinity observed in 2017 and 2018 in the MicroCAT time-series plots (Figure VI-22 through Figure VI-26) is apparent in Figure VI-32 and Figure VI-33. When plotted in  $\sigma_\theta$  coordinates (Figure VI-33), the salinity maximum seems to be centered roughly between 24 and 24.5  $\sigma_\theta$ .

Records from the WHOTS-14 MicroCATs (Figure VI-34) deployed near the bottom of the mooring (4715 m) detected temperature and salinity changes related to episodic ‘cold events’ apparently caused by bottom water moving between abyssal basins (Lukas et al., 2001). These events are being monitored by instruments at the ALOHA Cabled Observatory (ACO, Howe et al., 2011), a deep water observatory located at the bottom of Station ALOHA (about 6 nautical miles west from the WHOTS-14 anchor), since June 2011. Figure VI-34 shows temperature and salinity records from the WHOTS-14 MicroCATs superimposed on the ACO data. The MicroCAT data agreed with the temperature decrease and the salinity variability registered by ACO instruments during three cold events in August 2017, January 2018, and April 2018, during the WHOTS-14 period.

Figure VI-38 through Figure VI-40 show time series of the zonal, meridional, and vertical currents recorded with the moored ADCPs during the WHOTS-14 deployment. Figure VI-35 through Figure VI-37 shows contours of the ADCP current components in context with data from the previous deployments. Despite the gaps in the data, an apparent variability is seen in the zonal and meridional currents, apparently caused by passing eddies. On top of this variability, there have been periods of intermittent positive or negative zonal currents, for instance, during 2007-2008. The contours of vertical current component (Figure VI-37) show a transition in the magnitude of the contours near 47 m, indicating that the 300 kHz ADCP located at 126 m moves more vertically than the 600 kHz ADCP located at 47.5 m.

A comparison between the moored ADCP data and the shipboard ADCP data obtained during the WHOTS-14 cruise is shown in Figure VI-41 and Figure VI-42 and a similar comparison during the WHOTS-15 cruise is shown in Figure VI-43 and Figure VI-44. Some of the differences seen especially in the zonal component, maybe due to the mooring motion, which was not removed from the data. Comparisons between the available shipboard ADCP from HOT-295, -298, and -300 cruises and the mooring data are shown in Figure VI-45 and Figure VI-46.

The motion of the WHOTS-14 buoy was registered by the Xeos-GPS receiver, and its positions are plotted in Figure VI-48. The buoy was located west of the anchor for the majority of the deployment, except after June 2018, when it was east of it. The power spectrum of these data (Figure VI-49) shows extra energy at the inertial period (~31 hr). Combining the buoy motion with the tilt (a combination of pitch and roll) from the ADCP data (Figure VI-50), showed that the tilt increased as the buoy distance from the anchor WHOTS-14 increased. This was expected since the inclination of the cable increases as the buoy moves away from the anchor.

## A. CTD Profiling Data

Profiles of temperature, salinity, and potential density ( $\sigma_\theta$ ) from the casts obtained during the WHOTS-14 deployment cruise are presented in Figure VI-1 through Figure VI-6 together with the results of bottle determination of salinity. Figure VI-7 through Figure VI-11 shows the results of the CTD profiles during the WHOTS-15 cruise.

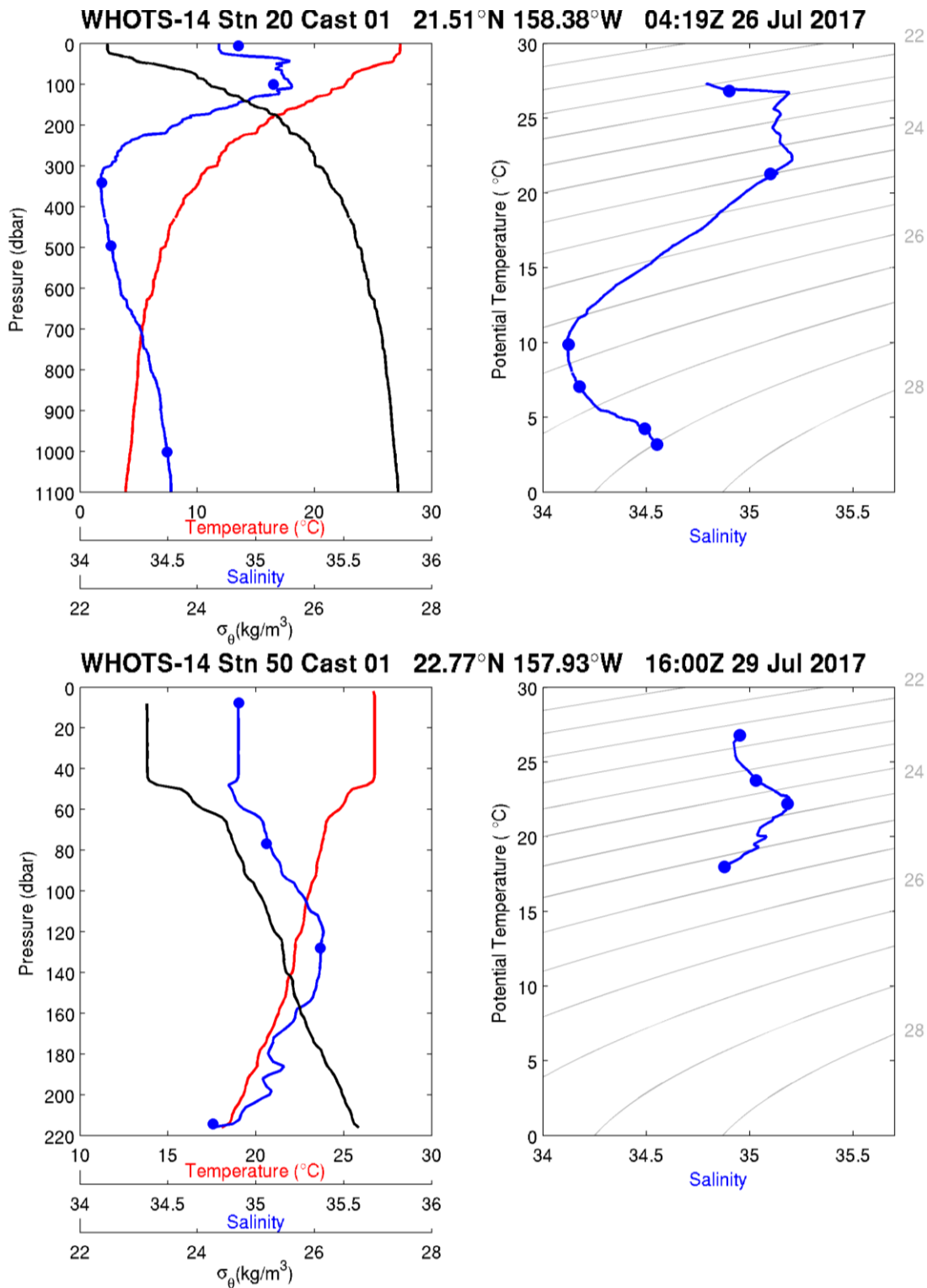


Figure VI-1 [Upper left panel] Profiles of CTD temperature, salinity, and potential density ( $\sigma_\theta$ ) as a function of pressure, including discrete bottle salinity samples (when available) for station 20 cast 1 during the WHOTS-14 cruise. [Upper right panel] Profiles of CTD salinity as a function of potential temperature, including discrete bottle salinity samples (when available) for station 20 cast 1 during the WHOTS-14 cruise. [Lower left panel] Same as in the upper left panel, but for station 50 cast 1. [Lower right panel] Same as in the upper right panel, but station 50 cast 1.

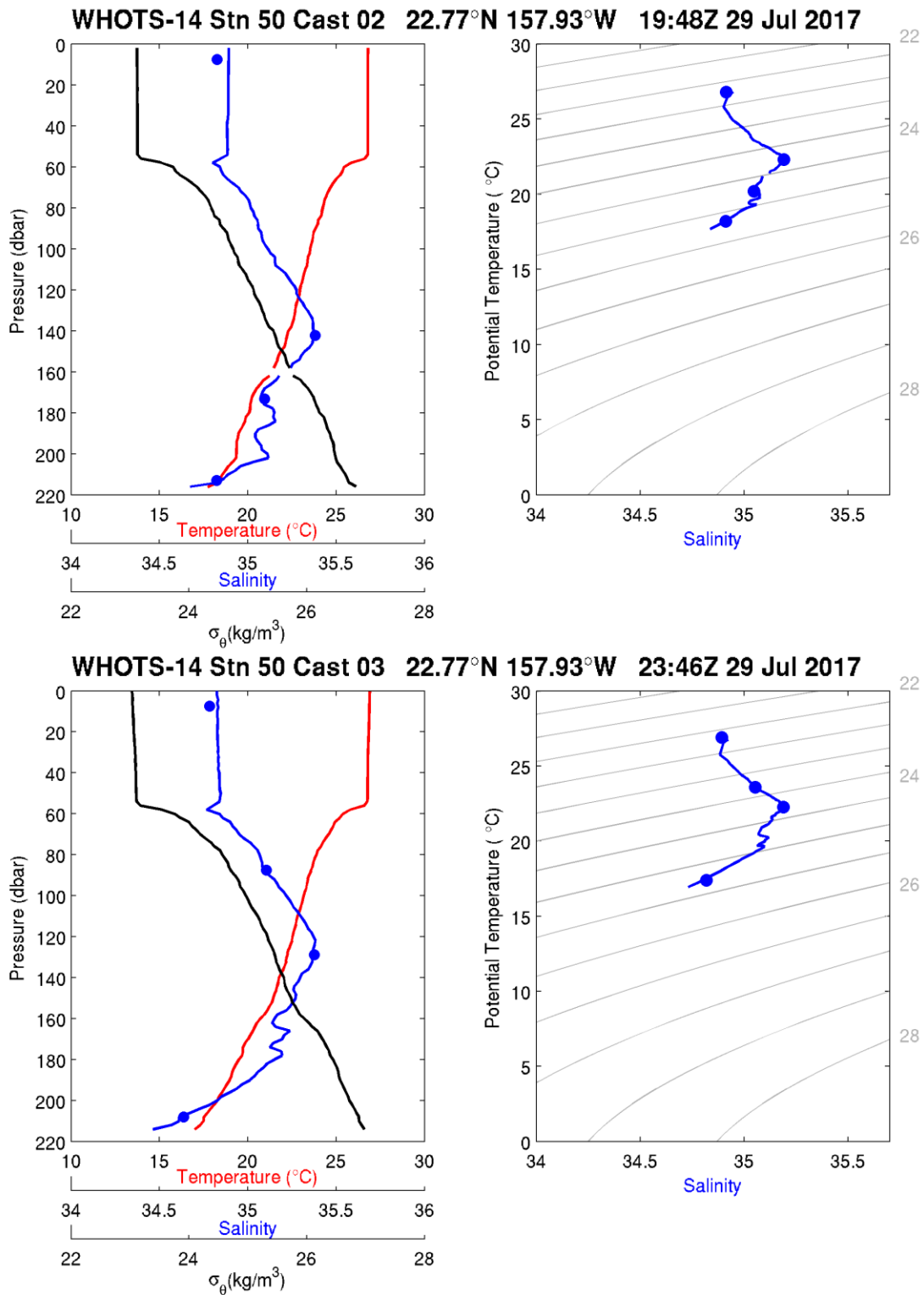


Figure VI-2. [Upper panels] Same as in Figure VI-1, but for station 50, cast 2. [Lower panels] Same as Figure VI-1, but for station 50, cast 3.

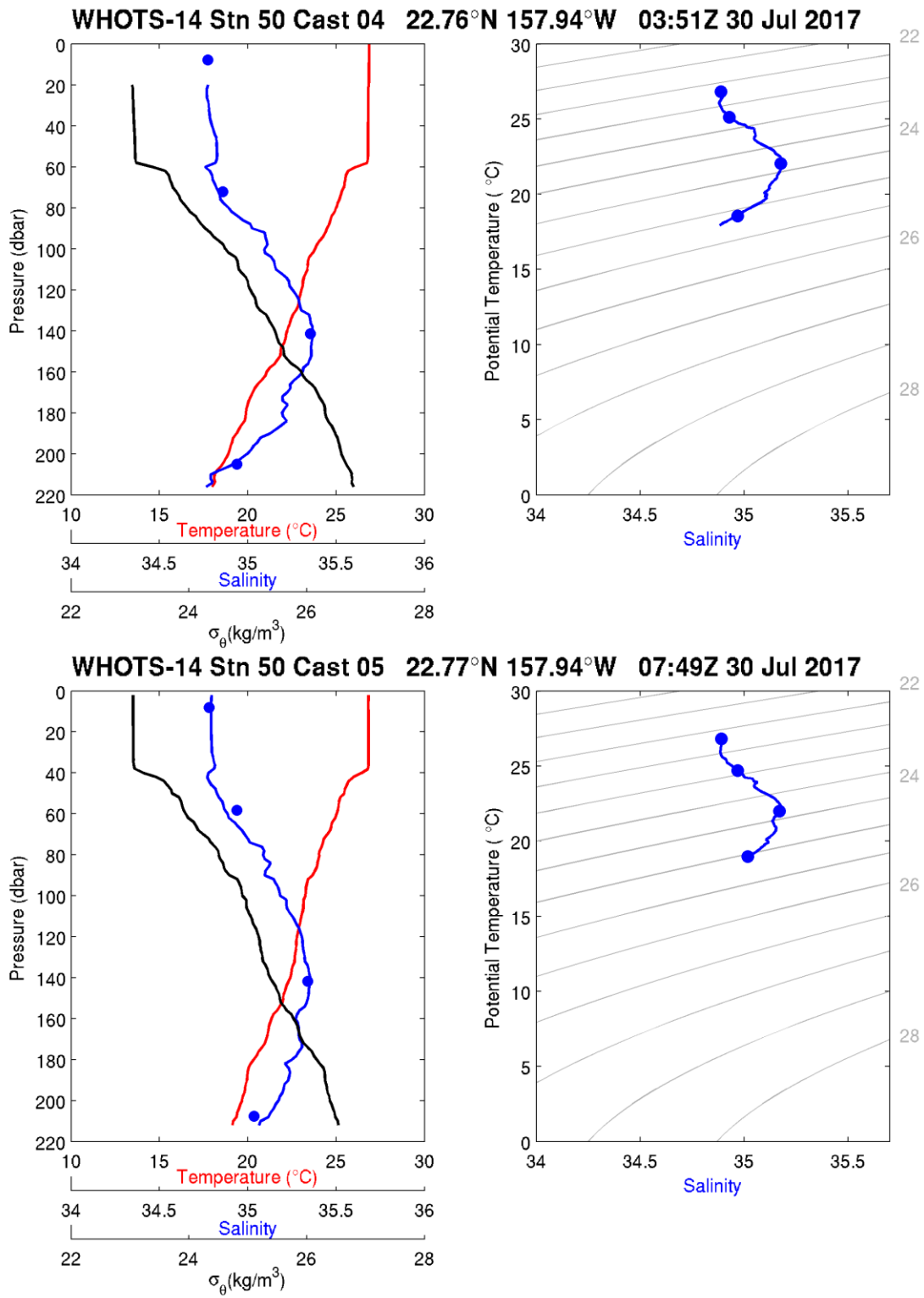


Figure VI-3. [Upper panels] Same as in Figure VI-1, but for station 50, cast 4. [Lower panels] Same as in Figure VI 1, but for station 50 cast 5.

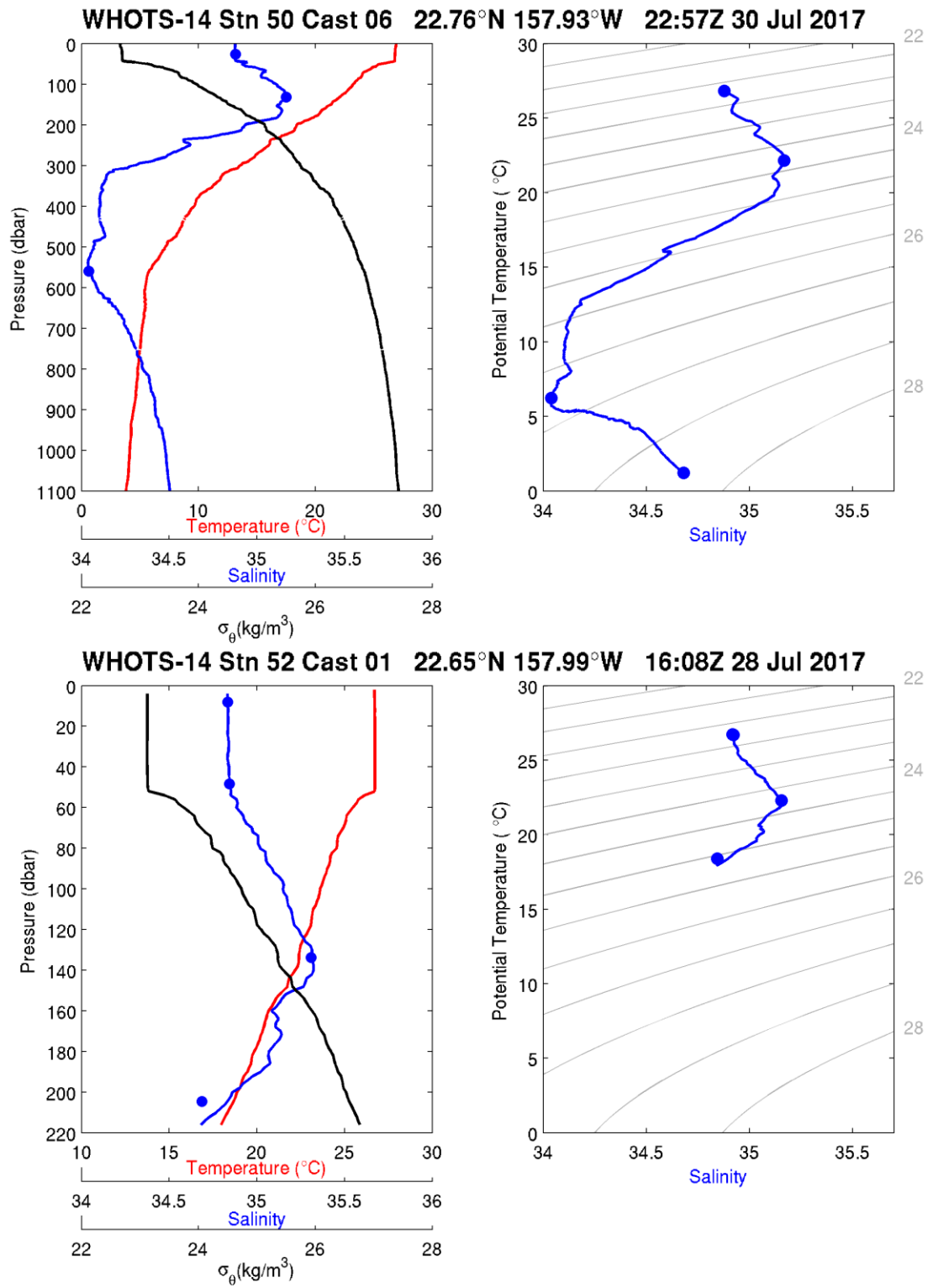


Figure VI-4. [Upper panels] Same as in Figure VI-1, but for station 50, cast 6. [Lower panels] Same as in Figure VI 1, but for station 52, cast 1.

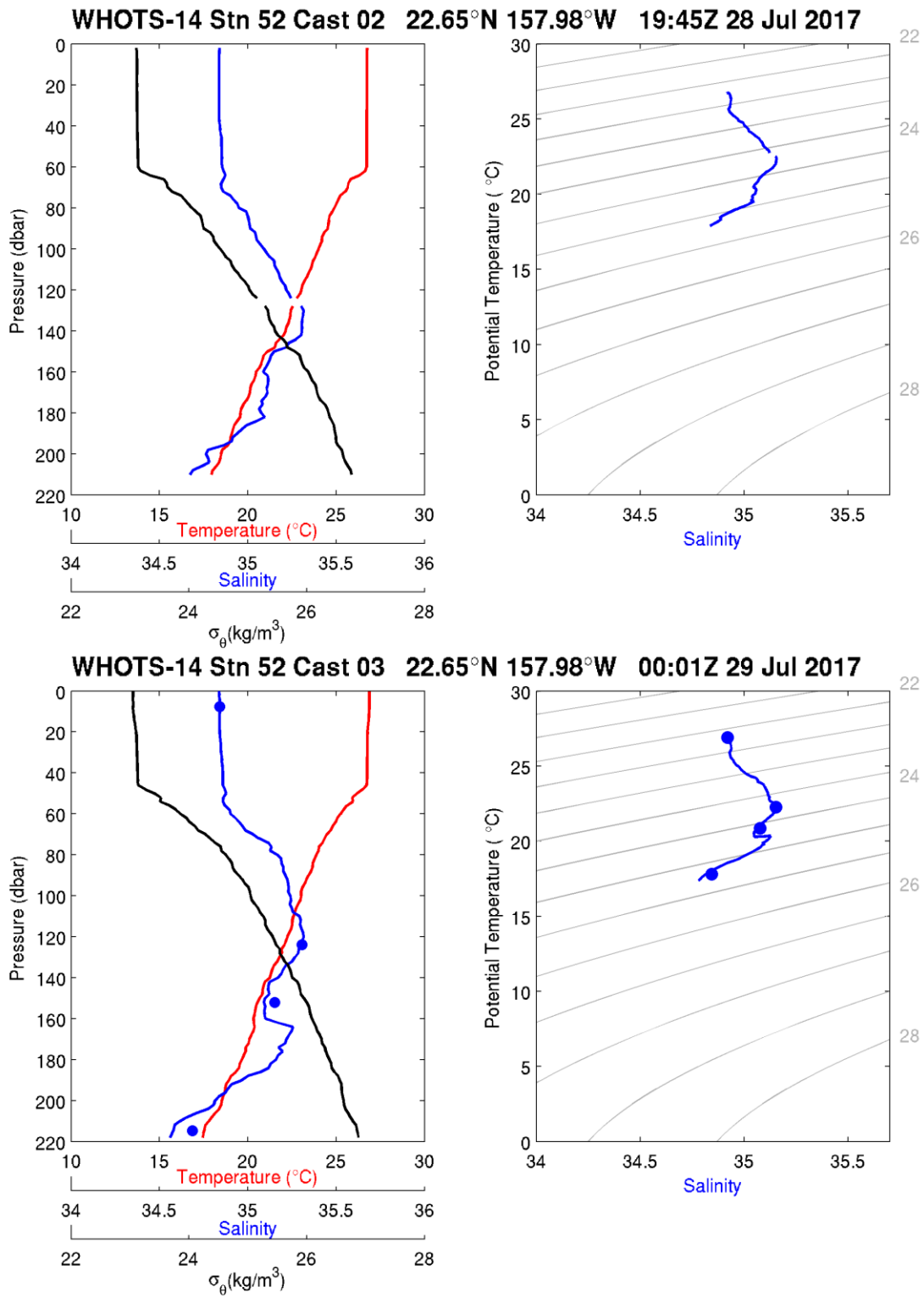


Figure VI-5. [Upper panels] Same as in Figure VI-1, but for station 52, cast 2. [Lower panels] Same as in Figure VI 1, but for station 52 cast 3.

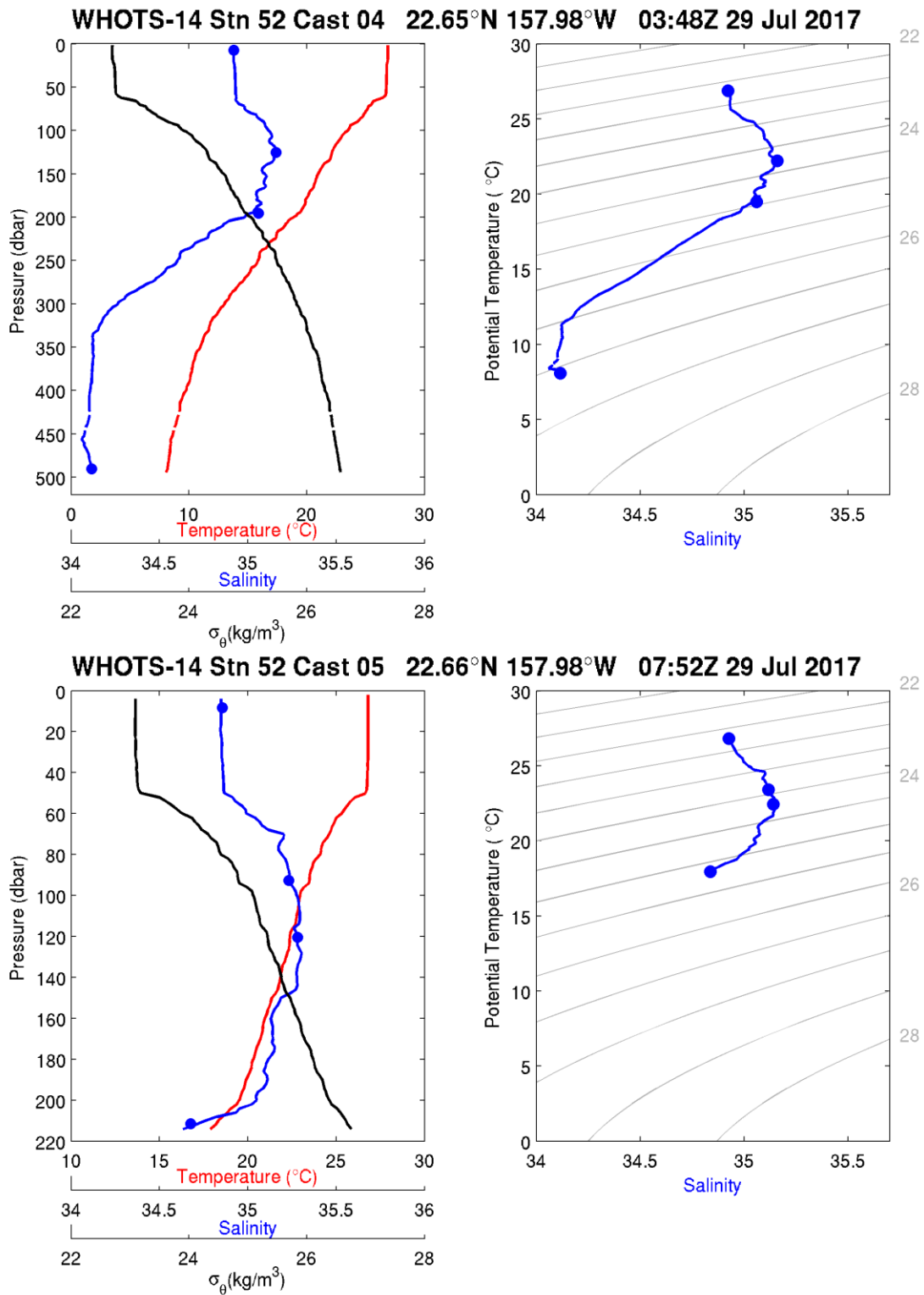


Figure VI-6. [Upper panels] Same as in Figure VI-1, but for station 52, cast 4. [Lower panels] Same as in Figure VI 1, but for station 52 cast 5.

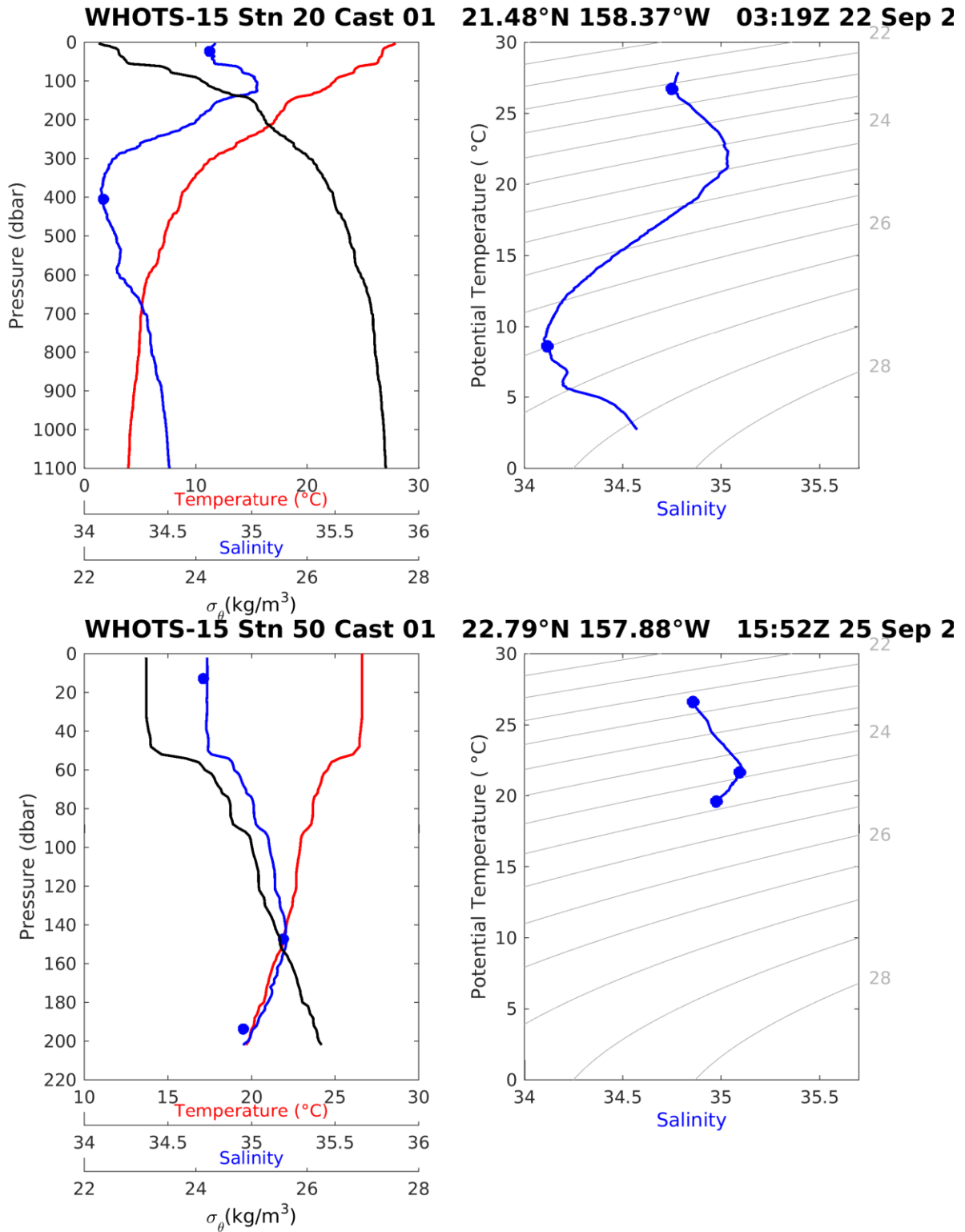


Figure VI-7. [Upper left panel] Profiles of CTD temperature, salinity, and potential density ( $\sigma_\theta$ ) as a function of pressure, including discrete bottle salinity samples (when available) for station 20 cast 1 during the WHOTS-15 cruise. [Upper right panel] Profiles

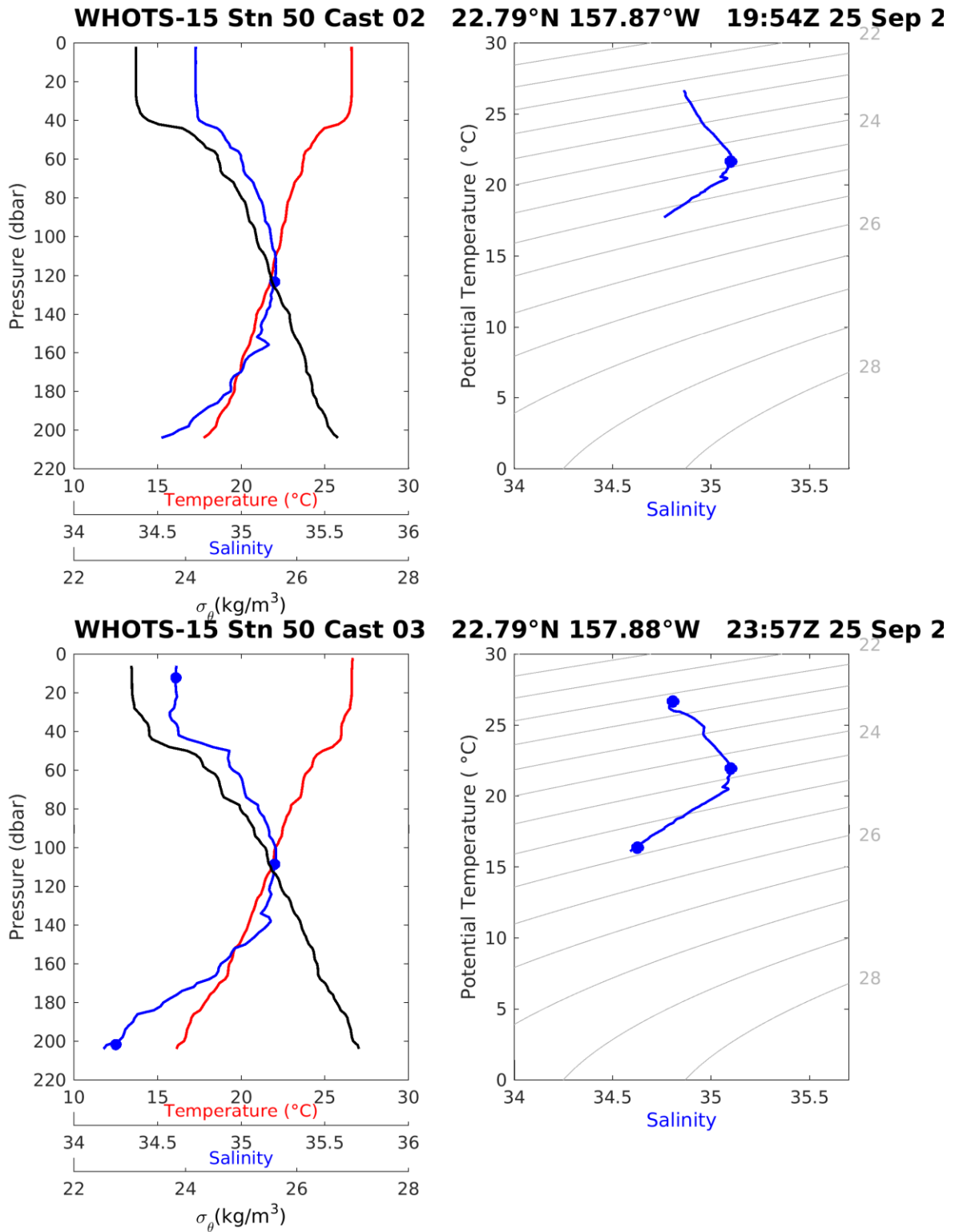


Figure VI-8. [Upper panels] Same as in Figure VI-7, but for station 50, cast 2. [Lower panels] Same as in Figure VI-7, but for station 50, cast 3.

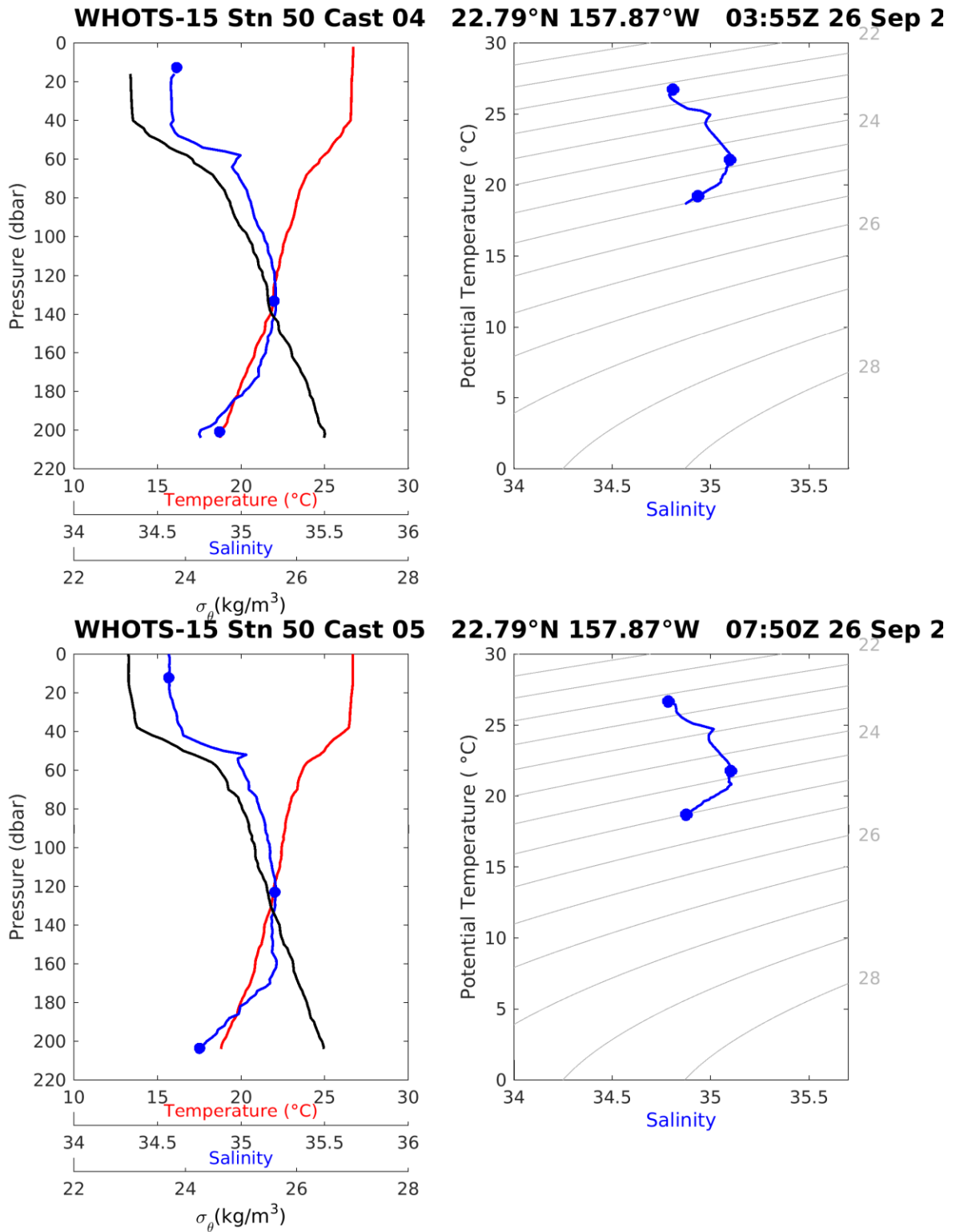


Figure VI-9. [Upper panels] Same as in Figure VI-7, but for station 50, cast 4. [Lower panels] Same as in Figure VI-7, but for station 50 cast 5.

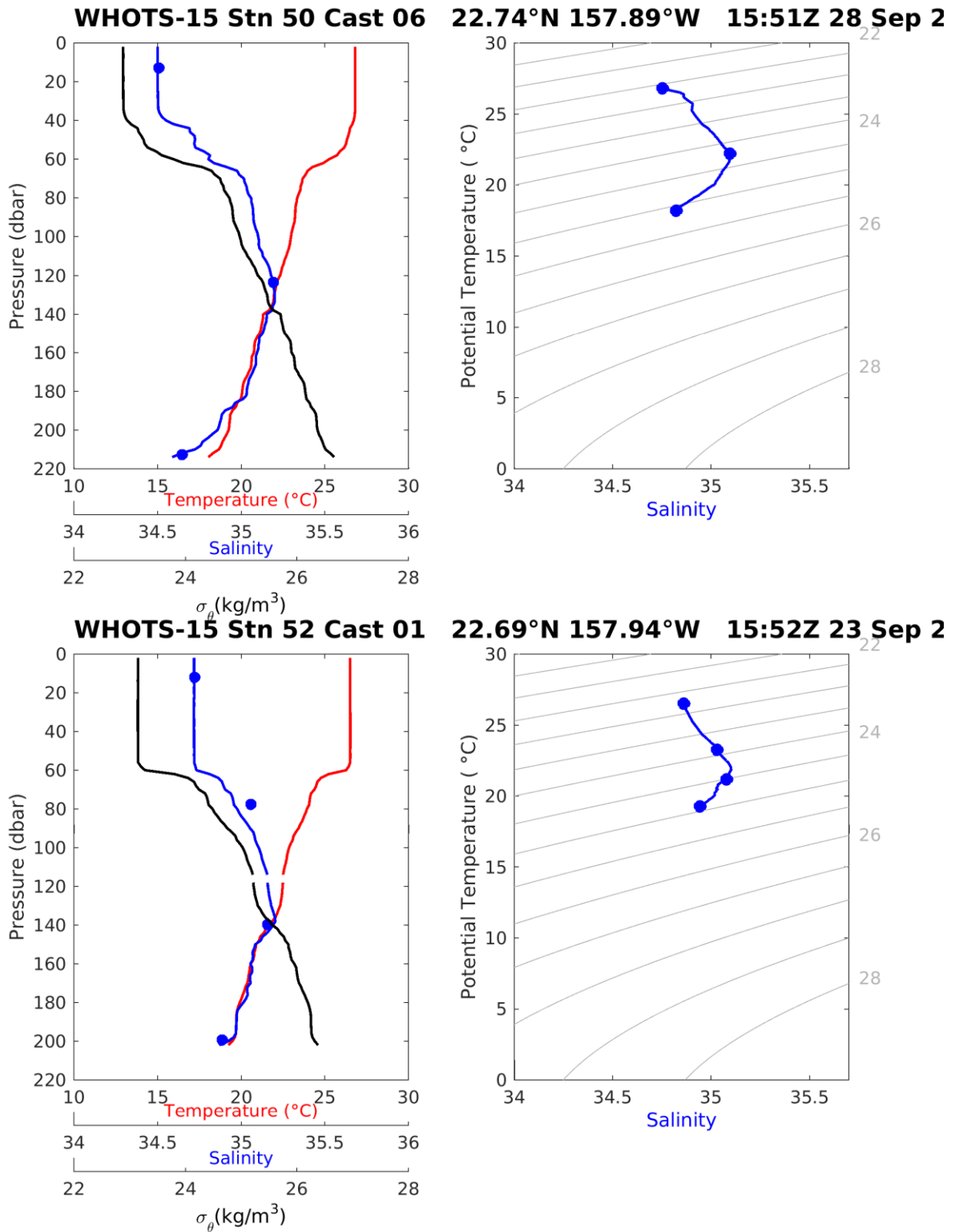


Figure VI-10. [Upper panels] Same as in Figure VI-7, but for station 50, cast 6. [Lower panels] Same as in Figure VI-7, but for station 52, cast 1.

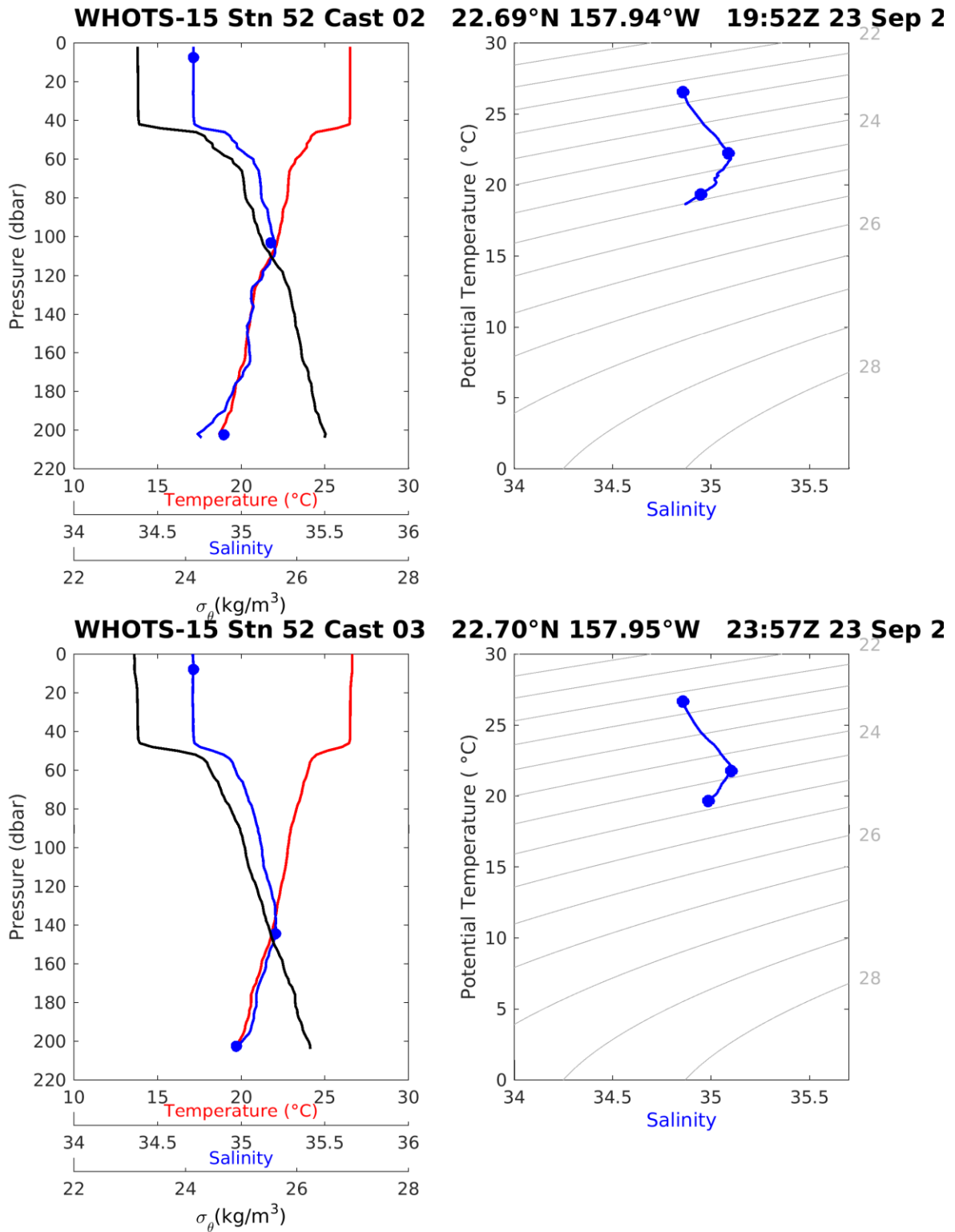


Figure VI-11. [Upper panels] Same as in Figure VI-7, but for station 52, cast 2. [Lower panels] Same as in Figure VI-7, but for station 52, cast 3.

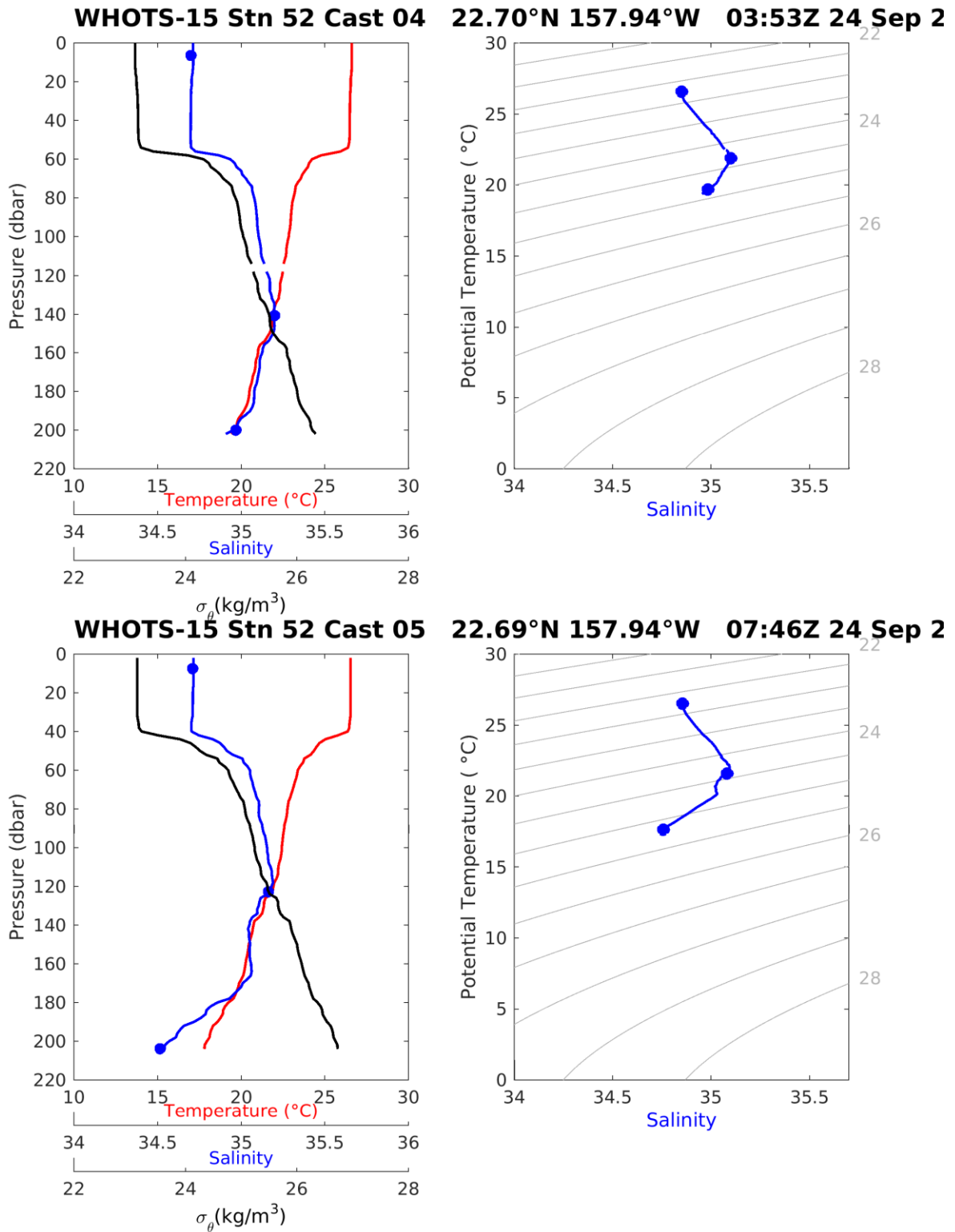


Figure VI-12. Same as in Figure VI-7, but for station 52, cast 4. [Lower panels] Same as in Figure VI-7, but for station 52, cast 5.

## B. Thermosalinograph data

Underway measurements of near-surface temperature and salinity from the thermosalinograph (TSG) system onboard the R/V Hi'ialakai cruise are presented in Figure VI-13 and navigational data is presented in Figure VI-14 for the WHOTS-14 cruise. TSG and navigational data during the WHOTS-15 cruise are presented in Figure VI-15 and Figure VI-16.

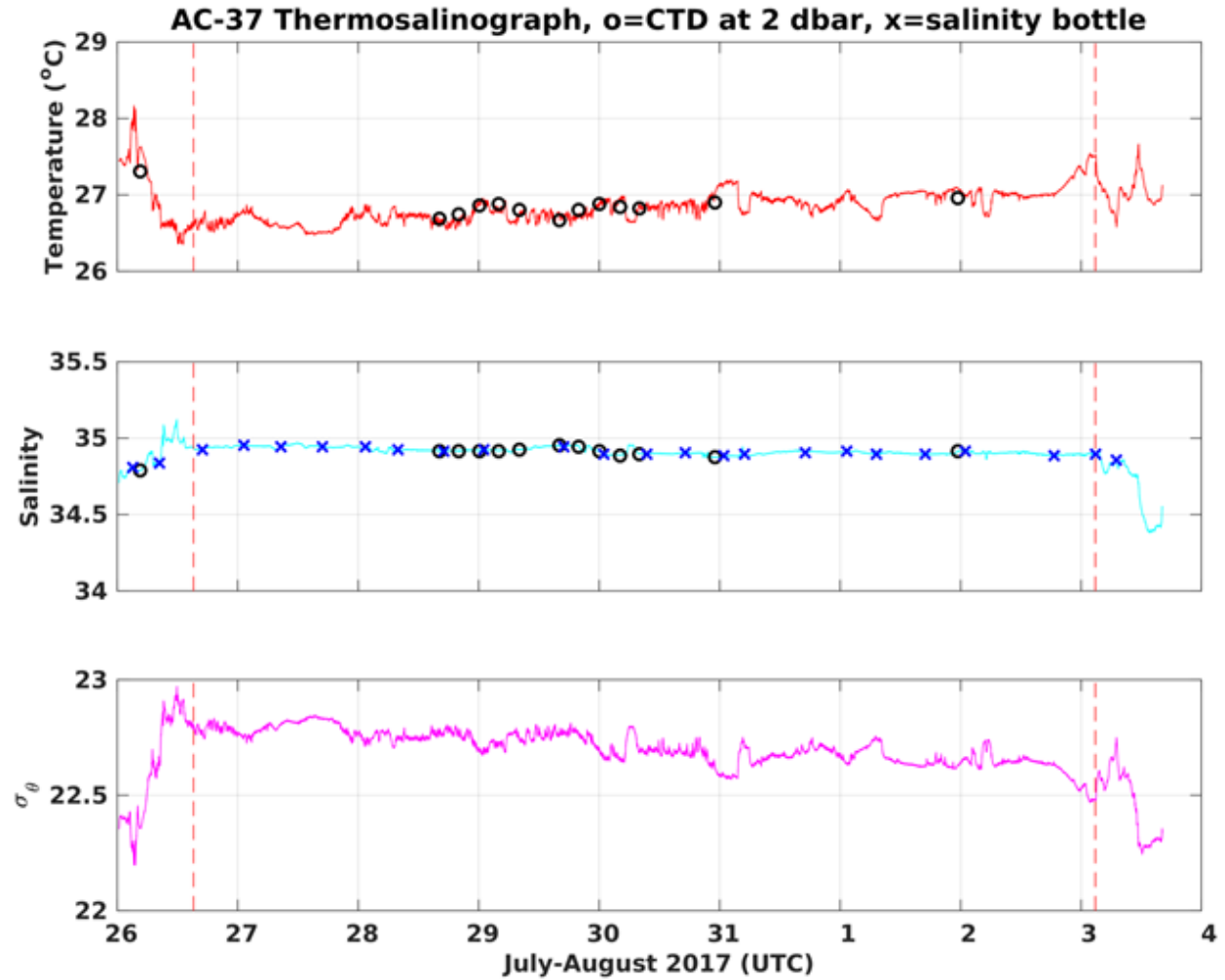


Figure VI-13. Final processed temperature (upper panel), salinity (middle panel), and potential density ( $\sigma_\theta$ ) (lower panel) data from the continuous underway system onboard the R/V Hi'ialakai during the WHOTS-14 cruise. Temperature and salinity taken from 6-dbar CTD data (circles) and salinity bottle sample data (crosses) are superimposed. The dashed vertical red line indicates the period of occupation of Station ALOHA and the WHOTS site.

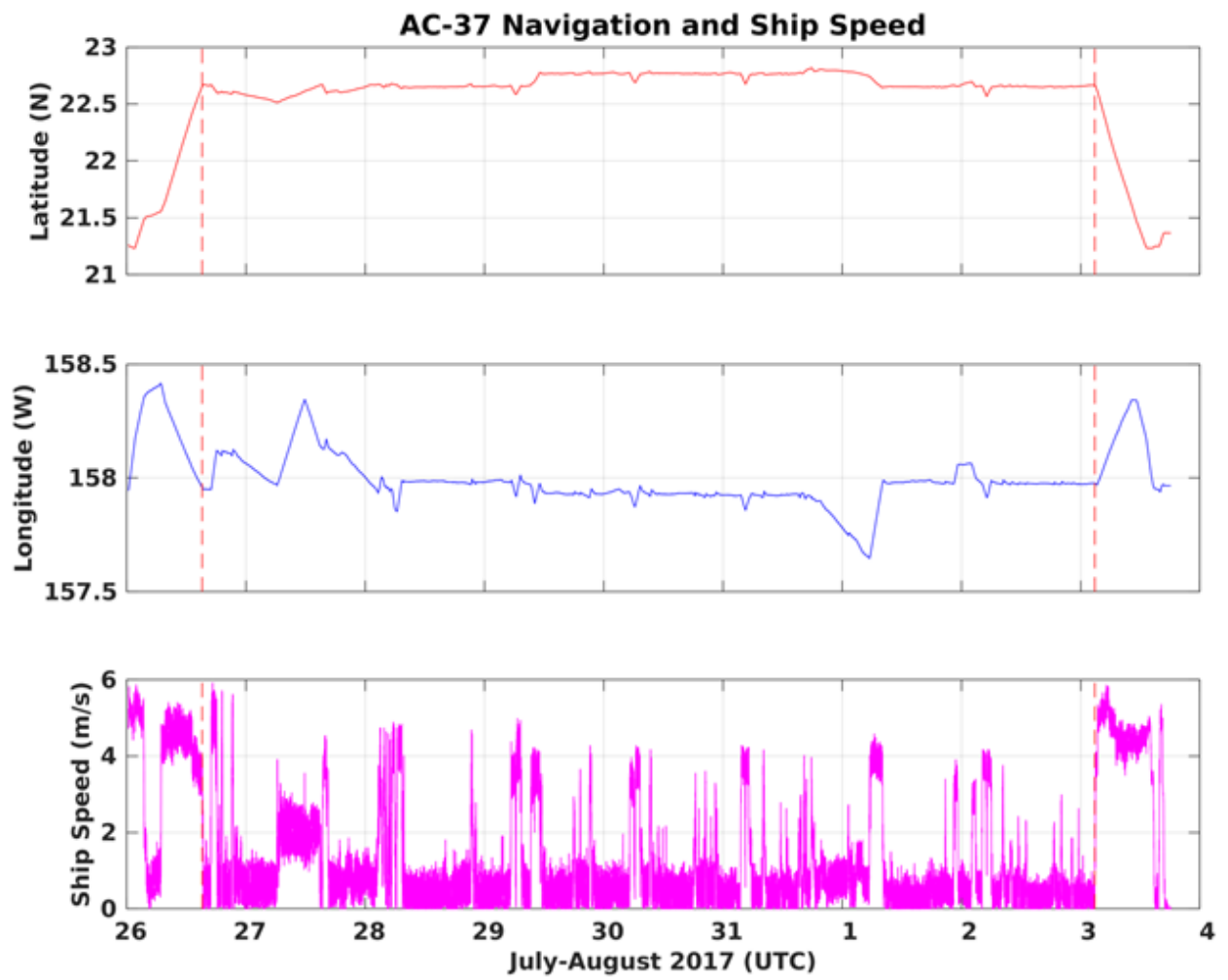


Figure VI-14. Timeseries of latitude (upper panel), longitude (middle panel), and ship's speed (lower panel) during the WHOTS-14 cruise.

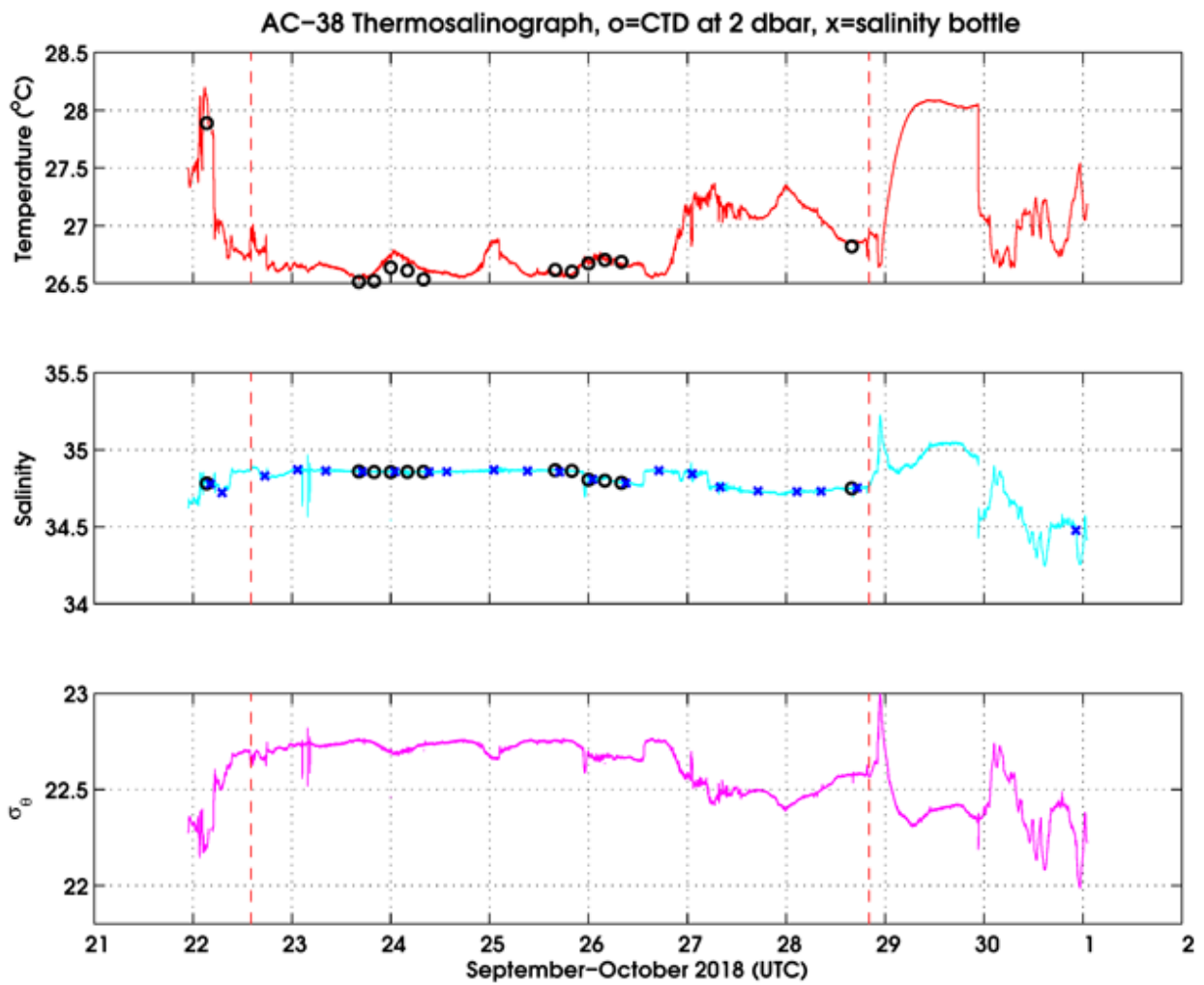


Figure VI-15. Final processed temperature (upper panel), salinity (middle panel), and potential density ( $\sigma_\theta$ ) (lower panel) data from the continuous underway system onboard the R/V *Hi'ialakai* during the WHOTS-15 cruise. Temperature and salinity were taken from 6-dbar CTD

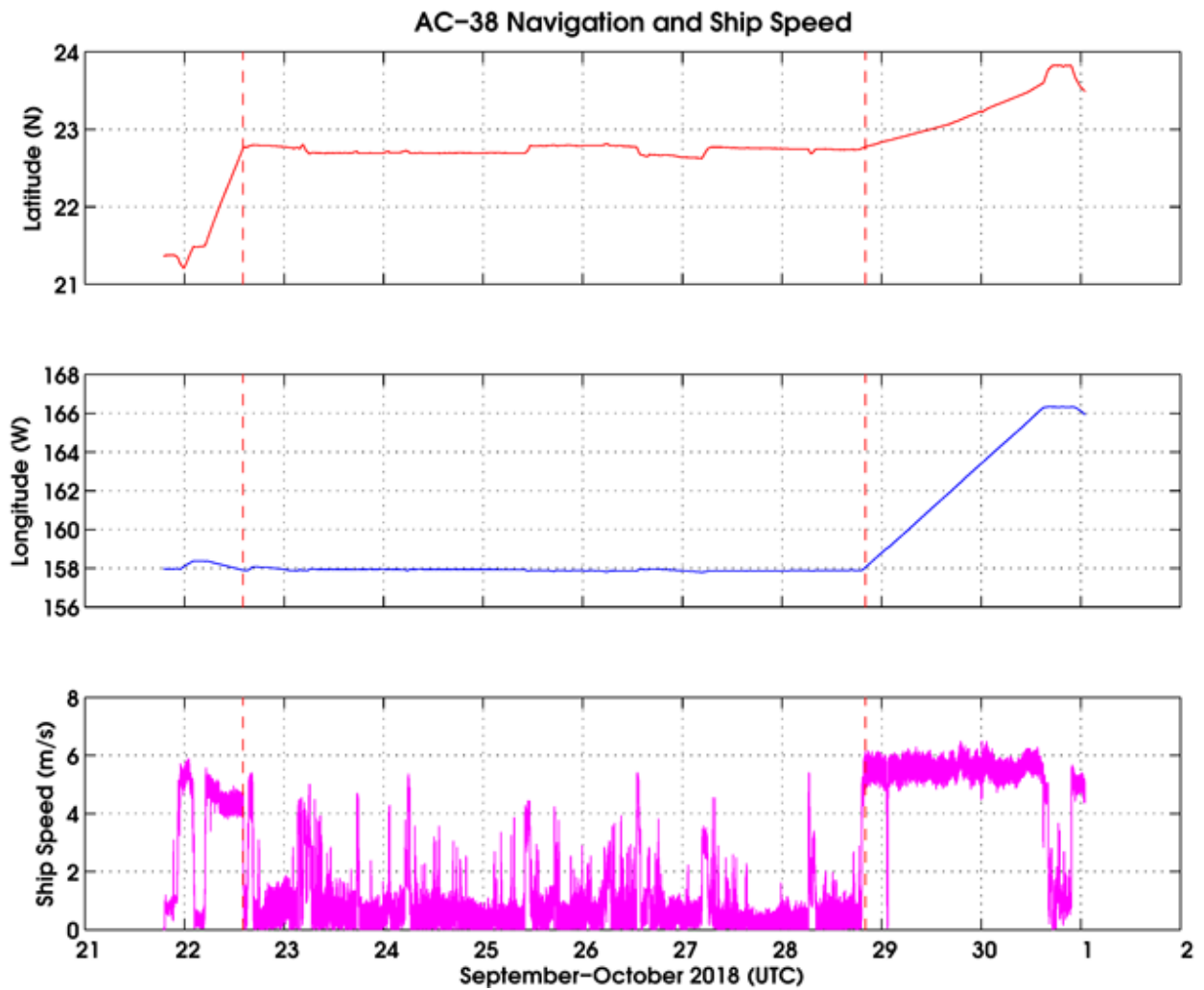


Figure VI-16. Final processed temperature (upper panel), salinity (middle panel), and potential density ( $\sigma_\theta$ ) (lower panel) data from the continuous underway system onboard the R/V *Hi'ialakai* during the WHOTS-15 cruise. Temperature and salinity taken from 6-dbar CTD data (circles) and salinity bottle sample data (crosses) are superimposed. The dashed vertical red line indicates the period of occupation of Station ALOHA and the WHOTS site. The ship had to leave Station ALOHA to head for the French Frigate Shoals to save a group of scientists before hurricane Walaka hit land.

### **C. MicroCAT/SeaCAT data**

The temperature measured by MicroCATs during the mooring deployment for WHOTS-14 is presented in Figure VI-17 through Figure VI-21 for each of the depths where the instruments were located. The salinity is plotted in Figure VI-22 through Figure VI-26. The potential density ( $\sigma_\theta$ ) is plotted in Figure VI-27 through Figure VI-31.

Contoured plots of temperature and salinity as a function of depth are presented in Figure VI-32, and contoured plots of potential density ( $\sigma_\theta$ ) as a function of depth, and of salinity as a function of  $\sigma_\theta$  are in Figure VI-33.

The potential temperature and salinity measured by the deep SeaCATs during the mooring deployment are shown in Figure VI-34. Also shown in the plot are the potential temperature and salinity data obtained with a MicroCAT (SBE-37) installed in the ALOHA Cabled Observatory, about 6 nautical miles north from the WHOTS-13 anchor, the instrument is located 2 m above the bottom.

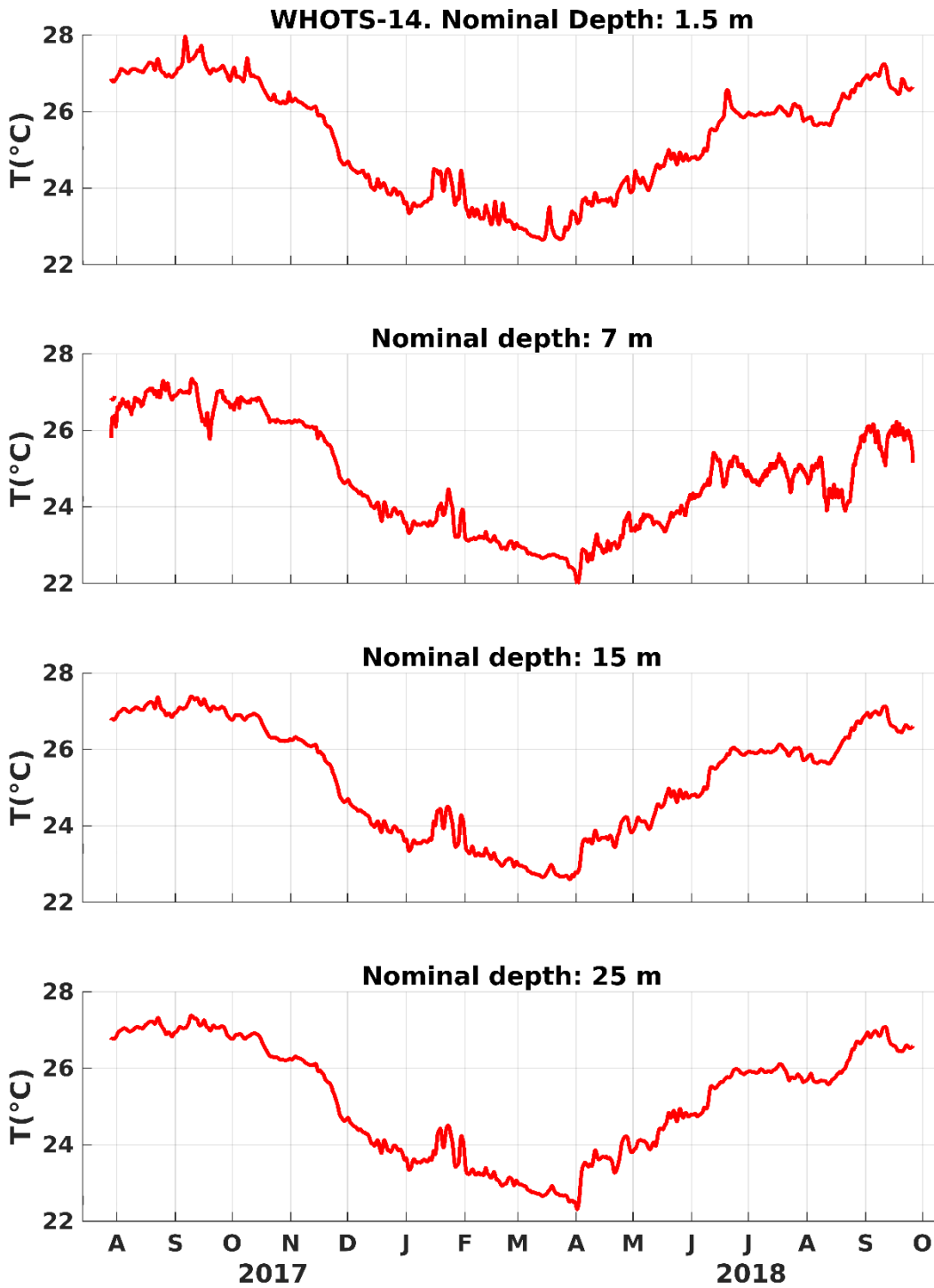


Figure VI-17. Temperatures from MicroCATs during WHOTS-14 deployment at 1.5, 7, 15, and 25 m.

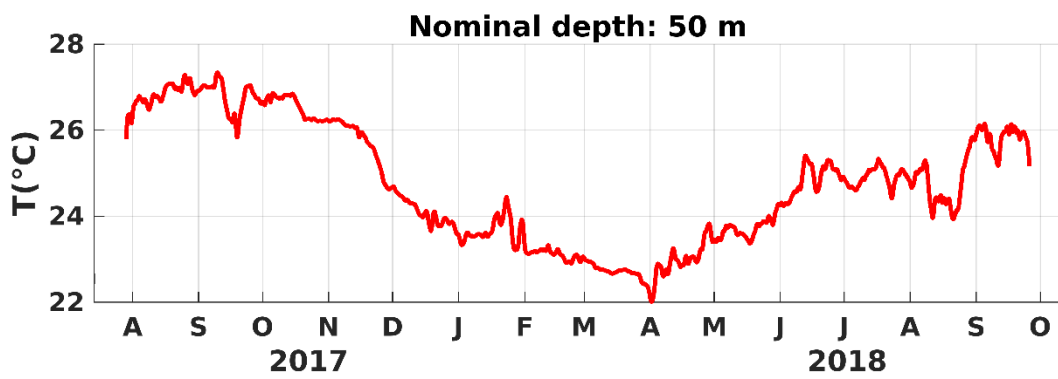
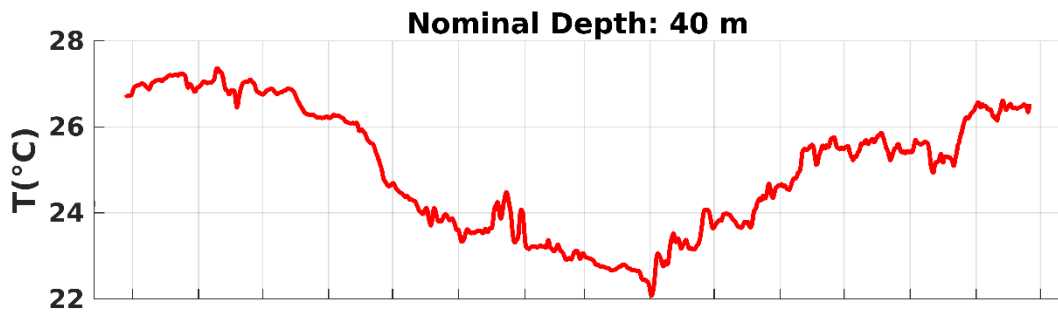


Figure VI-18. Same as in Figure VI-17, but at 35, 40, 45, and 50 m.

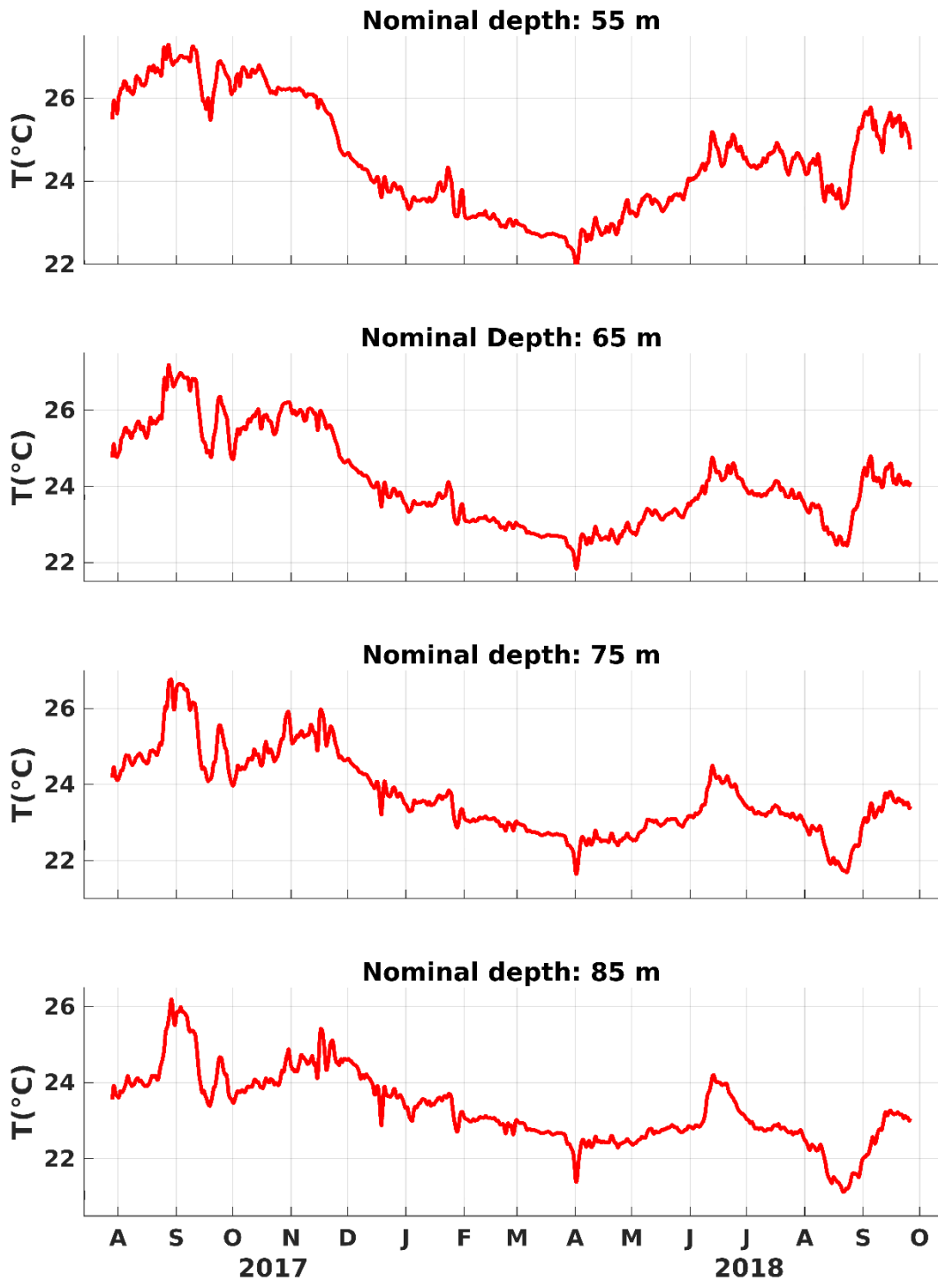


Figure VI-19. Same as in Figure VI-17, but at 55, 65, 75, and 85 m.

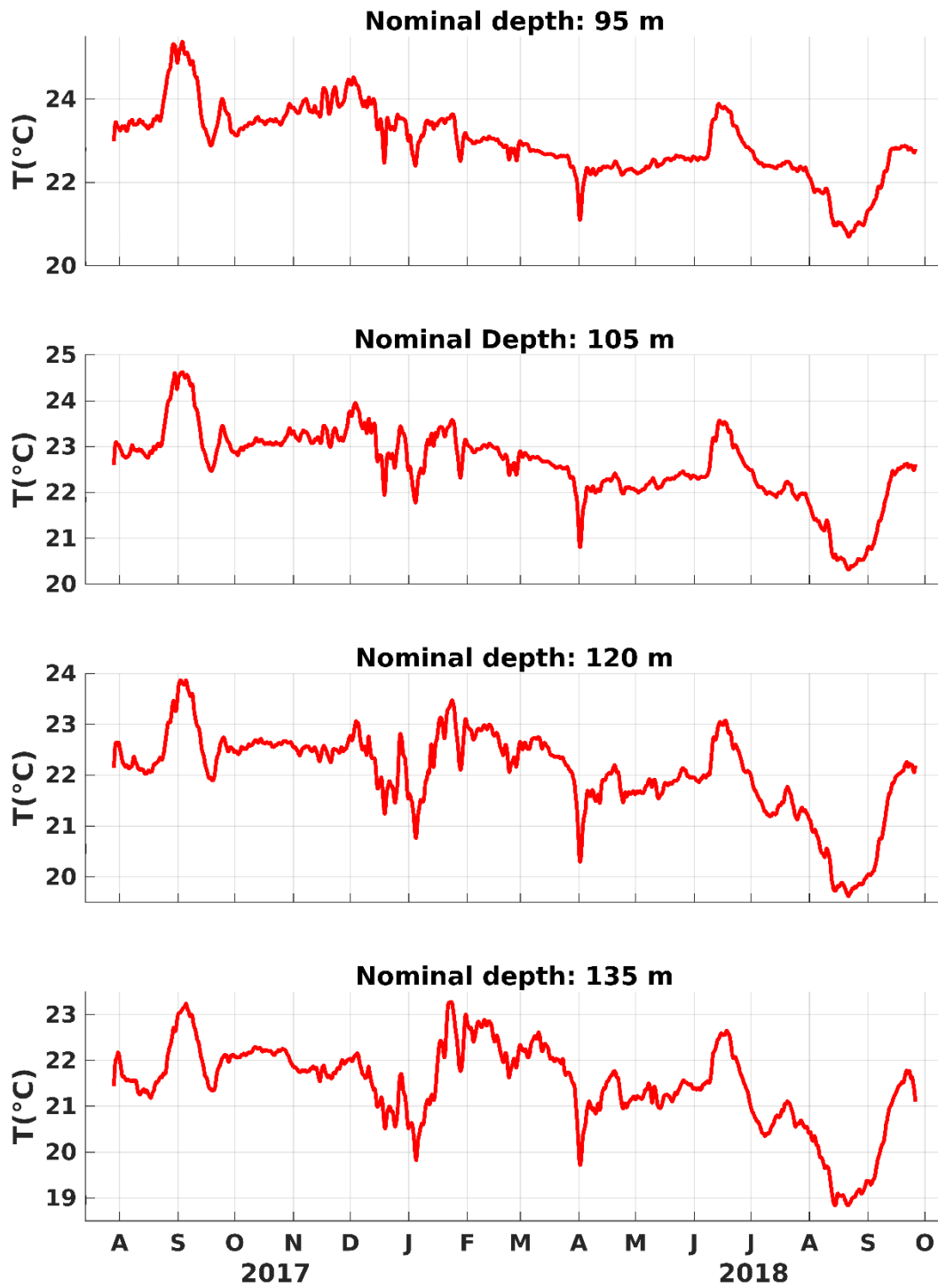
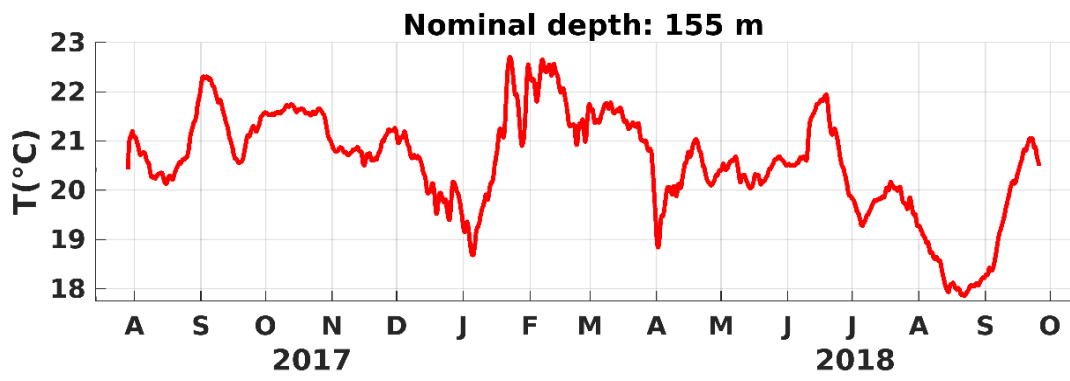


Figure VI-20. Same as in Figure VI-17, but at 95, 105, 120, and 135 m.



*Figure VI-21. Same as in Figure V-17, but at 155 m.*

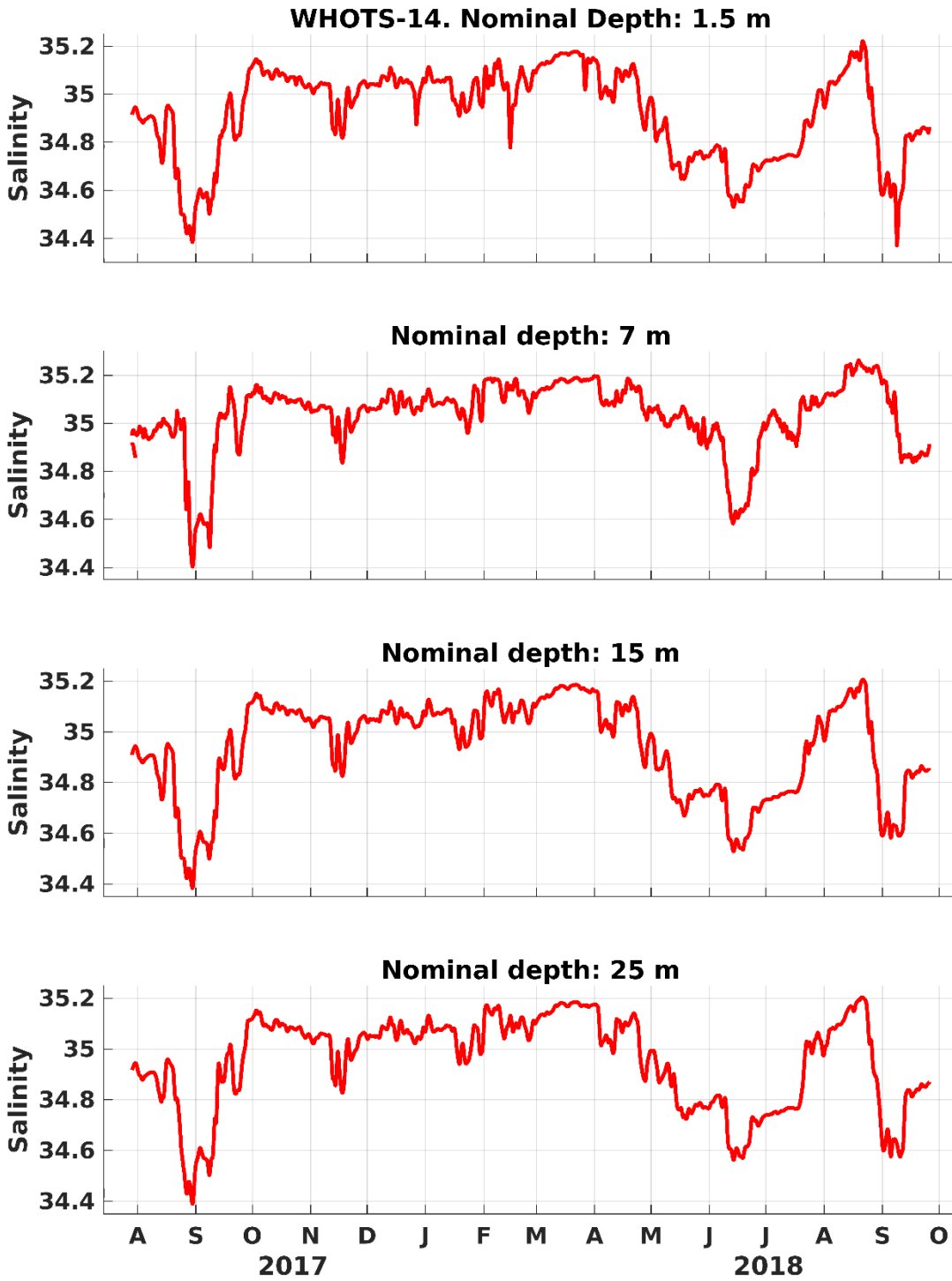


Figure VI-22. Salinities from MicroCATs during WHOTS-14 deployment at 1.5, 7, 15, and 25 m

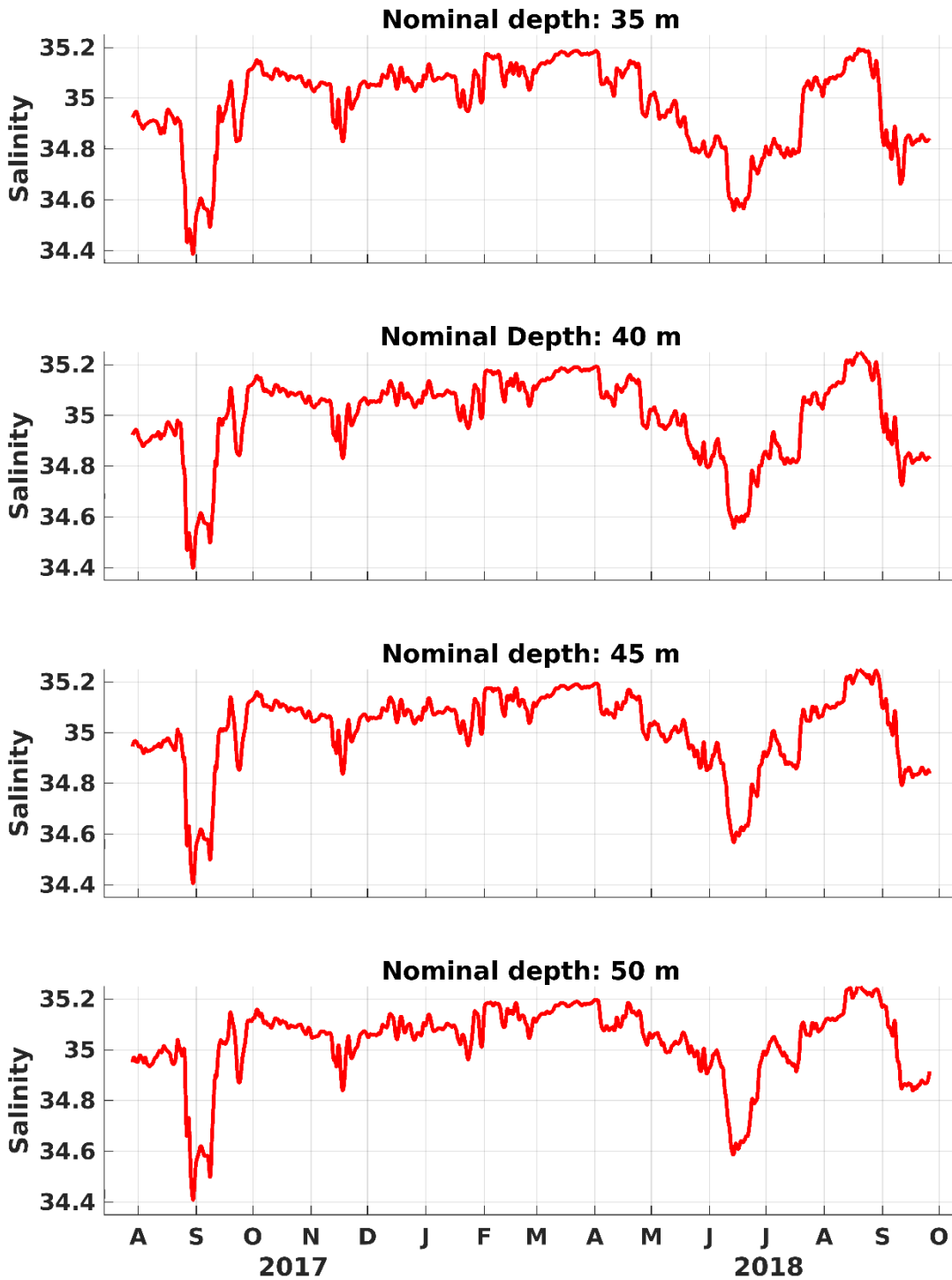


Figure VI-23. Same as in Figure VI-22, but at 35, 40, 45, and 50 m.

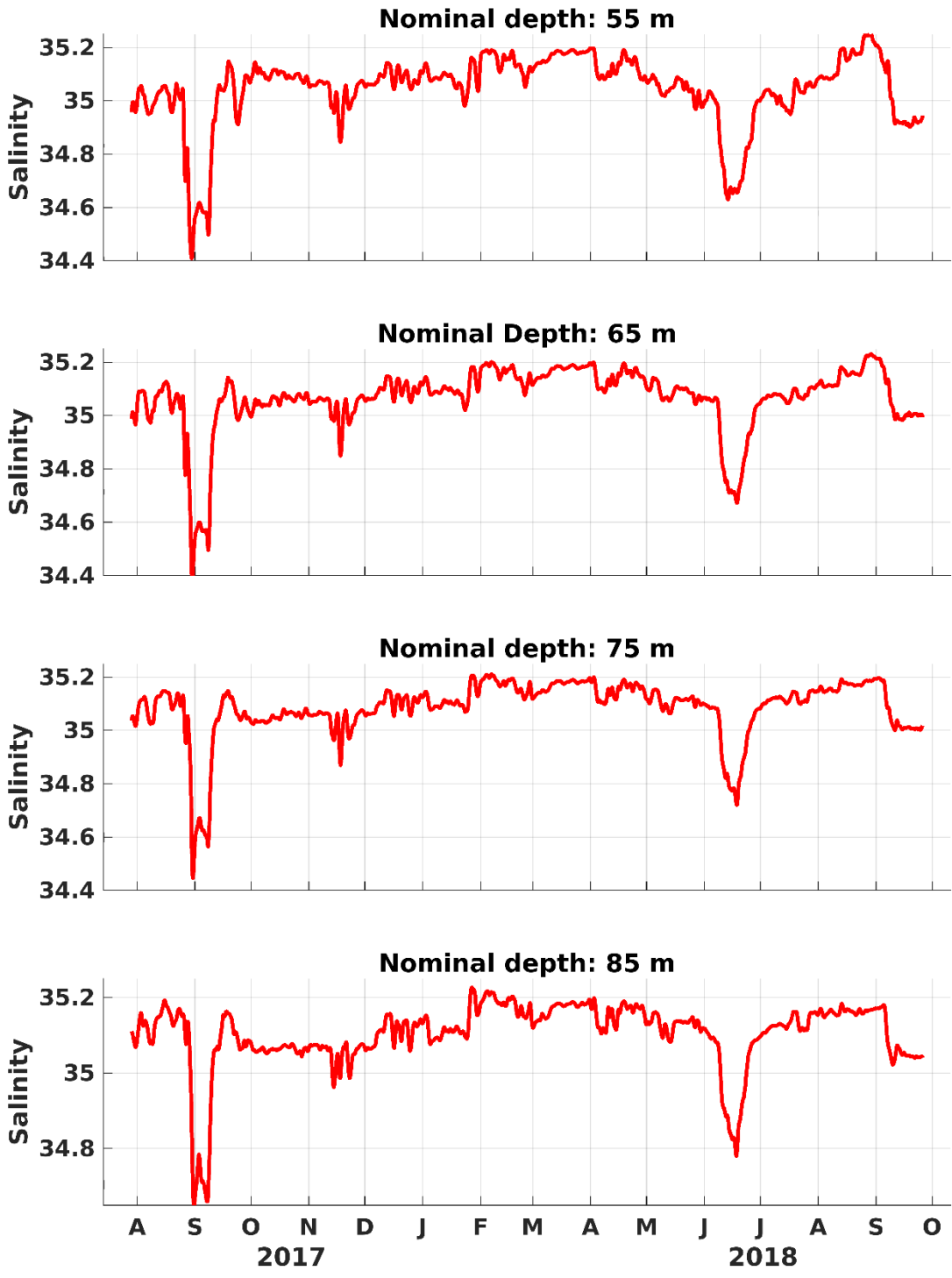


Figure VI-24. Same as in Figure VI-22, but at 55, 65, 75, and 85 m

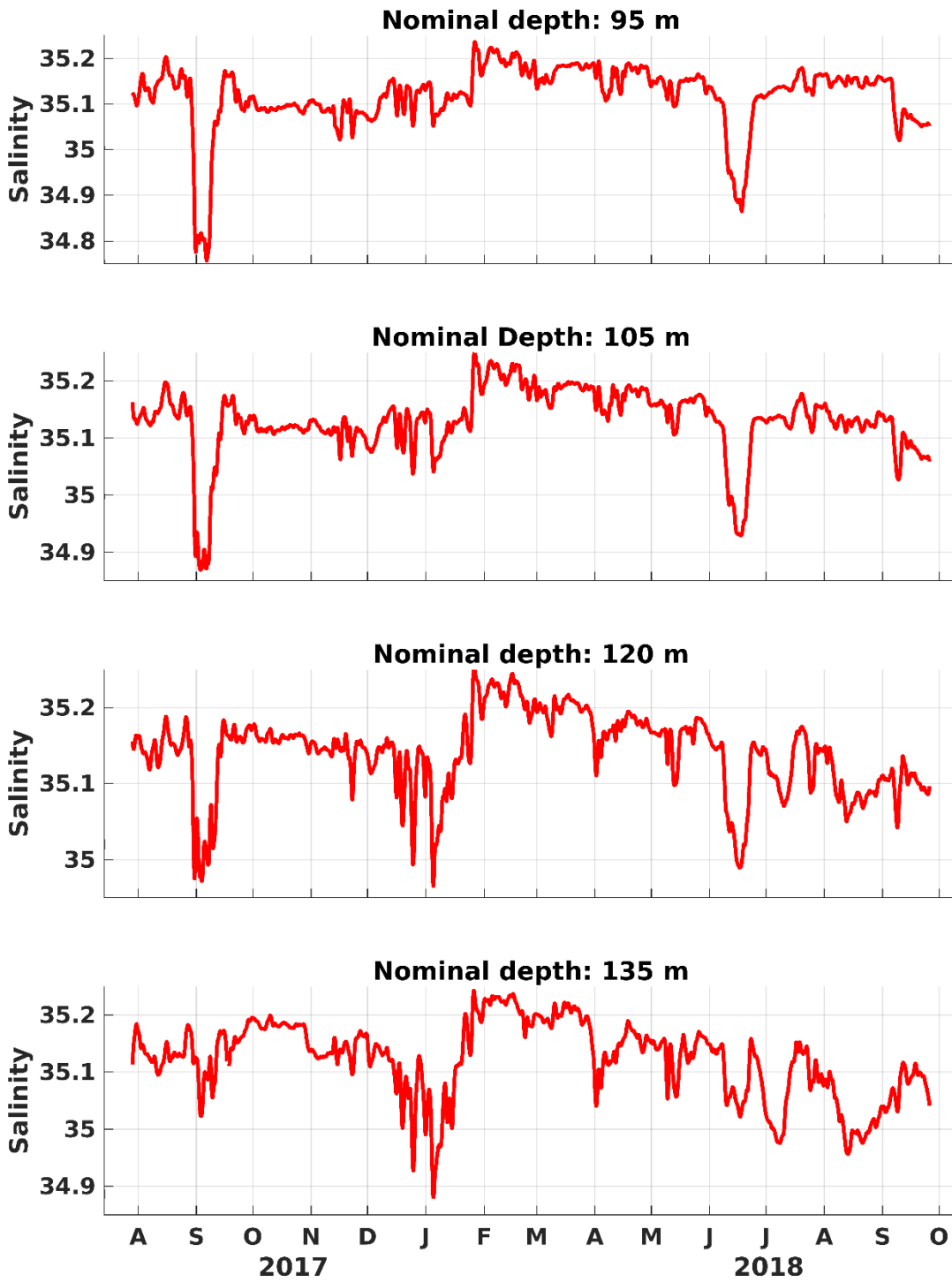
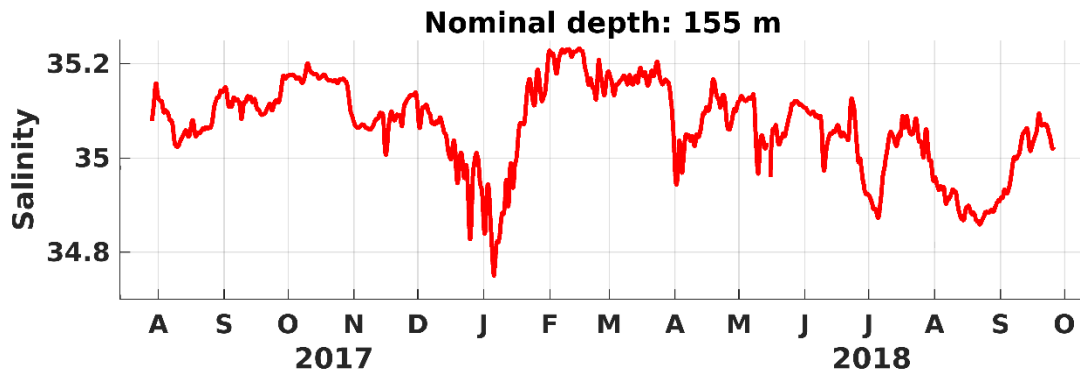


Figure VI-25. Same as in Figure VI-22, but at 95, 105, 120, and 135 m.



*Figure VI-26. Same as in Figure V-22, but at 155 m.*

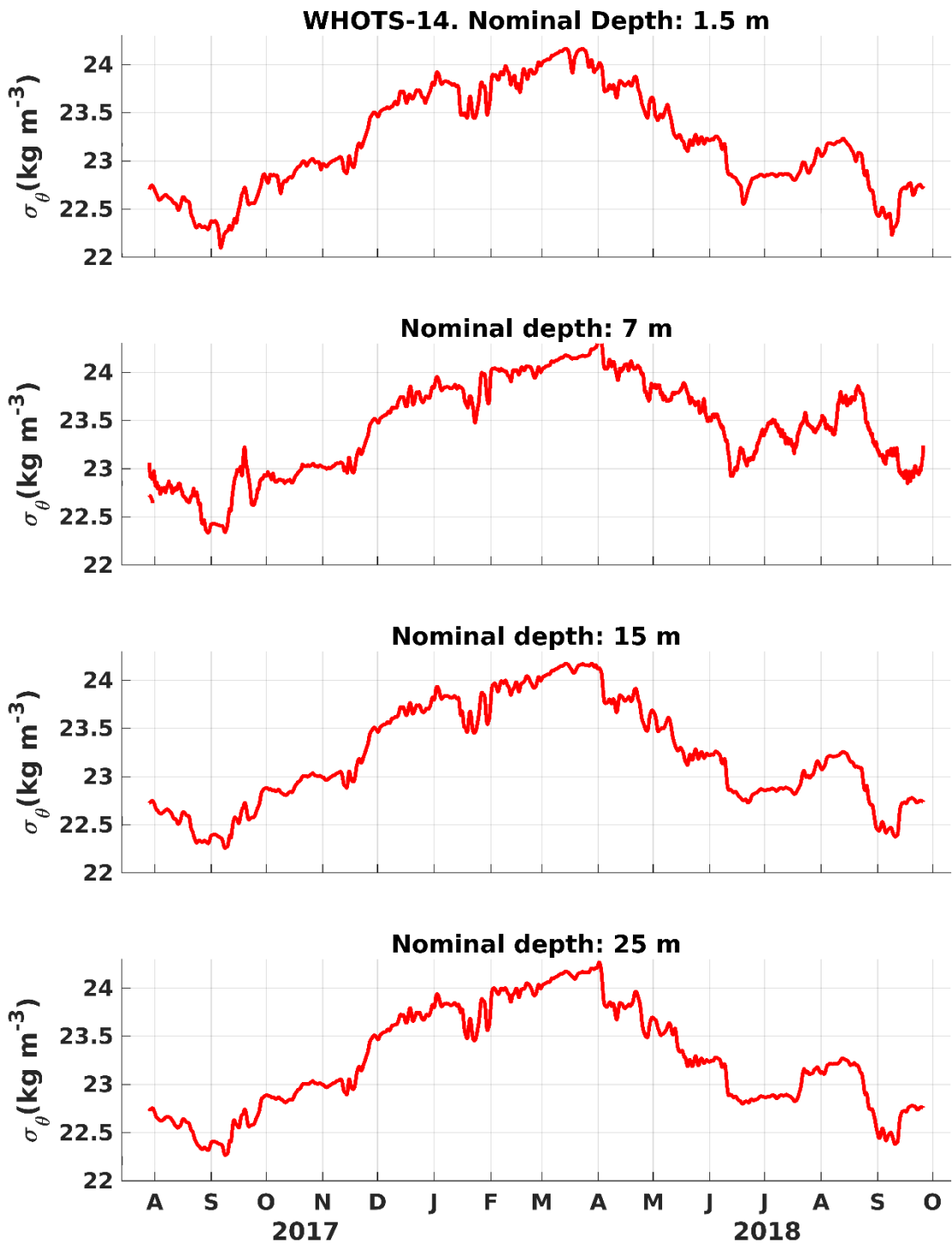


Figure VI-27. Potential densities ( $\sigma_\theta$ ) from MicroCATs during WHOTS-14 deployment at 1.5, 7, 15, and 25 m.

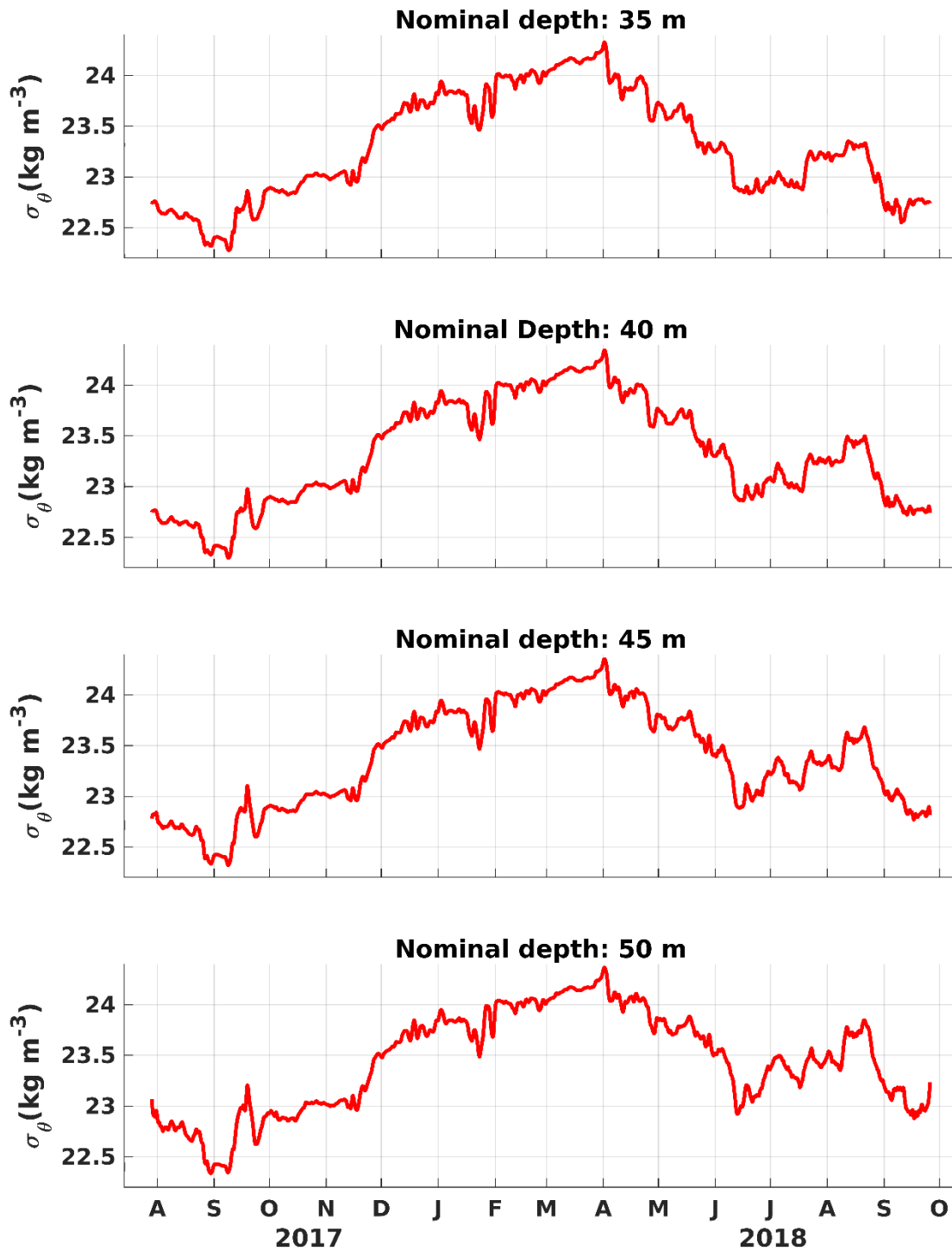


Figure VI-28. Same as in Figure VI-27, but at 35, 40, 45, and 50 m.

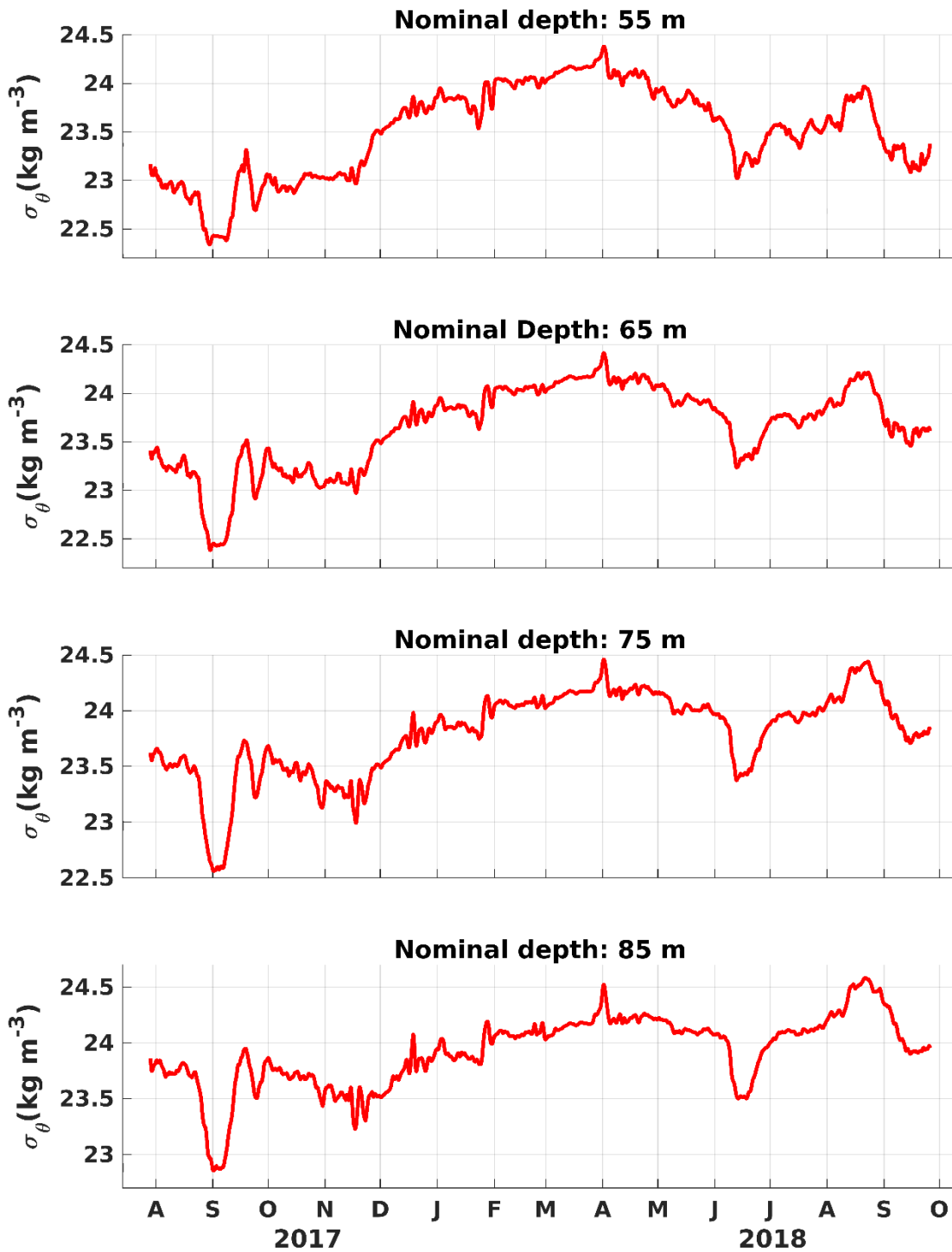


Figure VI-29. Same as in Figure VI-27, but at 55, 65, 75, and 85 m.

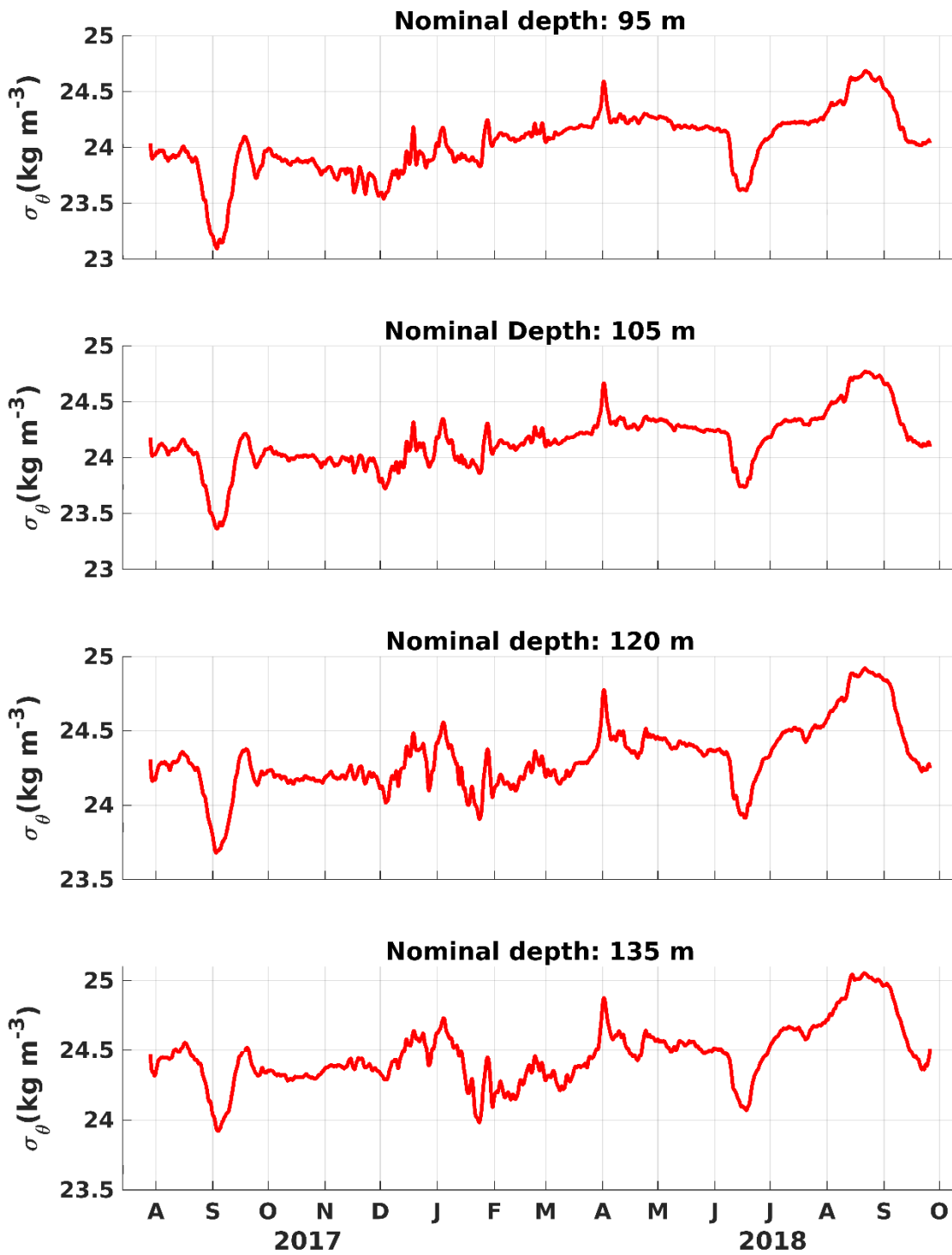


Figure VI-30. Same as in Figure VI-27, but at 95, 105, 120, and 135 m.

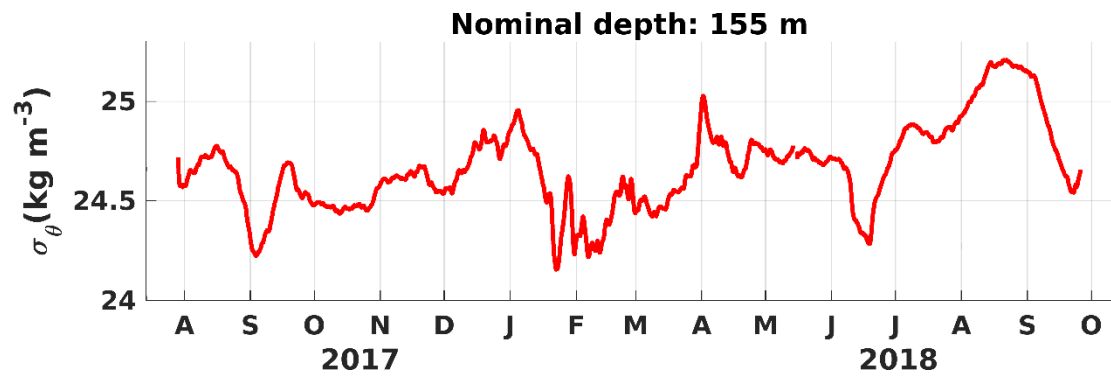


Figure VI-31. Same as in Figure VI-27, but at 155 m.

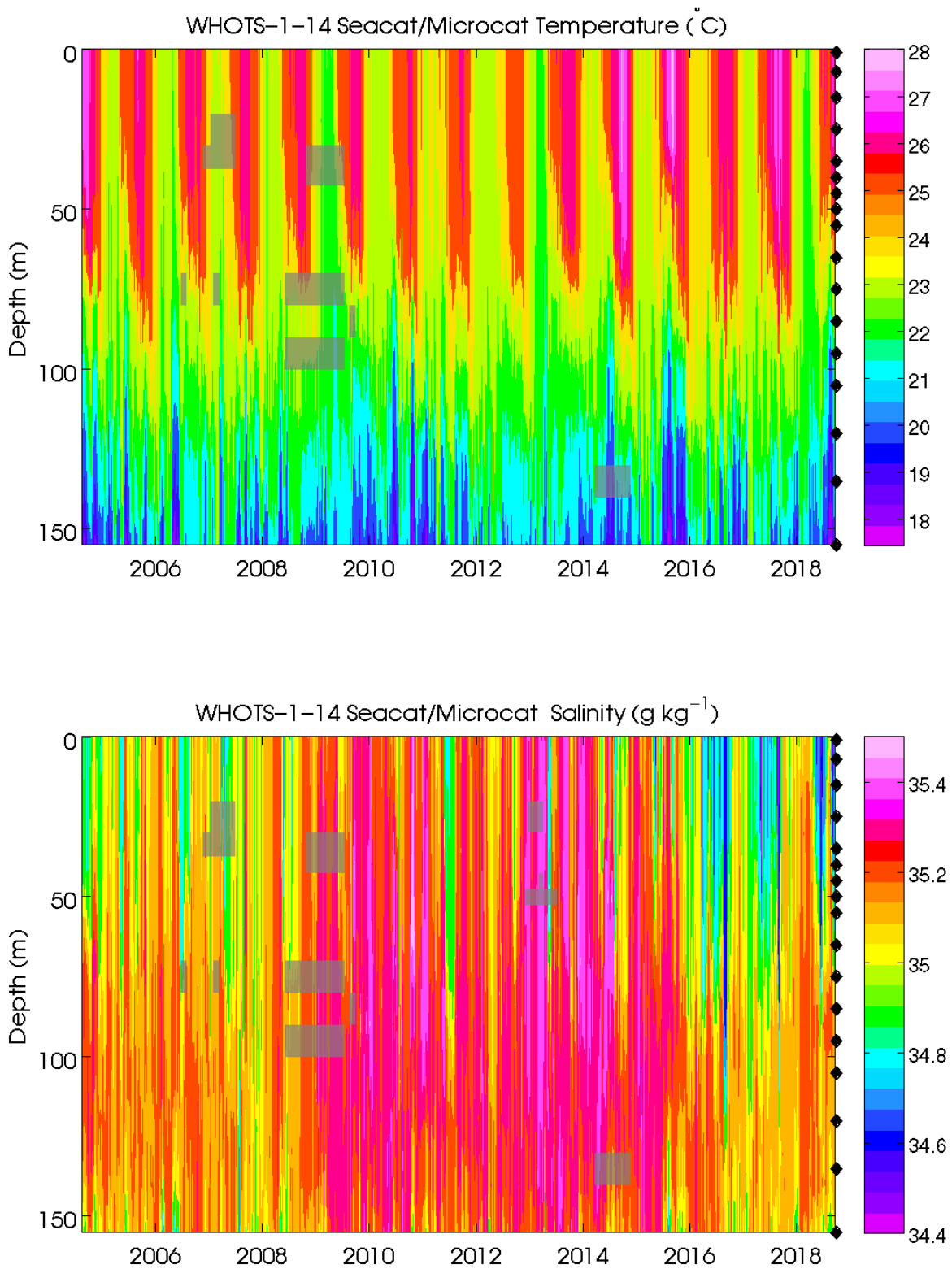


Figure VI-32. Contour plots of temperature (upper panel), and salinity (lower panel) versus depth from SeaCATs/ MicroCATs during WHOTS-1 through WHOTS-14 deployments. The shaded areas indicate missing data. The diamonds along the right axis indicate the depths of the instrument.

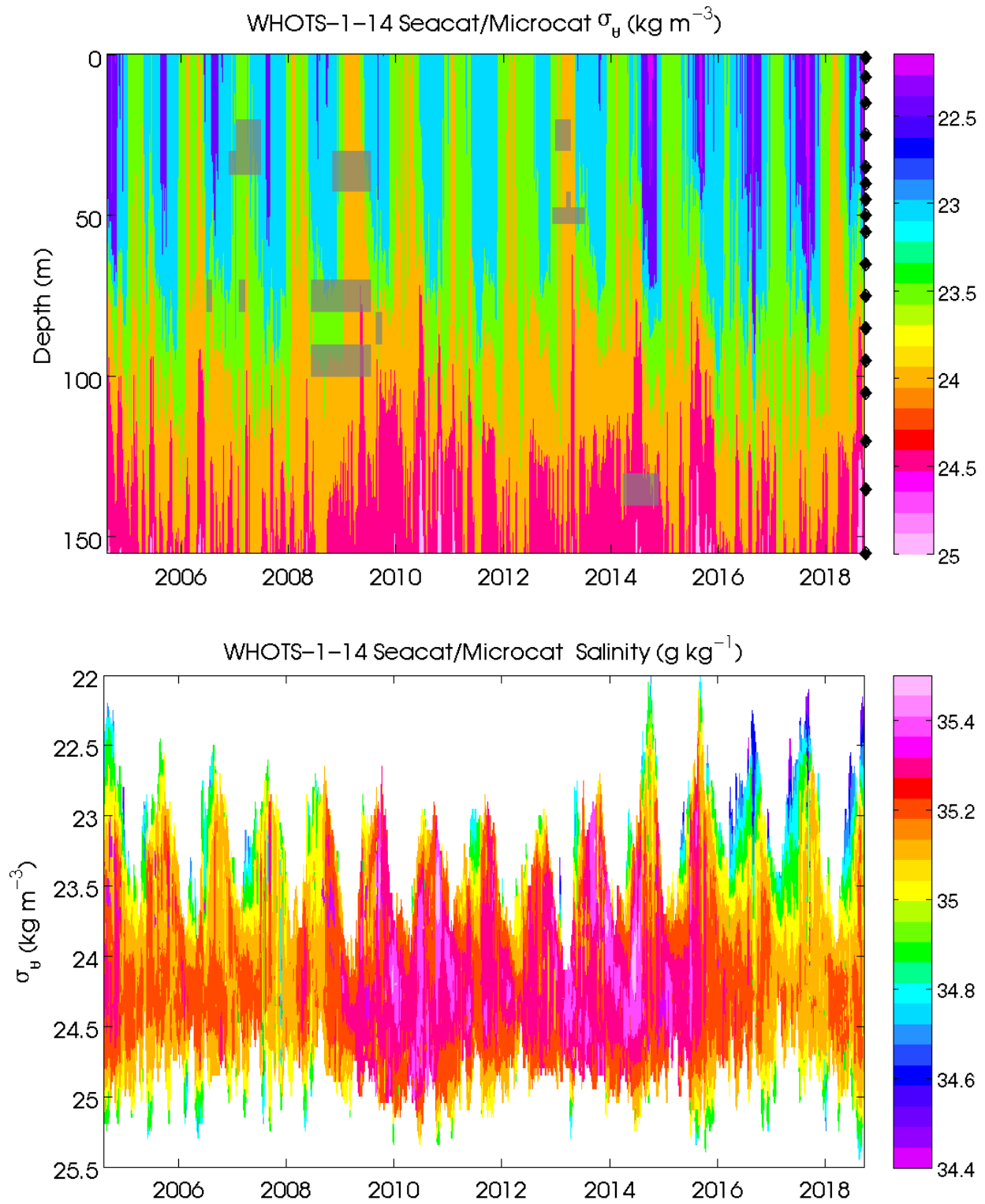
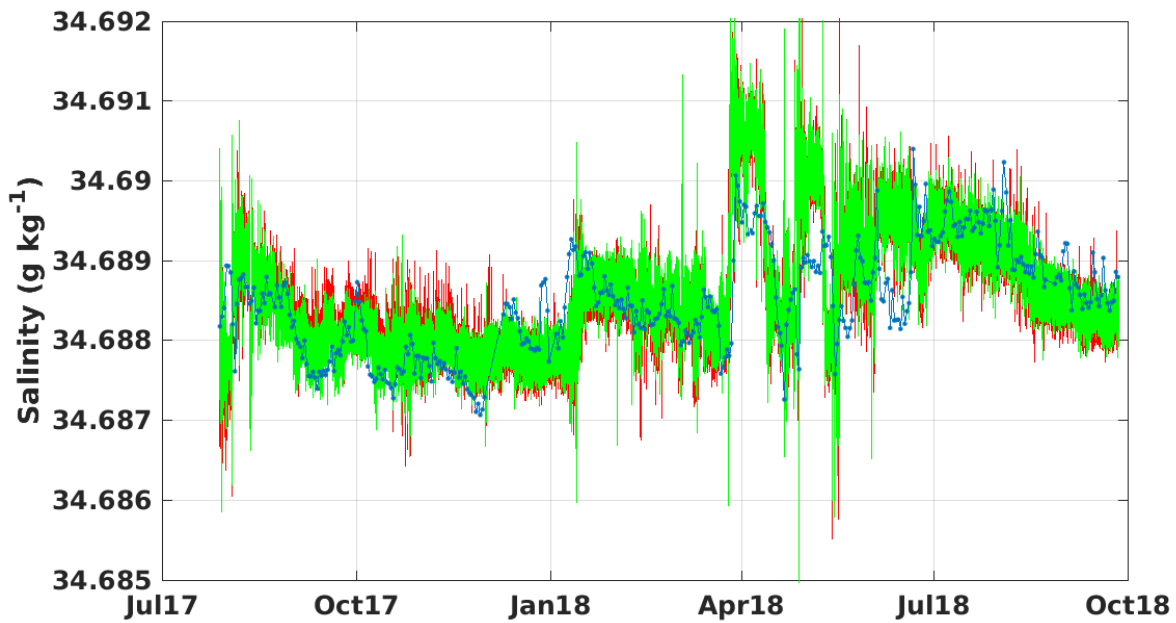
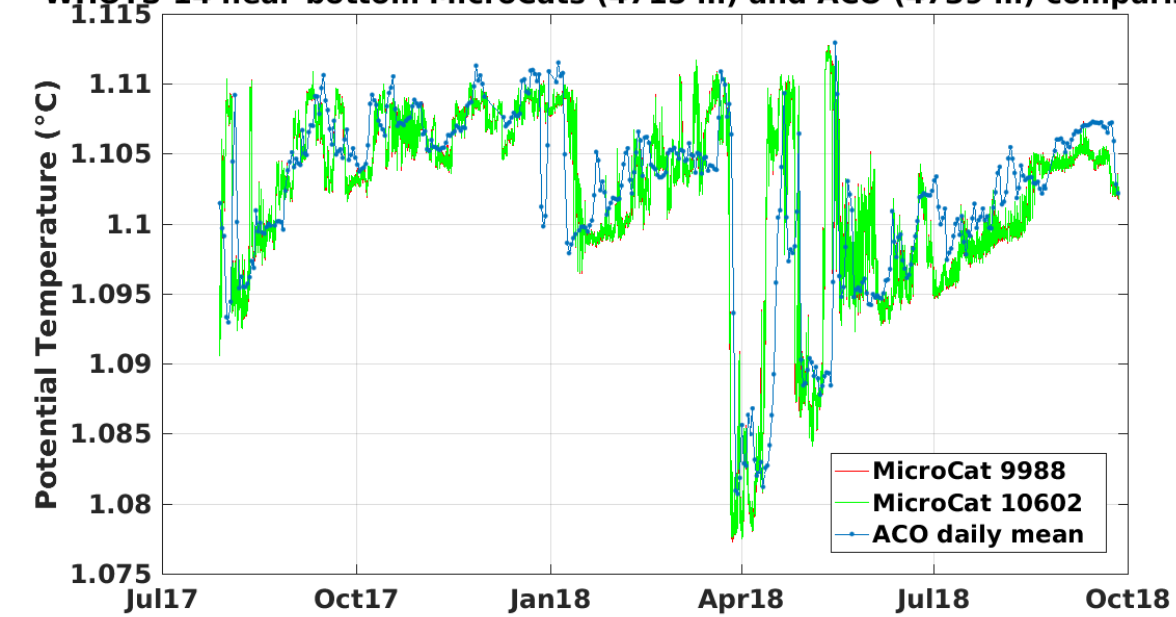


Figure VI-33. Contour plots of potential density ( $\sigma_\theta$ , upper panel), versus depth, and of salinity versus  $\sigma_\theta$  (lower panel) from SeaCATs/MicroCATs during WHOTS-1 through WHOTS-14 deployments. The shaded areas indicate missing data. The diamonds along the right axis in the upper figure indicate the depths of the instrument.

**WHOTS-14 near-bottom MicroCats (4715 m) and ACO (4739 m) comparisons**



*Figure VI-34. Potential temperature (upper panel) and salinity (lower panel) time-series from the ALOHA Cabled Observatory (ACO) sensors and the WHOTS-14 MicroCATs 9988 and 10602.*

#### D. Moored ADCP data

Contoured plots of smoothed horizontal (east and north component) and vertical velocity as a function of depth during the mooring deployments 1 through 13 are presented in Figure VI-35 through Figure VI-37. A staggered time-series of smoothed horizontal and vertical velocities are shown in Figure VI-38 through Figure VI-40. Smoothing was performed by applying a daily running mean to the data and then interpolating the data on to an hourly grid.

Contours of east and north velocity components from the Ship *Hi'ialakai's* Ocean Surveyor broadband 75 kHz shipboard ADCP, and the moored 300 kHz ADCP from the WHOTS-14 deployment as a function of time and depth, during the WHOTS-14 cruise, are shown in Figure VI-41 and Figure VI-42.

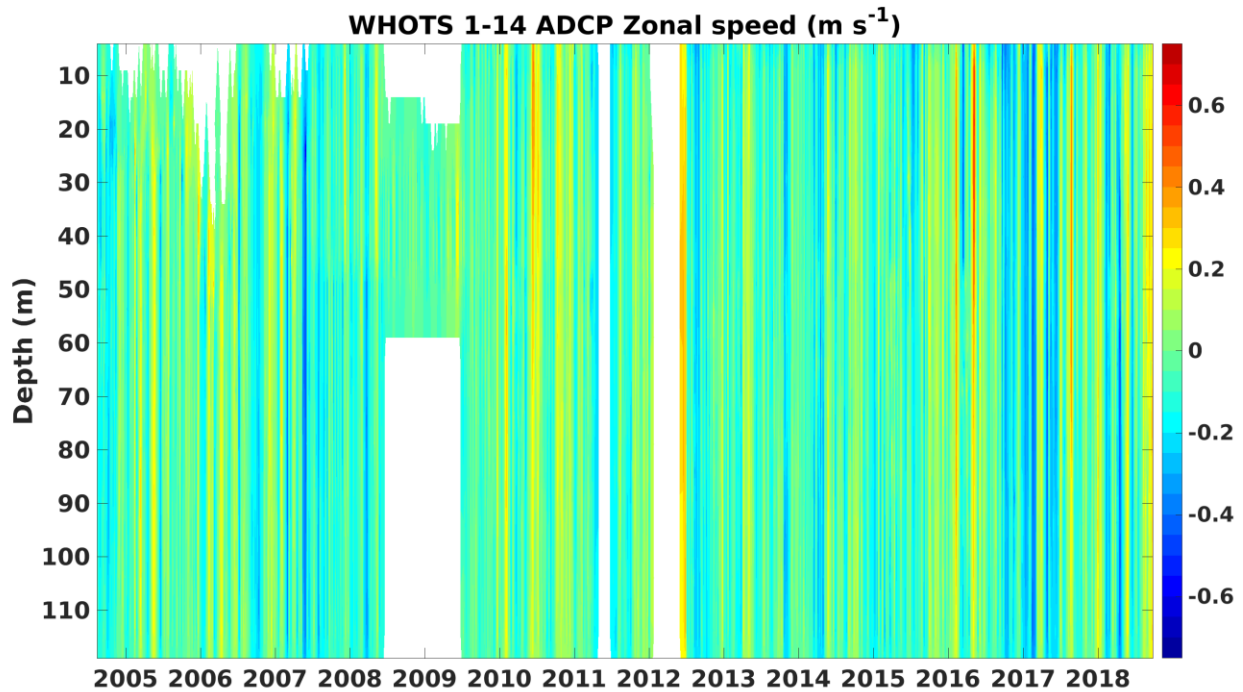


Figure VI-35. Contour plot of east velocity component (m s<sup>-1</sup>) versus depth and time from the moored ADCPs from the WHOTS-1 through -14 deployments.

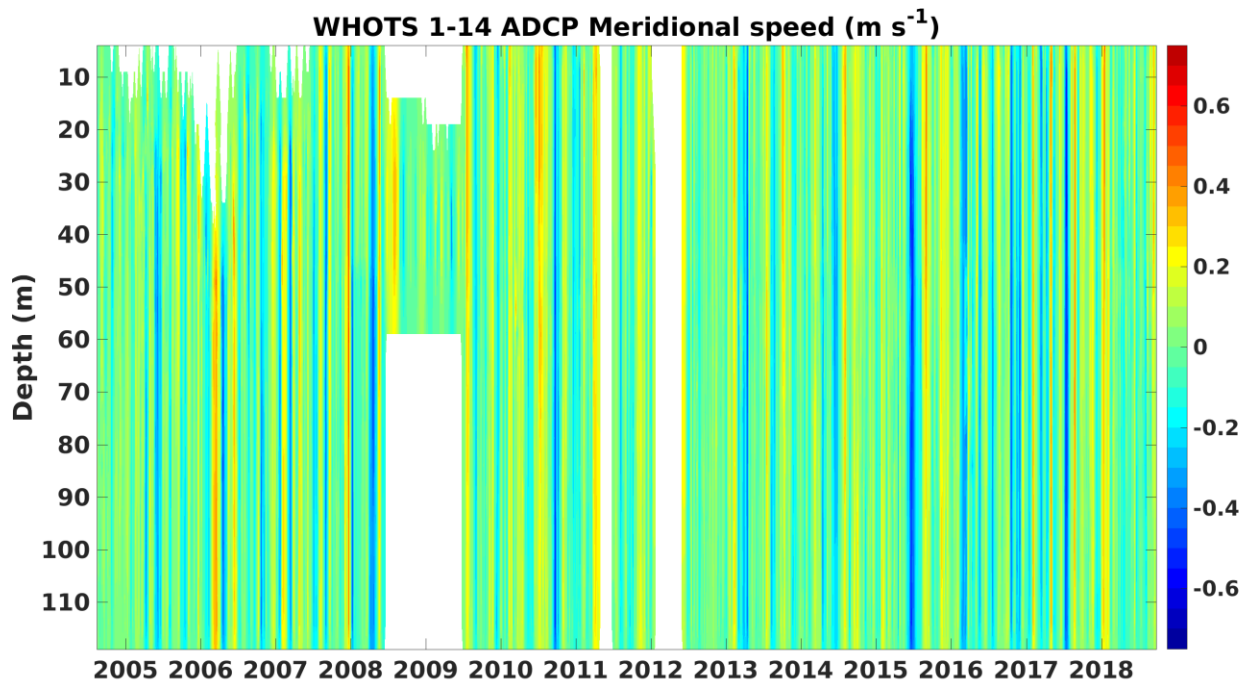


Figure VI-36. Contour plot of north velocity component ( $m s^{-1}$ ) versus depth and time from the moored ADCPs from the WHOTS-1 through -14 deployments.

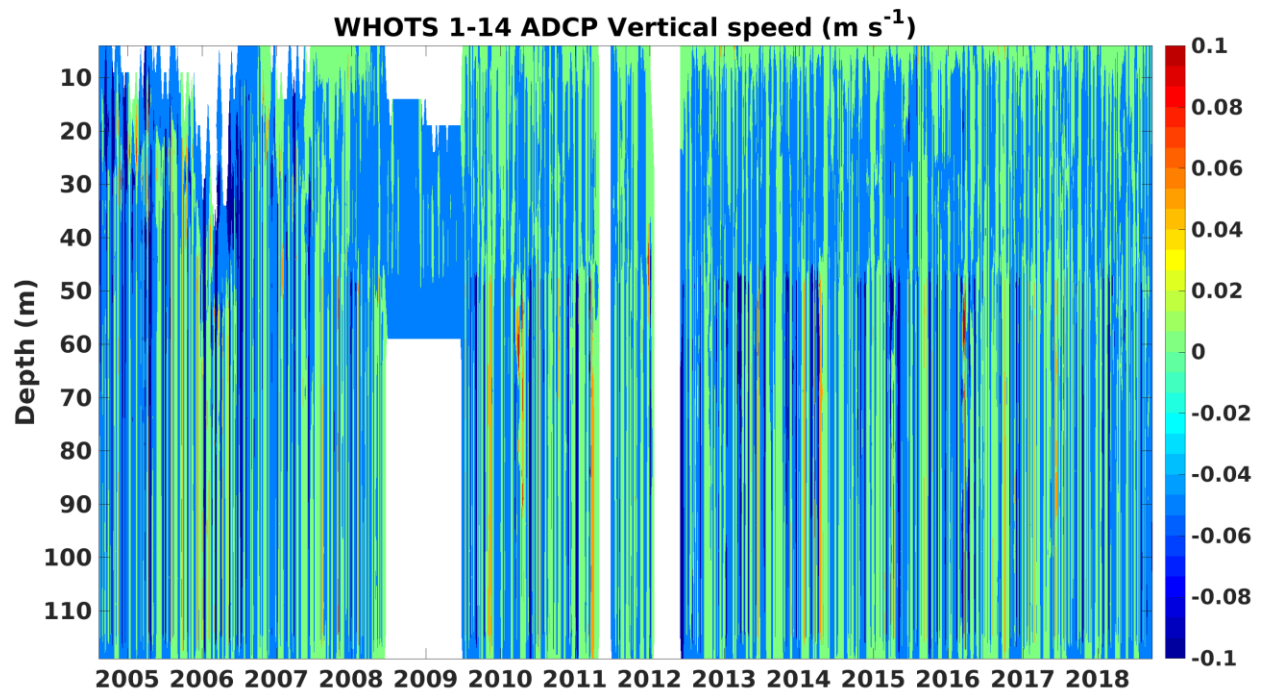


Figure VI-37. Contour plot of vertical velocity component ( $m s^{-1}$ ) versus depth and time from the moored ADCPs from the WHOTS-1 through -14 deployments.

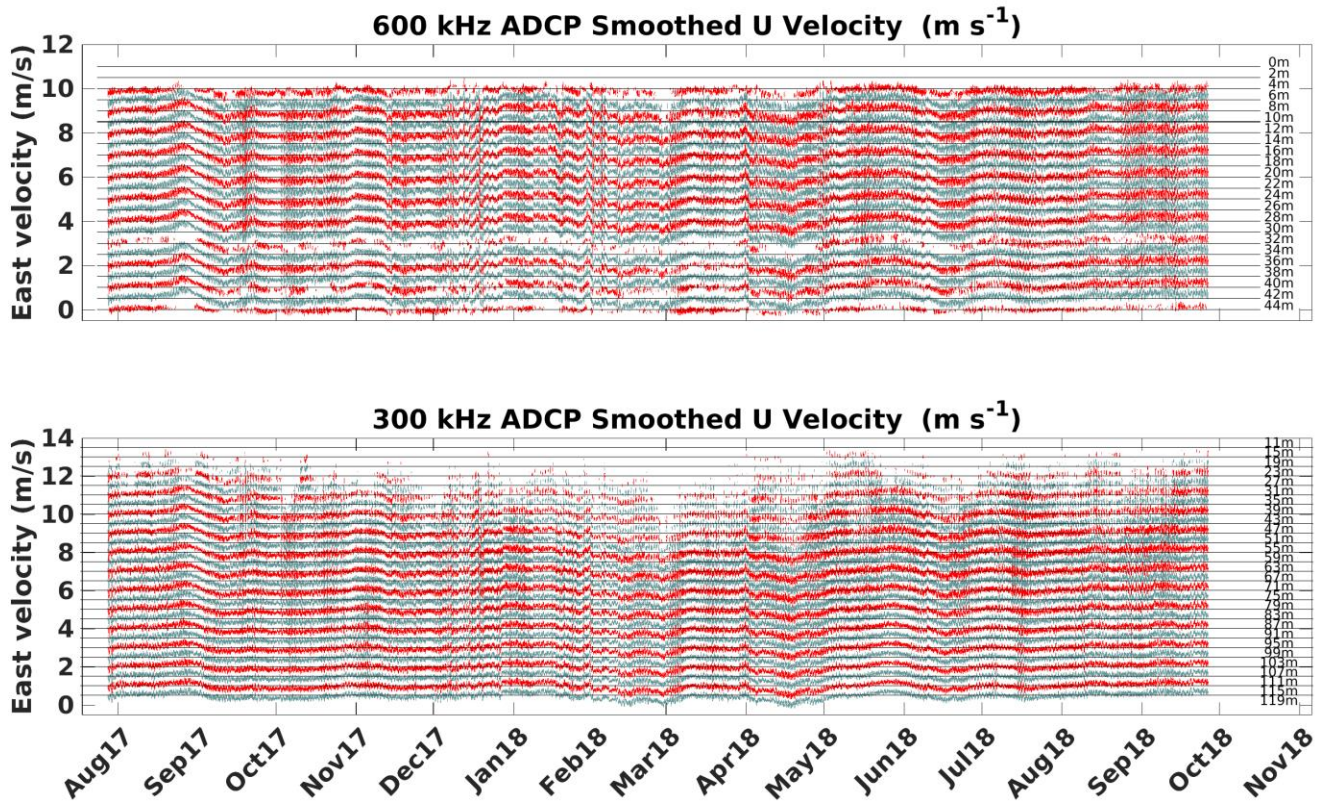


Figure VI-38. Staggered time-series of east velocity component (m s<sup>-1</sup>) for each bin of the 600 kHz (upper panel), and 300 kHz (lower panel) moored ADCPs during WHOTS-14. The time-series are offset upwards by 0.5 m s<sup>-1</sup>; the depth of each bin is on the right.

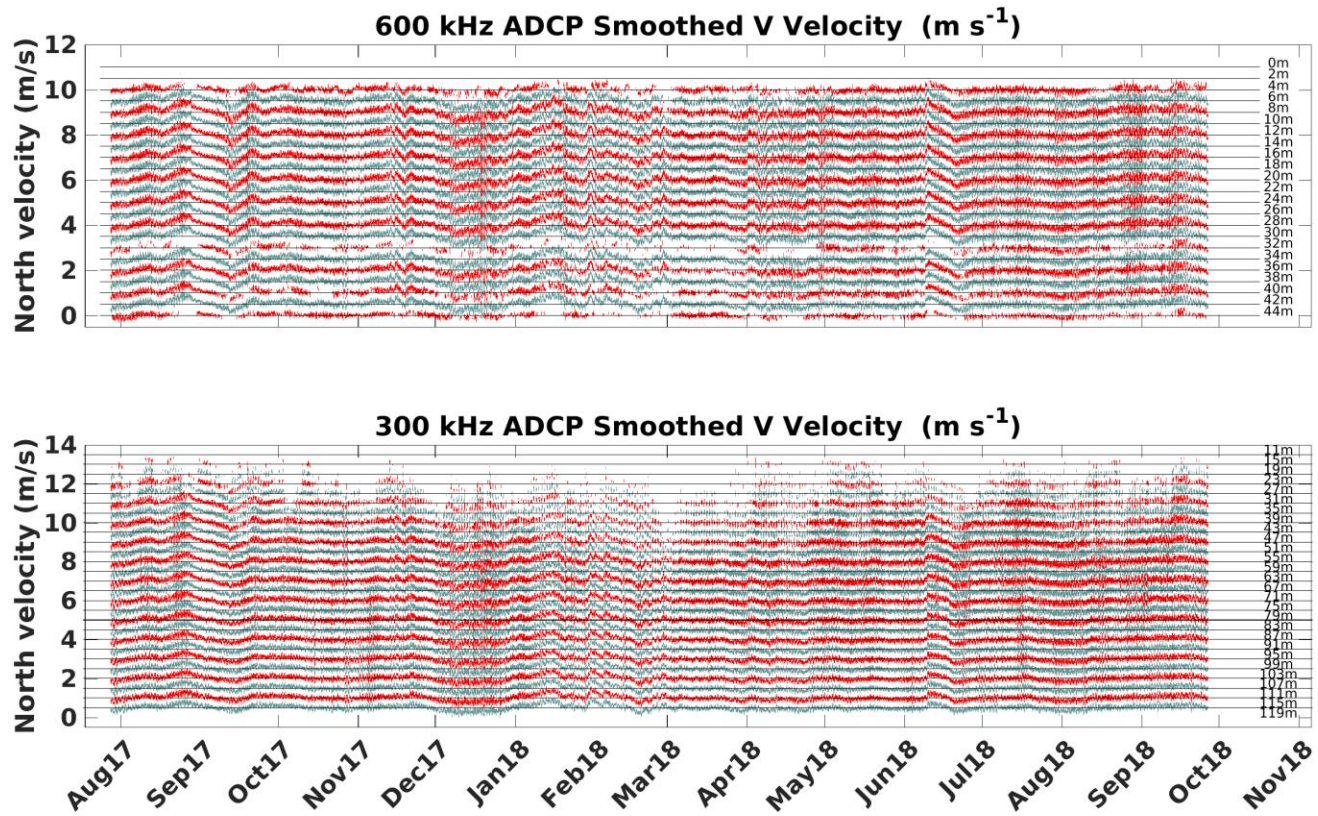


Figure VI-39. Same as Figure VI-38 but for north velocity component.

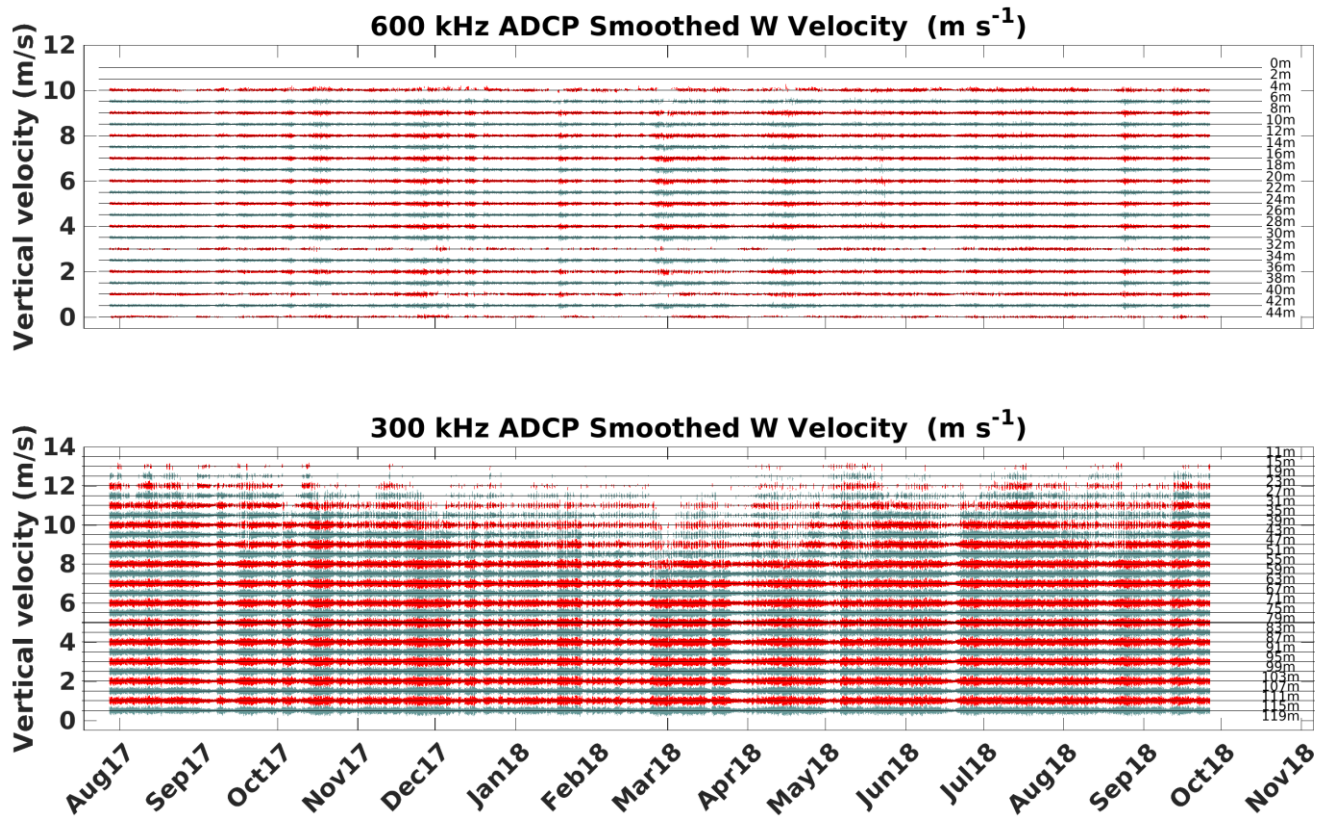


Figure VI-40. Same as Figure VI-38, but for vertical velocity component.

### E. Moored and Shipboard ADCP comparisons

Contours of zonal and meridional current components from the Ship *Hi'ialakai's* Ocean Surveyor broadband 75 kHz shipboard ADCP, and the moored 300 kHz ADCP from the WHOTS-14 deployment as a function of time and depth, during the WHOTS-14 cruise, are shown in Figure VI-41 and Figure VI-42. Similar comparisons during the WHOTS-15 cruise are in Figure VI-43 and Figure VI-44

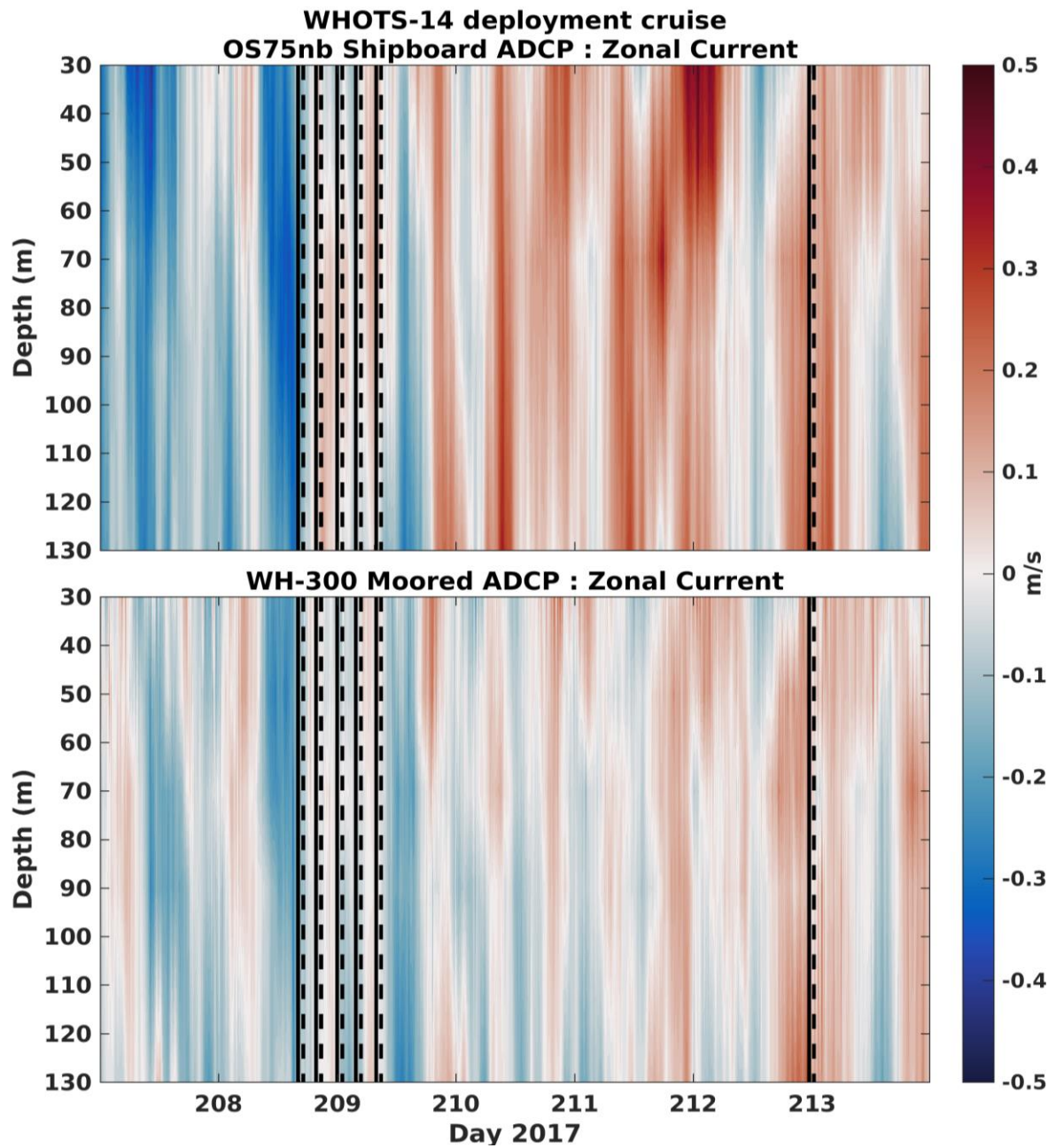


Figure VI-41. The contour of zonal currents ( $m\ s^{-1}$ ) from the Ship *Hi'ialakai's* Ocean Surveyor narrowband 75 kHz shipboard ADCP (upper panel), and the moored 300 kHz ADCP from the WHOTS-14 mooring (bottom panel) as a function of time and depth, during the WHOTS-14 cruise. Times, when the CTD rosette was in the water, are identified between solid and dashed black lines.

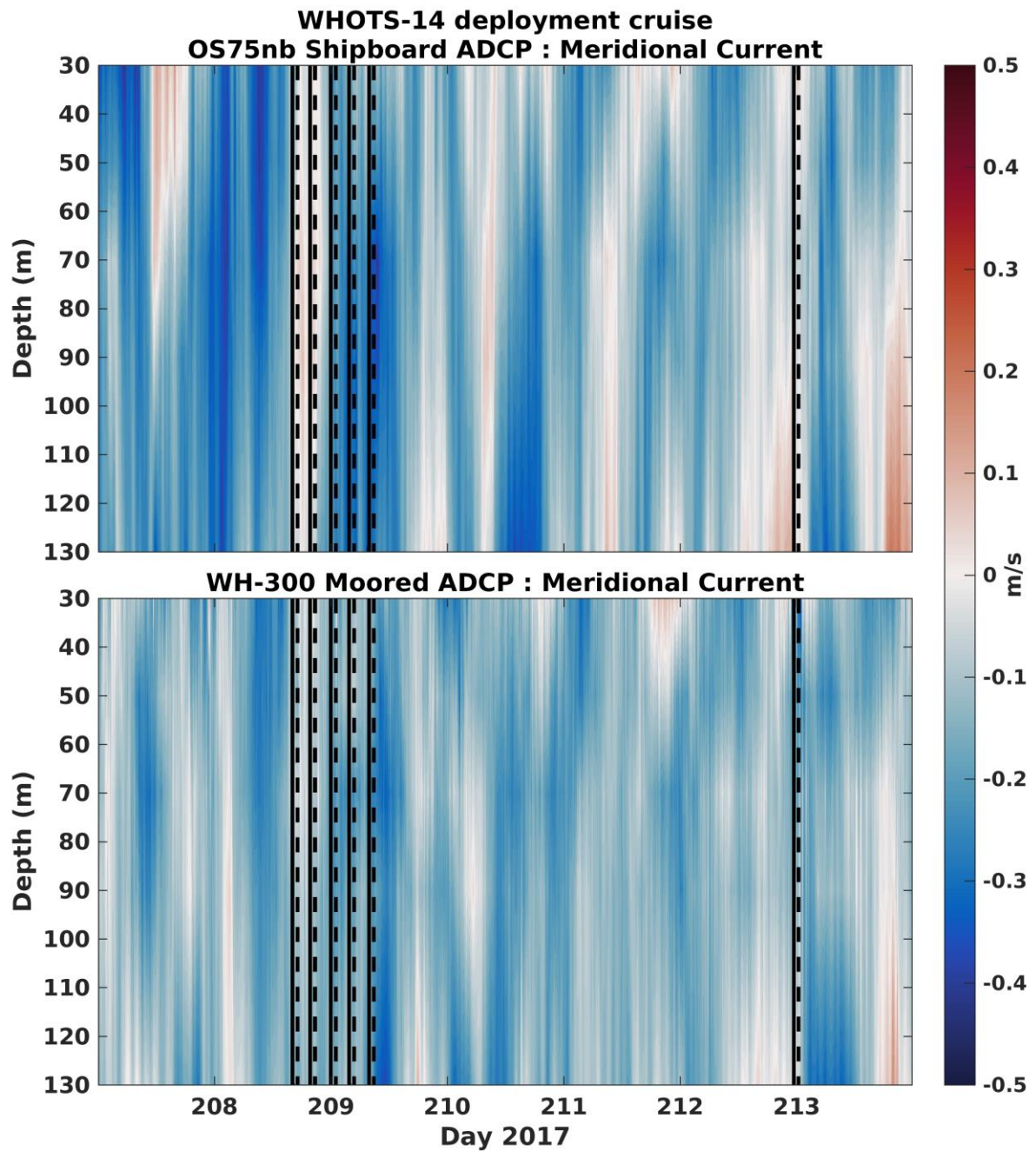


Figure VI-42. The contour of meridional currents ( $m\ s^{-1}$ ) from the Ship *Hi'ialakai's* Ocean Surveyor narrowband 75 kHz shipboard ADCP (upper panel), and the moored 300 kHz ADCP from the WHOTS-14 mooring (bottom panel) as a function of time and depth, during the WHOTS-14 cruise. Times, when the CTD rosette was in the water, are identified between solid and dashed black lines.

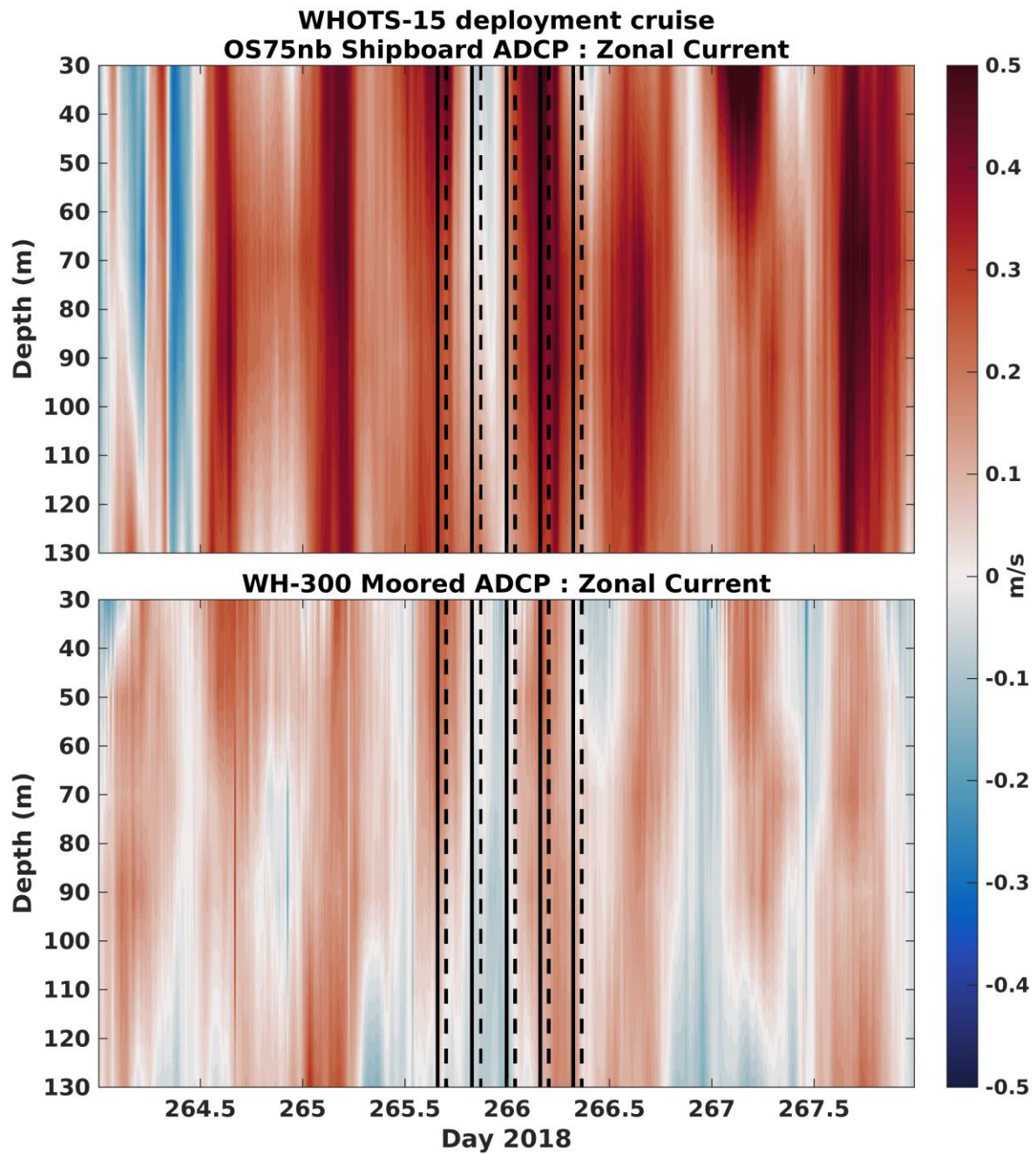


Figure VI-43. The contour of zonal currents ( $m\ s^{-1}$ ) from the Ship *Hi'ialakai's* Ocean Surveyor narrowband 75 kHz shipboard ADCP (upper panel), and the moored 300 kHz ADCP from the WHOTS-14 mooring (bottom panel) as a function of time and depth, during the WHOTS-15 cruise. Times, when the CTD rosette was in the water, are identified between solid and dashed black lines.

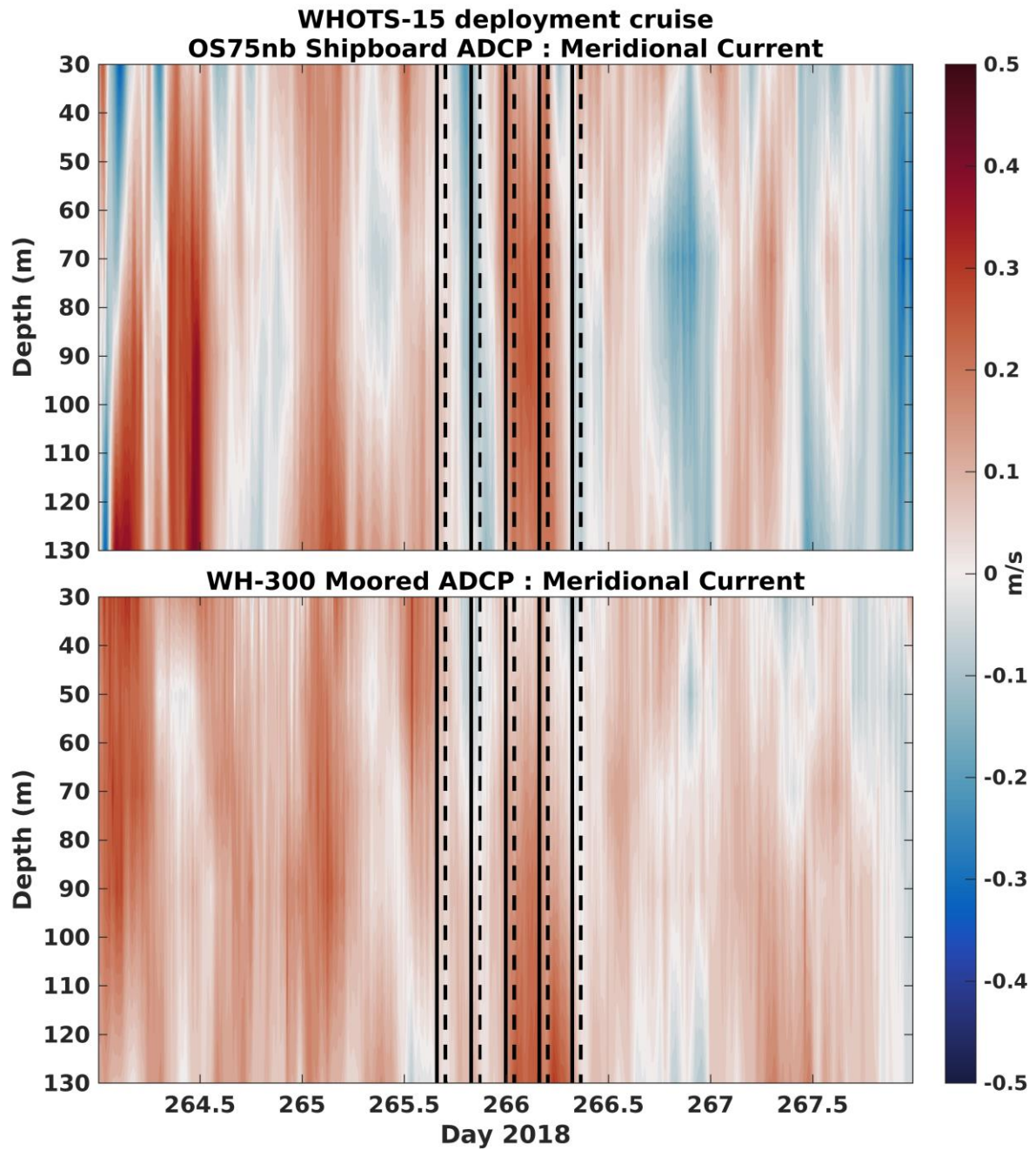


Figure VI-44. Contours of meridional currents ( $m\ s^{-1}$ ) from the Ship *Hi'ialakai's* Ocean Surveyor narrowband 75 kHz shipboard ADCP (upper panel), and the moored 300 kHz ADCP from the WHOTS-14 mooring (lower panel) as a function of time and depth, during the WHOTS-15 cruise. Times, when the CTD/rosette was in the water, are identified between the solid and dashed black lines.

Comparisons between quality-controlled moored ADCPs during the WHOTS-14 deployment and available shipboard ADCP obtained during regular HOT cruises 295 to 305, and during the mooring deployment (WHOTS-14) and recovery (WHOTS-15) cruises are shown in Figure VI-45 for the 300 kHz ADCP, and Figure VI-46 for the 600 kHz ADCP. Median and mean velocity profiles were computed when HOT CTD casts were being conducted near the WHOTS mooring specifically intended to calibrate moored instrumentation (see V.A4). The HOT shipboard profiles were taken when the ship was stationary, within 1 km of the mooring, and within 4 hours before the start and 4 hours after the end of the CTD cast conducted near the WHOTS mooring.

HOT cruises conducted on the R/V *Kilo Moana* (HOT-296, -297, -299, -300 and -305) used data from a TRDI Workhorse 300 kHz ADCP (wh300) with 4 m bin size, reaching 100 m, and averaging ensembles every 2 minutes; and from a TRDI Ocean Surveyor 38 kHz operating in broadband mode (os38bb) with 12 m bin size, reaching 1200 m, with 5-minute ensemble averages, and in narrow band mode (os38nb) with 24 m bin size, reaching 1500 m and also with 5-minute ensemble averages. Data from the wh300 were used for the comparisons with the moored ADCP data, or from the os38bb if the wh300 data were not available. HOT cruises conducted on the R/V *Ka'Imikai-O-Kanaloa* (HOT-295, -298 and -301 through -304) used data from a TRDI Workhorse 300 kHz ADCP (wh300) with 4 m bin size, reaching 100 m, and averaging ensembles every 2 minutes. WHOTS cruises conducted on the Ship *Hi'ialakai's* used an Ocean Surveyor TRDI 75 kHz shipboard ADCP working in narrowband mode with a vertical resolution of 16 m, and in broadband mode with a vertical resolution of 8 m.

The moored ADCP data were collected from the upward facing 300 kHz ADCP located at 125 m and the upward facing 600 kHz ADCP located at 47.5 m over the same period. Zonal (U) and meridional (V) current components from the shipboard and moored vertical profiles were interpolated to the profile resolution of the shipboard ADCP, and ensemble mean and median profiles were obtained for each data set to compute differences and correlation coefficients between them. Bins with less than 50% of data were excluded.

Comparisons between the 300 kHz and the shipboard ADCP were available for HOT-295, -298, and -300; data from all other HOT cruises were excluded due to a lack of comparable data. Comparisons between the moored 600 kHz and the shipboard ADCP were only evaluated for cruises featuring the Workhorse 300 kHz ADCP (wh300) due to the larger vertical resolution with the other ADCP models (os38bb, os75nb).

### WHOTS-14 300 kHz to HOT Shipboard ADCP Comparisons

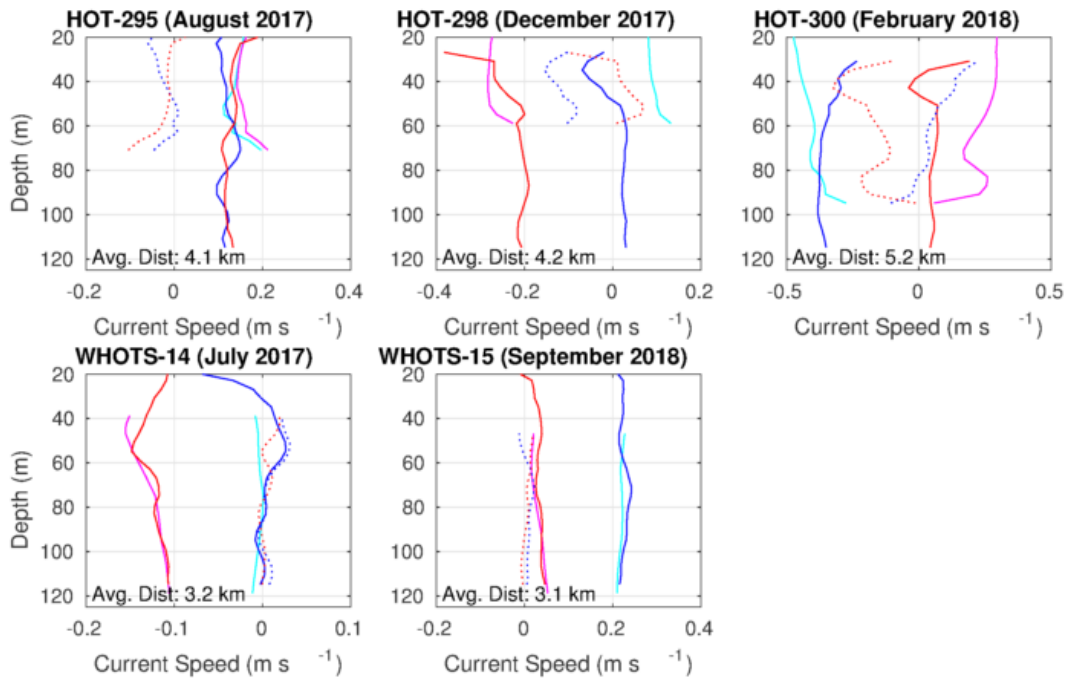


Figure VI-45. Mean current profiles during shipboard ADCP (cyan: zonal, magenta: meridional) versus moored 300 kHz ADCP (blue: zonal, red: meridional) intercomparisons from HOT-295 through HOT-305 and from WHOTS-14 and WHOTS-15 cruises. Moored minus shipboard ADCP differences shown in dotted lines (blue: zonal, red: meridional)

### WHOTS-14 600 kHz to HOT Shipboard ADCP Comparisons

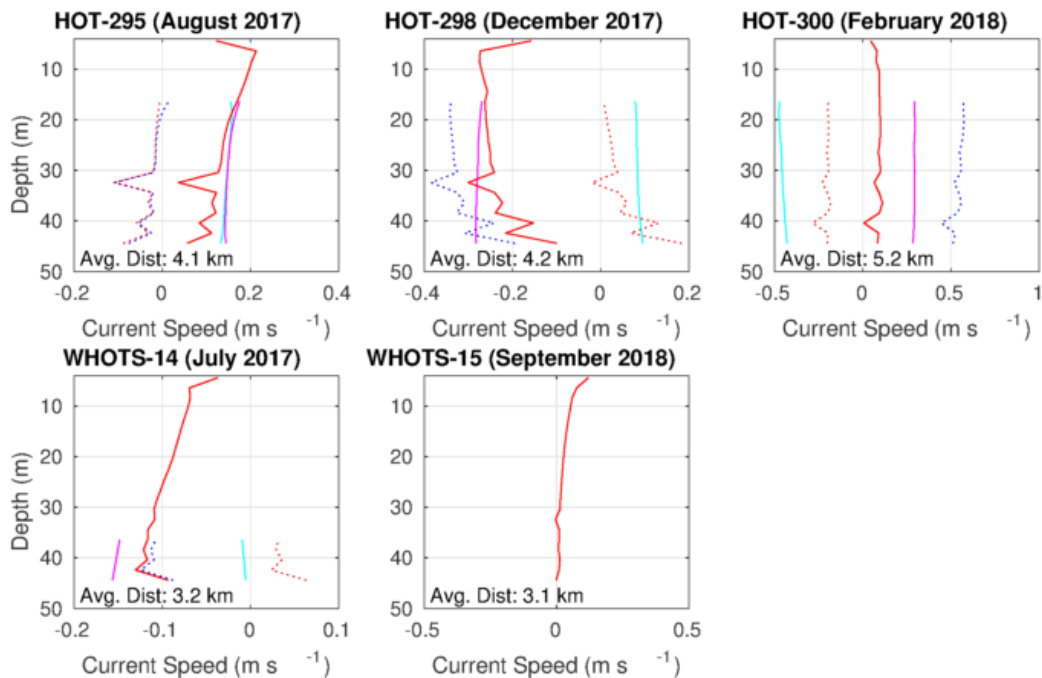


Figure VI-46. Mean current profiles during shipboard ADCP (cyan: zonal, magenta: meridional) versus moored 600 kHz ADCP (blue: zonal, red: meridional) intercomparisons from HOT-295 through HOT-305 and from WHOTS-14 and WHOTS-15 cruises. Moored minus shipboard ADCP differences shown in dotted lines (blue: zonal, red: meridional).

## F. Next Generation Vector Measuring Current Meter data (VMCM)

Time-series of daily mean horizontal velocity components for the VMCM current meters deployed during WHOTS-14 at 10 m and 30 m are presented in Figure VI-47

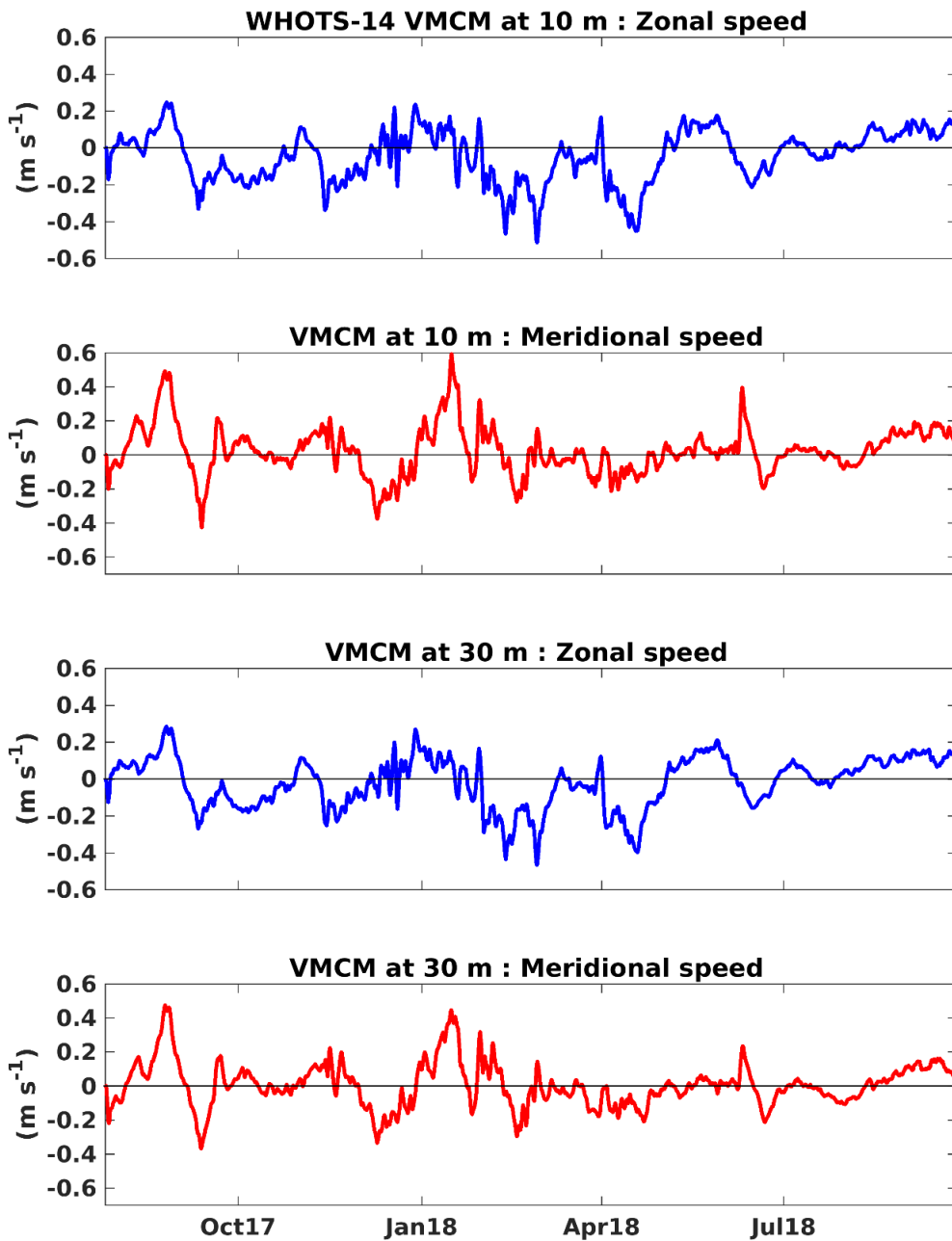


Figure VI-47. Horizontal velocity data ( $\text{m/s}$ ) during WHOTS-14 from the VMCMs at 10 m depth (first and second panel) and at 30 m depth (third and fourth panel)

## G. GPS data

Time-series of latitude and longitude of the WHOTS-14 buoy from GPS data are presented in Figure VI-48, and spectra of the time-series are shown in Figure VI-49.

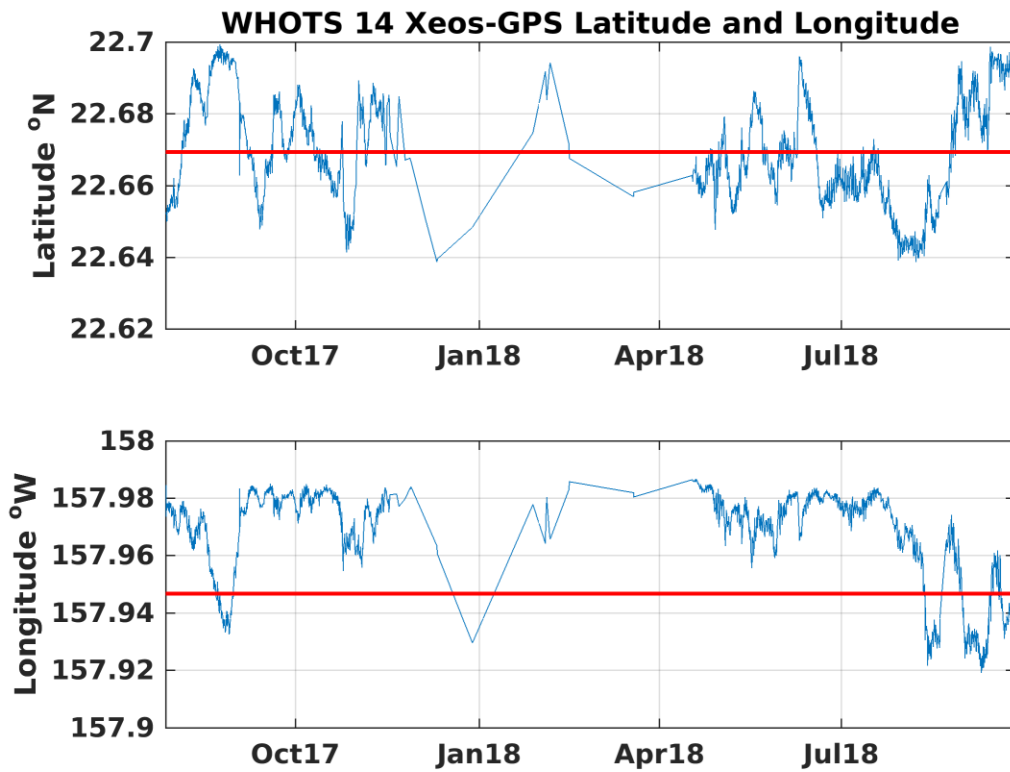


Figure VI-48. GPS Latitude (upper panel) and longitude (lower panel) time series from the WHOTS-14 deployment the instrument failed and was not able to collect data between November 2018 and April 2019 (See Sect. V-D).

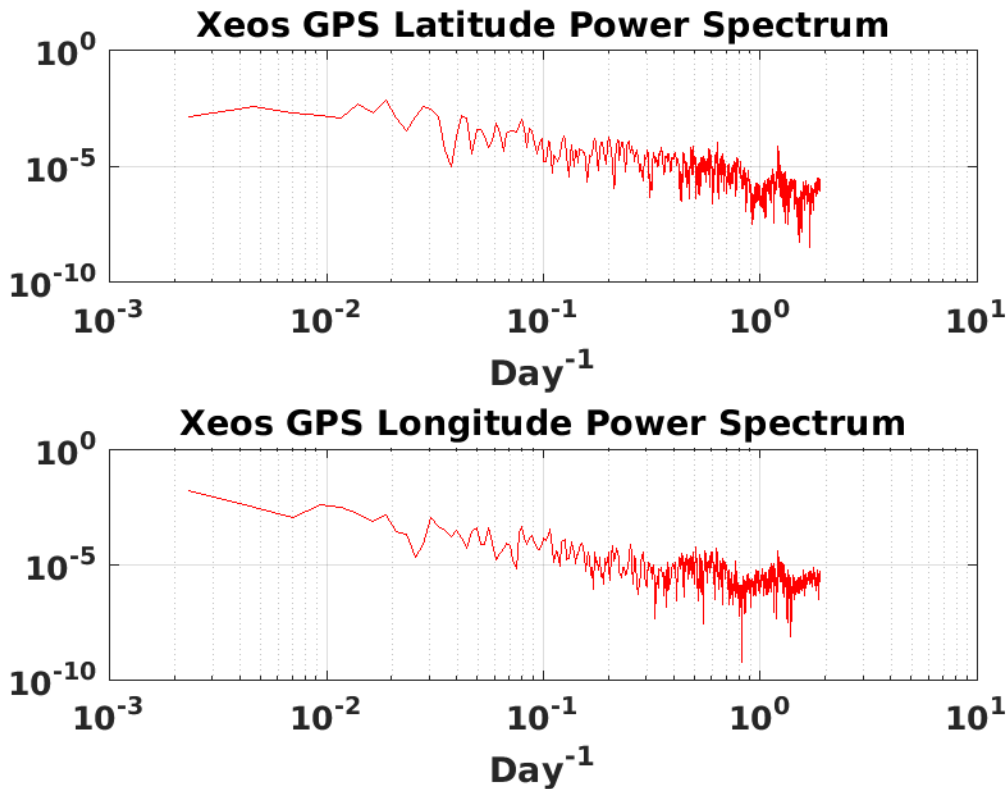


Figure VI-49. The power spectrum of latitude (upper panel) and longitude (lower panel) for the WHOTS-14 deployment.

## H. Mooring Motion

The position of the mooring with respect to its anchor was determined from the ARGOS positions, as shown in Section 0. Additional information on the mooring motion was provided by the ADCP data of pitch, roll, and heading, shown in this section.

Figure VI-50 shows the ADCP data of the instrument's tilt (a combination of the pitch and roll), plotted against the buoy's distance from its anchor (derived from ARGOS positions), for both WHOTS-14 ADCP's. The red line in the plot is a quadratic fit to the median tilt calculated every 0.2 km distance bins. The figure shows that during both deployments, the ADCP tilt increased as the distance from the anchor increased. This tilting was caused by the deviation of the mooring line from its vertical position as it was pulled by the anchor. The tilting of the line also caused the rising of the instruments attached to the line.

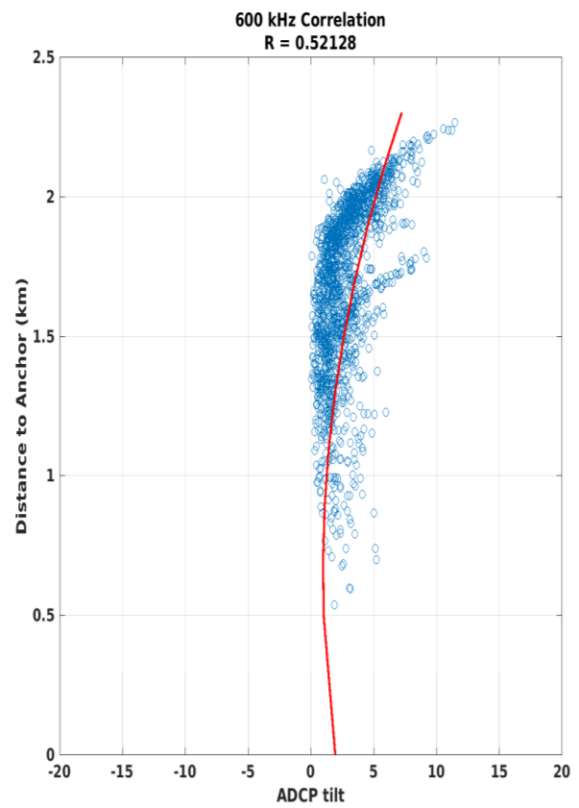
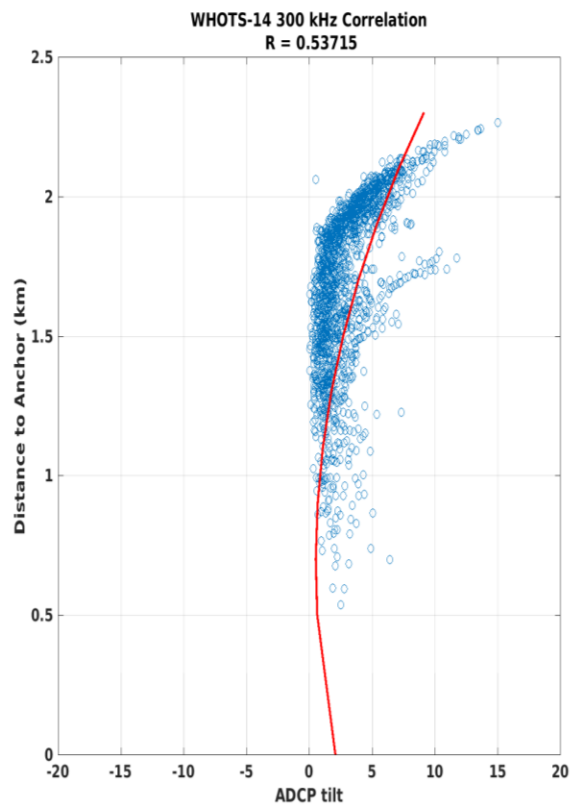


Figure VI-50. Scatter plots of ADCP tilt and distance of the buoy to its anchor for the 300 kHz (left panel), and the 600 kHz ADCP deployments (right panel, blue circles). The red line is a quadratic fit to the median tilt calculated every 0.2 km distance bins.

## VII. References

- Colbo, K., R. Weller, 2009. Accuracy of the IMET Sensor Package in the Subtropics. *J. Atmos. Oceanic Technol.*, 26, 1867-1890.
- Firing, E., 1991. Acoustic Doppler Current Profiling measurements and navigation. In *WOCE Hydrographic Operations and Methods*. WOCE Operations Manual, WHP Office Report WHPO 91-1, WOCE Report No. 68/91, 144pp.
- Freitag, H. P., M. E. McCarty, C. Nosse, R. Lukas, M. J. McPhaden, and M. F. Cronin, 1999. COARE Seacat data: Calibrations and quality control procedures. NOAA Technical Memorandum, ERL PMEL-115. 93 pp.
- Fukieki, L., F. Santiago-Mandujano, K. Trifonova, R. Lukas, and D. Karl, 2019. Hawaii Ocean Time-series Data Report 29: 2017, School of Ocean and Earth Science and Technology, University of Hawaii, SOEST Publication #10803, 436 pp.
- Hasbrouck, E., R.A. Weller, F. Santiago-Mandujano, B. Blomquist, K. Maloney, J. Snyder, A. Clabaugh, S. Adams, K. Rosburg, A. King, S. Natarov, N. Howins, G. Hebert, and R. Lukas, 2019, WHOI Hawaii Ocean Timeseries Station (WHOTS): WHOTS-14 Mooring Turnaround Cruise Report, Woods Hole Oceanographic Institution, Technical Report WHOI-2019-04, 112 pp.
- Hosom, D. R. Weller, R. Payne, and K. Prada, 1995. The IMET (Improved Meteorology) Ship and Buoy Systems. *J. Atmos. Oceanic Technol.*, 12, 527-540.
- Howe, B. M., R. Lukas, F. Duennebieer, and D. Karl, ALOHA cabled observatory installation, 2011. *OCEANS 2011*, 19-22 Sept. 2011.
- Kara, A. B., P. A. Rochford, and H. E. Hulbert, 2000. Mixed layer depth variability and barrier layer formation over the North Pacific Ocean, *J. Geophys. Res.*, 105, 16,803–16,821.
- Lukas, R., F. Santiago-Mandujano, F. Bingham and A. Mantyla, 2001. Cold bottom water events observed in the Hawaii Ocean time-series: Implications for vertical mixing. *Deep-Sea Res. I*, 48 (4), 995-1021
- Owens, W. B., and R. C. Millard, 1985. A new algorithm for CTD oxygen calibration. *Journal of Physical Oceanography*, 15, 621-631.
- Plueddemann, A.J., R.A. Weller, R. Lukas, J. Lord, P.R. Bouchard, and M.A. Walsh, 2006, WHOI Hawaii Ocean Timeseries Station (WHOTS): WHOTS-2 Mooring Turnaround Cruise Report, Woods Hole Oceanographic Institution, Technical Report WHOI-2006-08, 68 pp.
- Santiago-Mandujano, F., J. Snyder, S. Natarov, K. Maloney, N. Howins, G. Hebert, and R. Lukas, 2019. UH Contributions to WHOTS-15 Cruise Report. School of Ocean and Earth Science and Technology, University of Hawaii. ([http://www.soest.hawaii.edu/whots/proc\\_reports/WHOTS-15\\_CruiseRpt.pdf](http://www.soest.hawaii.edu/whots/proc_reports/WHOTS-15_CruiseRpt.pdf))

Santiago-Mandujano, F., P. Lethaby, R. Lukas, J. Snyder, Weller, A. Plueddeman, J. Lord, S. Whelan, P. Bouchard, and N. Galbraith, 2007. Hydrographic Observations at the Woods Hole Oceanographic Institution (WHOI) Hawaii Ocean Timeseries (HOT) Site (WHOTS): 2004-2006. School of Ocean and Earth Science and Technology, University of Hawaii. ([http://www.soest.hawaii.edu/whots/data\\_report1.html](http://www.soest.hawaii.edu/whots/data_report1.html))

Tupas, L., F. Santiago-Mandujano, D. Hebel, R. Lukas, D. Karl, and E. Firing, 1993. Hawaii Ocean Time-series Data Report 4, 1992, School of Ocean and Earth Science and Technology, University of Hawaii, 93-14, 248 pp.

Tupas, L., F. Santiago-Mandujano, D. Hebel, C. Nosse, L. Fujieki, E. Firing, R. Lukas, D. Karl, 1997. Hawaii Ocean Time-series Data Report 8, 1996, School of Ocean and Earth Science and Technology, University of Hawaii, 97-7, 296 pp.

UNESCO. 1981. Tenth Report of the Joint Panel on Oceanographic Tables and Standards. UNESCO Technical Papers in Marine Science, No. 36, UNESCO, Paris.

Whelan S., R. Weller, R. Lukas, F. Bradley, J. Lord, J. Smith, F. Bahr, P. Lethaby, J. Snyder, 2007. WHOI Hawaii Ocean Timeseries Station (WHOTS): WHOTS-3 Mooring Turnaround Cruise Report. Technical Report. Woods Hole Oceanographic Institution, WHOI-2007-03, 103 pp.

# VIII. Appendices

## A. Appendix 1: WHOTS-14 300 kHz - SERIAL 4981

File Size 47,015,670 bytes  
Data Structure BB/WH/OS  
Ensemble Length 754 bytes  
Program Version 50.4  
System Frequency 300 kHz  
Convex  
Sensor Configuration #1  
Transducer Head Attached TRUE  
Orientation UP  
Beam Angle 20 Degrees  
Transducer 4 Beam Janus

### Real Data

CPU Serial Number: 63 00 00 03 87 A5 E4 09  
False Target Threshold Maximum (WA) 70 counts  
Bandwidth Control (WB) 0  
Low Correlation Threshold (WC) 64 counts  
  
Blank After Transmit, cm (WF) 176 cm  
Minimum Percent Good (WG) 0  
Water Reference Layer (WL) 002, 006, first bin, last bin  
Mode (WM) 1  
No. of depth cells (bins) (WN) 30  
Pings per ensemble (WP) 40  
Depth Cell Size (bin length), cm (WS) 400 cm  
Ambiguity Velocity, cm/s radial (WV) 175 cm/s  
  
Heading Alignment, deg (EA) 0.00 degrees  
Heading Bias, deg (EB) 9.61degrees  
Coord Transform (EX) 00011111 Earth Coordinates  
Sensor Source (EZ) 01111101cdhprst  
Sens Avail 00011101cdhprst  
Time per Ping, sec (TP) 00:04.00  
Time per Ensemble, min (TE) 10:00.00

Hardware 4 Beams  
Code Reps. 9  
Lag Length 0.50  
Xmt Length 4.42 m  
1st Bin 6.22 m

First Ensemble 00000001 17/07/24 00:00:00.00  
Last Ensemble 00062355 18/09/30 00:19:59.96

## B. Appendix 2: WHOTS-14 600 kHz ADCP Configuration (serial 1825)

File Size 40,597,050 bytes  
Data Structure BB/WH/OS  
Ensemble Length 654bytes  
Program Version 51.4  
System Frequency 600 kHz  
Convex  
Sensor Configuration #1  
Transducer Head Attached TRUE  
Orientation UP  
Beam Angle 20 Degrees  
Transducer 4 Beam Janus

### Real Data

CPU Serial Number: 97 00 00 02 00 3F BB 09  
False Target Threshold Maximum (WA) 70 counts  
Bandwidth Control (WB) 0  
Low Correlation Threshold (WC) 64 counts  
Error Velocity Threshold, mm/s (WE) 2000 mm/s  
Blank After Transmit, cm (WF) 88 cm  
Minimum Percent Good (WG) 0  
Water Reference Layer (WL) 002, 006, first bin, last bin  
Mode (WM) 1  
No. of depth cells (bins) (WN) 25  
Pings per ensemble (WP) 80  
Depth Cell Size (bin length), cm (WS) 200 cm  
Ambiguity Velocity, cm/s radial (WV) 175 cm/s  
  
Heading Alignment, deg (EA) 0.00 degrees  
Heading Bias, deg (EB) 9.61 degrees  
Coord Transform (EX) 00011111 Earth Coordinates  
Sensor Source (EZ) 01111101 cdhprst  
Sens Avail 00111101 cdhprst  
Time per Ping, sec (TP) 00:02.00  
Time per Ensemble, min (TE) 10:00.00

Hardware 4 Beams  
Code Reps. 9  
Lag Length 0.25 m  
Xmt Length 2.22 m  
1st Bin 3.11 m

First Ensemble 00000001 17/07/26 00:00:00.00  
Last Ensemble 00062075 18/09/30 01:39:59.96